Coop Agreement
University
of
Idaho

THESIS/
REPORTS

SHARMA, S.

A Technical Manual For Slope Analysis With XSTABL

June 1992

Coop Agreement
University
of
Idaho

FINAL REPORT FOR RESEARCH JOINT VENTURE AGMT
#INT-89416-RJVA with
UNIVERSITY OF IDAHO
FS CONTACT: **Carol HAMMOND**
Co-op CONTACT: Sunil Sharma

A Technical Manual for

SLOPE ANALYSIS

WITH

XSTABL

prepared for the

Intermountain Research Station
Forest Service
U.S. Department of Agriculture
Moscow, ID 83843

by

Sunil Sharma
Department of Civil Engineering
University of Idaho
Moscow, ID 83843

June, 1992

Contract # INT – 89416 – RJV

NOTICE

All problems presented in Chapter 5 were prepared using the slope stability program, **XSTABL**®, Version 4.1. The practical problems, and their solutions, have been carefully reviewed to minimize the possibility of errors. Readers should ***not*** presume that the solutions presented by the author provide a single unique method that can be used to evaluate the stability of all slopes. Such procedures must necessarily rely on considerable practical experience and engineering judgement for each individual site.

The views expressed in this report are those of the author and do not necessarily reflect the views of the sponsors: USDA – Forest Service and the University of Idaho.

This research was supported in part by funds provided by the Intermountain Research Station, Forest Service, U.S. Department of Agriculture and the University of Idaho. *The Federal Government reserves a royalty-free, nonexclusive, and irrevocable right to reproduce, publish, or otherwise use, and to authorize others to use, this report for Government purposes. Additionally, the report may be freely reproduced in whole, or in part, for* ***personal*** *use only.*

ACKNOWLEDGEMENTS

In preparing this technical report, the author has relied heavily on the original reports prepared by Siegel (1975), Boutrup (1977) and Lovell, et. al. (1985). These reports concerned the development and implementation of the slope stability program, STABL, at Purdue University, West Lafayette, Indiana. This material has been included in this report to provide USDA - Forest Service personnel, and other users, a concise and accurate review of the capabilities and limitations of the slope stability analysis algorithms used in the program **XSTABL** that has been developed for the personal computer.

This report was prepared with financial support provided by a cooperative project agreement, # INT-89416-RJVA, between the University of Idaho and the Intermountain Research Station, USDA - Forest Service, Moscow, Idaho. The author would also like to thank the many current and prospective **XSTABL** users who provided useful information that improved the quality of this manual considerably. Hopefully, this extra effort will be appreciated by existing, and future, **XSTABL** users.

And finally, I would like to acknowledge the encouragement and support provided by Rod Prellwitz, USDA - Forest Service, Missoula, Montana. This support was a fundamental factor in the initial development and final completion of this project.

TABLE OF CONTENTS

1.0 **INTRODUCTION** 1

2.0 **METHODS OF ANALYSIS** 5

2.1 Simplified Janbu Method 10
2.2 Simplified Bishop Method 13
2.3 Reinforced Slope Analysis 15
2.4 Non-linear Mohr-Coulomb Envelope 19
2.5 Factor of Safety Iteration 20
2.6 Control of Negative Effective Stresses 21
2.7 Comparison of Results with Other Methods 24

3.0 **SEARCHING TECHNIQUES** 27

3.1 Random Numbers 27
3.2 Circular Surface Generation 28
Adjustment of $\Delta\theta$ 32
3.3 Irregular Surface Generation 35
3.4 Block Surface Generation 38
Rankine Wedges 39
Block Wedges 41
Search Boxes 42

4.0 **DETERMINATION OF SLICE DATA** 45

4.1 Determination of Slice Widths 45
4.2 Calculation of Slice Weight 46
4.3 Pore Pressure Calculations 47
Phreatic Surface 48
Piezometric 50
Pore Pressure Grid 51
4.4 Submerged Slopes 52
4.5 Earthquake Loads 53
4.6 Boundary Surcharge Loads 53

Table of Contents, continued . . . . .

5.0 **SLOPE STABILITY EXAMPLES** 55

5.1 Pore Water Pressures 55
EXAMPLES 56
Search for Critical Surface 56
Analysis of Critical Surface 58
Summary and Conclusions 60
5.2 Typical USDA-Forest Service Examples 61
Example 1 61
Example 2 63
Example 3 67
Bearing Capacity 68
Overall Stability 72
5.3 Anisotropic Subsoils 75
Example of Anisotropic Strength 76
5.4 Seismic Analysis 79
5.5 Curved Mohr-Coulomb Envelope 82
5.6 Geotextile Reinforcement 87
5.7 Negative Effective Stresses 91
Example 1 91
Example 2 93
5.8 Random Search for Critical Surface 95

6.0 **SPENCER'S ANALYSIS** 99

6.1 Spencer's method 100
Force Equilibrium 101
Moment Equilibrium 102
6.2 Factor of Safety 103
6.3 Example Applications 105
Problem 1 105
Problem 2 109
6.4 Summary 112
6.5 Conclusions and Recommendations 113

7.0 **REFERENCES** 115

8.0 **APPENDIX** 119

CHAPTER 1

INTRODUCTION

The design and assessment of the stability of slopes is a critical component of successful slope management of USDA - Forest Service lands. The stability of natural or constructed slopes has to be assessed routinely for safety and hazard mitigation. Such work requires the development of practical solutions on the basis of sophisticated or simple analytical tools that are an integral part of slope stability analysis. However in all cases, it must be emphasized that the final analytical assessment is a function of the overall geology of the area and the strength of the soils and the pore water pressures within the slope. These are the most significant features that form the essential input data for the analytical part of slope analysis.

The available analytical procedures rely heavily on numerical methods that are implemented into computer programs. The earliest programs for general slope stability analysis were written in the late 1950's (Little and Price, 1958). Unfortunately, since these programs required mainframe computers, they were not readily accessible to practicing geotechnical engineers. The benefits of such programs were only apparent via design charts that were generated by several researchers for typical site conditions. However, the accessibility of computers has changed rapidly and now one can readily perform sophisticated analyses using desktop computers.

This technical manual discusses the use of the computer program, **XSTABL** (I.S. Designs, Inc., 1992) for slope stability analysis and design by USDA - Forest Service engineers and geologists. Since the program is available for use on all USDA - Forest Service projects, this report provides background information in an attempt to instruct the user about the general operation of the program. The current version of the **XSTABL** program (version 4.1) consists of about 140 subroutines and about 16,000 lines of FORTRAN code along with many additional subroutines written in assembly language for controlling the graphics and interactive screen displays. The program development was started in 1988 (Sharma, 1988)

under a grant from the Idaho Transportation Department. The original version was slow and only allowed the user to create and edit data files which could then be used with a version of STABL4 that had been modified to generate high quality plots of the slope and failure surface geometry on a dot-matrix printer.

The data creation and analysis portions were combined in 1989 to produce an integrated version that included context-sensitive help and an improved technique for handling data errors. This version was strongly supported by USDA - Forest Service and after additional improvements and extensive testing released as Version 3.0 in Spring, 1990. This version was made available to USDA - Forest Service personnel in 1990. Subsequent work has considerably enhanced the program, making available different graphical formats, a reinforced slope option and removing the restriction that the input data must correspond to a left facing slope. This version was released in October, 1991, as Version 4.0. The additional reviews and comments by users since that time has resulted in the release of **XSTABL**, Version 4.1. *This version has been used exclusively for the solution of all example problems discussed in this report.* The algorithms and the methodology employed by Version 4.1 of **XSTABL** are discussed in Chapters 2-4 and examples are presented in Chapter 5. The last three examples presented in chapter 5 should be carefully studied by all readers interested in the control of negative effective stresses and the search process for identifying the critical failure surface. Chapter 6 discusses Spencer's Method which is expected to be implemented into Version 5.0 under a forthcoming proposed joint venture between the University of Idaho and USDA - Forest Service.

The data files for all thirty-six examples presented in Chapter 5 are listed in the Appendix. If you would like to obtain these "*.IPT" data files in a readily useable format, please send a formatted, IBM-PC compatible disk to: Dr. Sunil Sharma, University of Idaho, Dept. of Civil Engineering, Moscow, ID 83843.

Slope analysis programs offer methods of analysis that can range in complexity from the relatively simple "Ordinary Method of Slices" to the highly complicated "Morgenstern-Price" method. The slope stability analysis program, **XSTABL**, uses the simplified Bishop and Janbu methods of analysis, as programmed into the original version of STABL4 that was available from Purdue University. Although the analytical technique is important, the user must be made aware of the capabilities and limitations that may have been implicitly included

during the development of the program. This concern has reached serious levels as more and more programs are provided in their binary (executable) form, thus preventing a closer examination of the program code and algorithms.

XSTABL is supplied only in its executable form and as the user does not have access to the program's code, this manual attempts to provide some useful background information concerning the operation of the program. These background details are provided for the analytical portion of the program, as well as the interactive portion. Hopefully, with this information, the user should be able to recognize the limitations of the program.

The analytical portion of **XSTABL** consists of a modified version of the STABL4, as described in reports by Siegel (1975a, 1975b), Siegel et al. (1980), Boutrup (1977) and Lovell et al. (1985). Since the material contained in these reports is rather voluminous, the following relevant aspects will be summarized:

1. methods of analysis,
2. discretization of the slope mass into slices,
3. search routines used to locate the critical surface,
4. pore water pressures for effective stress analysis,

Additional information is also provided concerning some of the new analytical features that are available in **XSTABL** version 4.1, and later. These new features include:

1. Improved algorithms for automatic surface generation,
2. Non-linear (or curved) Mohr-Coulomb Strength envelope,
3. Design of *reinforced* slopes,
4. Analysis of left facing ***and*** right-facing slopes,
5. Control of negative effective stresses,
6. Additional checks to identify misleading Factor of Safety values associated with negative effective stresses.
7. Details about the use of Spencer's method as the procedure is expected to be implemented in **XSTABL** Version 5.0 in 1993.

For slope analysis, the geotechnical engineer has available many commercial software packages as well as some public domain computer programs that have been developed as part of research supported by federal funds. A 1991 FHWA report evaluated 27 different slope stability analysis PC based programs that ranged in price from a nominal charge up to $ 3,500. The review considered features such as accuracy, available options, user-friendliness, output and found **XSTABL** to be strong in most categories. It is hoped that the publication of this supporting report will enhance the reputation and credibility of **XSTABL** within the USDA - Forest Service and general geotechnical engineering practice.

CHAPTER 2

METHODS OF ANALYSIS

XSTABL uses a modified version of the STABL4 program, originally developed at Purdue University, to calculate the factors of safety according to the simplified Bishop (1955) and simplified Janbu (1957) methods of analysis. Both of these methods use the limit equilibrium approach to analyze a slide-mass that is divided into n smaller slices as shown in Figure 2.1.

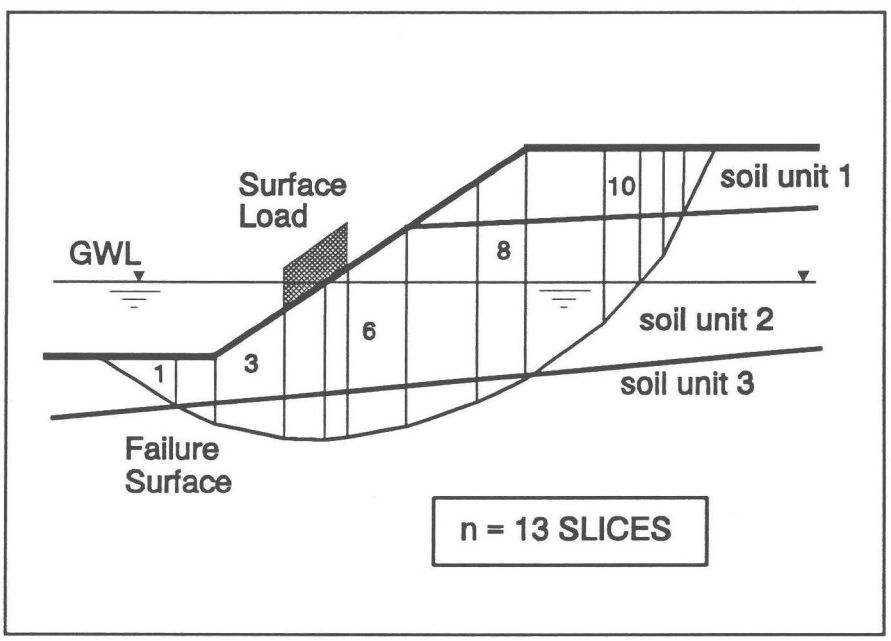

Figure 2.1. Division of potential sliding mass into slices

Each slice is affected by a general system of forces as shown in Figure 2.2. The thrust line indicated in the figure connects the points of application of the interslice forces, E_i. The location of this thrust line may be determined using a rigorous method of analysis that satisfies complete equilibrium. The popular simplified methods of analysis neglect the location of the interslice force because complete equilibrium is not satisfied for the failure mass.

For this system, there are (6n - 2) unknowns as listed in Table 2.1. Also, since only four equations can be written for the limit equilibrium for the system, the solution is statically indeterminate. However, a solution is possible providing the number of unknowns can be reduced by making some simplifying assumptions. One of the common assumptions is that

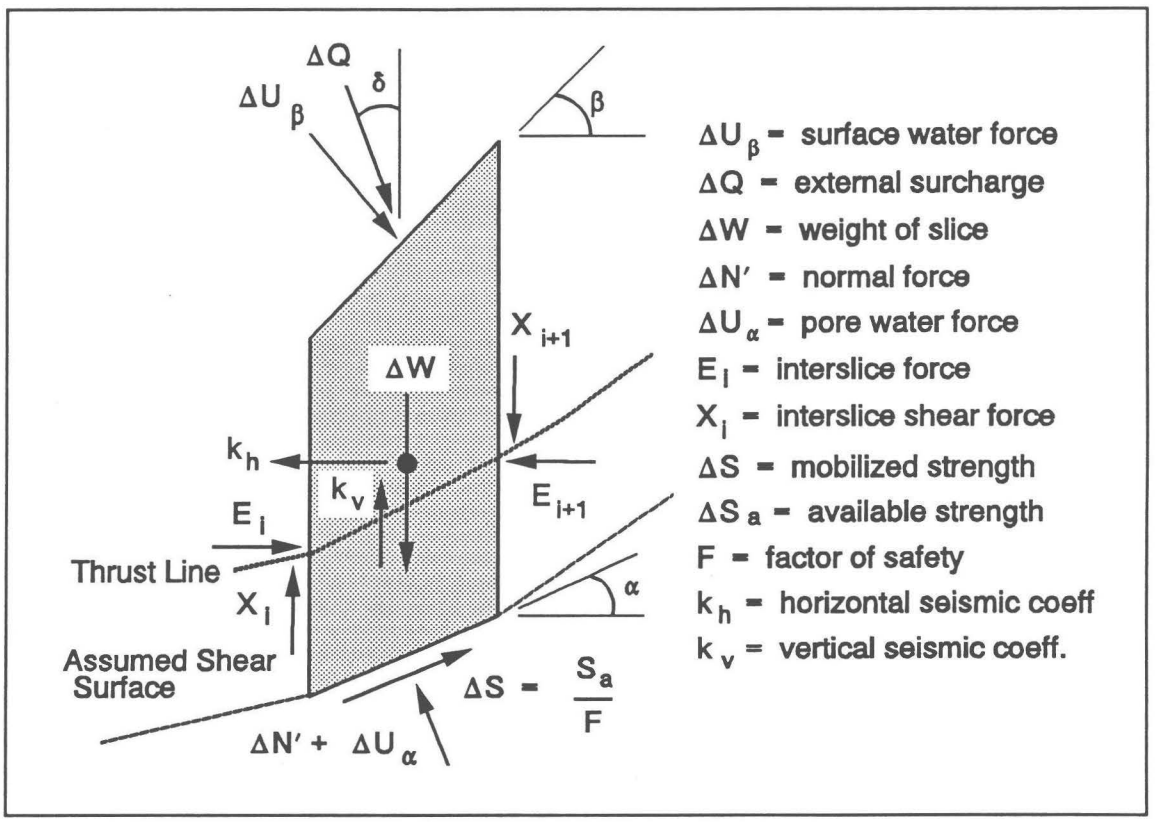

Figure 2.2. Forces acting on a typical slice

the normal force on the base of the slice acts at the midpoint, thus reducing the number of unknowns to (5n - 2). This then requires an additional (n-2) assumptions to make the problem determinate. Generally, the type and nature of these assumptions categorizes the available methods of analysis (Sharma and Lovell, 1983).

Table 2.2 lists the commonly available methods of analysis and the conditions of static equilibrium that are satisfied in determining the factor of safety. The assumptions made by each of these methods, to render the problem determinate, are summarized below.

Table 2.1. Equations and unknowns associated with the Method of Slices

Equations	Condition
n	Moment equilibrium for each slice
2n	Force equilibrium in two directions (for each slice)
n	Mohr-Coulomb relationship between shear strength and normal effective stress
4n	**Total number of equations**
Unknowns	
1	Factor of Safety
n	Normal force at base of each slice, $\Delta N'$
n	Location of normal force, $\Delta N'$.
n	Shear force at base of each slice, ΔS
n - 1	Horizontal interslice force, E
n - 1	Vertical interslice force, X
n - 1	Location of interslice force (line of thrust)
6n - 2	**Total number of unknowns**

Table 2.2. Static equilibrium conditions satisfied by Limit Equilibrium methods

METHOD	FORCE - EQUILIBRIUM		MOMENT EQUILIBRIUM
	x	y	
Ordinary Method of Slices	No	No	Yes
Bishop's Simplified	Yes	No	Yes
Janbu's Simplified	Yes	Yes	No
Bishops's Rigorous	Yes	Yes	Yes
Janbu's Generalized	Yes	Yes	Yes
Spencer	Yes	Yes	Yes
Morgenstern - Price	Yes	Yes	Yes

Ordinary Method of Slices neglects all interslice forces and fails to satisfy force equilibrium for the slide mass as well as for individual slices. However, this is one of the simplest procedures based on the method of slices.

Bishop's Simplified Method assumes that all interslice shear forces are zero, reducing the number of unknowns by (n - 1). This leaves (4n - 1) unknowns, leaving the solution over-determined as horizontal force equilibrium will not be satisfied for one slice.

Janbu's Simplified Method also assumes zero interslice shear forces, reducing the number of unknowns to (4n - 1). This leads to an over-determined solution that will not completely satisfy moment equilibrium conditions. However, Janbu presented a correction factor, f_o, to account for this inadequacy.

Bishop's Rigorous Method assumes (n - 1) interslice shear forces to calculate a factor of safety. Since this assumption leaves (4n - 1) unknowns, moment equilibrium cannot be directly satisfied for all slices. However, Bishop introduced an additional unknown by suggesting there exists a unique distribution of the interslice resultant force, out of a possible infinite number, that will rigorously satisfy the equilibrium equations.

Janbu's Generalized Method assumes a location of the thrust line, thereby reducing the number of unknowns to (4n - 1). Sarma (1979) points out that the position of the normal stress on the last (uppermost) slice is not used and hence moment equilibrium is not satisfied for this last slice. However, similar to the rigorous Bishop method, Janbu also suggested that the actual location of the thrust line is an additional unknown and thus equilibrium can be satisfied rigorously if the assumption selects the correct thrust line.

Spencer's Method rigorously satisfies static equilibrium by assuming that the resultant interslice force has a constant, but unknown, inclination. These (n - 1) assumptions again reduce the number of unknowns to (4n - 1), but the unknown inclination is an additional component which subsequently increases the number of unknowns to match the required 4n equations.

Morgenstern - Price method is similar to the Spencer's method, except that the inclination of the interslice resultant force is assumed to vary according to a "portion" of an arbitrary function. This additional "portion" of a selected function introduces and additional unknown, leaving 4n unknowns and 4n equations.

The rigorous methods, such as Morgenstern-Price and Spencer, may be used to analyze circular and noncircular failure surfaces. For these methods, moment equilibrium conditions are satisfied by either:

(a) taking overall moments about a common point (e.g. the center of a circle if a circular failure surface is being examined) for *all* slices, or

(b) by satisfying moment equilibrium for each *individual* slice by taking moments about the center of the slice base.

The second approach is used for presenting the formulation for the Spencer's method discussed in Chapter 6. In summary, only the Spencer and Morgenstern-Price (M & P) methods adequately satisfy all conditions of equilibrium. However, there are an infinite number of arbitrary functions that may be used to satisfy the interslice resultant force angles required for the M & P solution.

Once a factor of safety is computed, both Spencer's and the M & P methods require the user to verify the reliability and "reasonableness" of the calculated factor of safety. This additional complexity prevents use of these methods for automatic search procedures for location of the critical failure surface, reserving them for the analysis of well-defined, single surfaces only. Also these rigorous methods require a substantially higher level of familiarity if reasonable solutions are to be computed for practical problems.

Conversely, Bishop's and Janbu's simplified methods are popular because a factor of safety value can be quickly calculated for most surfaces. However, their assumptions and the factor of safety formulations often lead to the calculation of slightly different results. For circular failure surfaces, the factor of safety computed by Bishop's method is usually greater than the value from Janbu's formulation. Bishop's FOS value is also about the same as the FOS that may be calculated using a more rigorous approach such as the M-P or Spencer's method. So for the analysis of circular failure surfaces, the simplified Bishop's method is strongly recommended for analysis. However, Janbu's method is acceptable for circular and noncircular surfaces.

All these methods may lead to a different factor of safety (FOS) for the same surface and so it is important that the user understand details concerning the derivation of the FOS expressions.

2.1 Simplified Janbu Method

The simplified (or modified) Janbu method uses the method of slices to determine the stability of the slide mass. It is based on the forces shown, in Figure 2.2, for the free-body diagram of a typical slice. The simplified procedure assumes that there are no inter-slice shear forces. The geometry of each slice is described by its height, h, measured along its centerline, its width, Δx, and by the inclination of its base and top, α and β, respectively.

Janbu's method satisfies vertical force equilibrium for each slice, as well as overall horizontal force equilibrium for the entire slide mass (i.e., all slices). Vertical force equilibrium for each slice is given by:

$$\Sigma F_v = (\Delta N' + \Delta U_\alpha)\cos\alpha + \Delta S\sin\alpha - \Delta W\,(1 - k_v) - \Delta U_\beta \cos\beta - \Delta Q \cos\delta = 0 \qquad (2.1)$$

The above equation may be arranged for $\Delta N'$ as

$$\Delta N' = \frac{-\Delta U_\alpha\cos\alpha - \Delta S\sin\alpha + \Delta W\,(1 - k_v) + \Delta U_\beta \cos\beta + \Delta Q \cos\delta}{\cos\alpha} \qquad (2.2)$$

If the Factor of Safety (FOS) against shear failure is defined as **F**, and is assumed to be the same for all slices, the Mohr-Coulomb mobilized shear strength (ΔS) along the base of each slice is given by:

$$\Delta S = \frac{\Delta C + \Delta N'\tan\phi}{F} \qquad (2.3)$$

where ΔC and $\Delta N'\tan\phi$ are the cohesive and frictional shear strength components of the soil. By substituting Eq. 2.3 into 2.2, the effective normal force acting at the base of the slice can be determined as:

$$\Delta N' = \frac{1}{m_\alpha}\left[\Delta W(1 - k_v) - \frac{\Delta C\sin\alpha}{F} - \Delta U_\alpha\cos\alpha + \Delta U_\beta\cos\beta + \Delta Q\cos\delta\right] \qquad (2.4)$$

where

$$m_\alpha = \cos\alpha \left[1 + \frac{\tan\alpha\tan\phi}{F} \right] \tag{2.5}$$

Next, the overall horizontal force equilibrium is evaluated for all slices of the slide mass. In this case, for an individual slice i :

$$[F_H]_i = (\Delta N' + \Delta U_\alpha)\sin\alpha + \Delta W k_h + \Delta U_\beta \sin\beta + \Delta Q \sin\delta - \Delta S \cos\alpha \tag{2.6}$$

then substituting for ΔS from Eq. 2.3 and rearranging, overall horizontal force equilibrium for the slide mass is given by:

$$\begin{aligned} \sum_{i=1}^{n} [F_H]_i = \sum_{i=1}^{n} & (\Delta N' + \Delta U_\alpha)\sin\alpha + \Delta W k_h + \Delta U_\beta \sin\beta \\ & + \Delta Q \sin\delta - \frac{\Delta C + \Delta N' \tan\phi}{F} \cos\alpha \\ & = 0 \end{aligned} \tag{2.7}$$

Rearranging the above equation, the following expression may be obtained:

$$\begin{aligned} \sum_{i=1}^{n} & \left[(\Delta N' + \Delta U_\alpha)\sin\alpha + \Delta W k_h + \Delta U_\beta \sin\beta + \Delta Q \sin\delta \right] \\ & = \sum_{i=1}^{n} \left[\frac{1}{F} (\Delta C + \Delta N' \tan\phi) \cos\alpha \right] \end{aligned} \tag{2.8}$$

Then if each slice has the same factor of safety, F,

$$F = \frac{\sum_{i=1}^{n} [\Delta C + \Delta N' \tan\phi] \cos\alpha}{\sum_{i=1}^{n} A_1 + \sum_{i=1}^{n} \Delta N' \sin\alpha} \tag{2.9}$$

where $\Delta N'$ is given by Eq. 2.4. and

$$A_1 = \Delta U_\alpha \sin\alpha + \Delta W k_h + \Delta U_\beta \sin\beta + \Delta Q \sin\delta \tag{2.10}$$

Eq. 2.9 is a ratio of the horizontal components of the available resistance and the driving forces or alternatively one can consider it as the ratio of the *available* shear strength and *driving* shear force along the failure surface. This equation is programmed into **XSTABL** for computing the uncorrected Janbu factor of safety. This format allows the state of the effective stress to be determined and appropriate corrections implemented if $\Delta N'$ is calculated to be less than zero. These corrections are discussed in section 2.6. **XSTABL** also computes the total available shear strength along the failure surface, $\Sigma(C + N'\tan\phi)$, and uses it to determine the *actual* magnitude of the driving shear force, as reported in the output files.

The reported Janbu FOS value is calculated by multiplying the calculated F value by a modification factor, f_o,

$$FOS_{Janbu} = f_o \cdot FOS_{calculated}$$

This modification factor is a function of the slide geometry and the strength parameters of the soil. Figure 2.3 illustrates the variation of the f_o value as a function of the slope geometry (d and L) and type of soil.

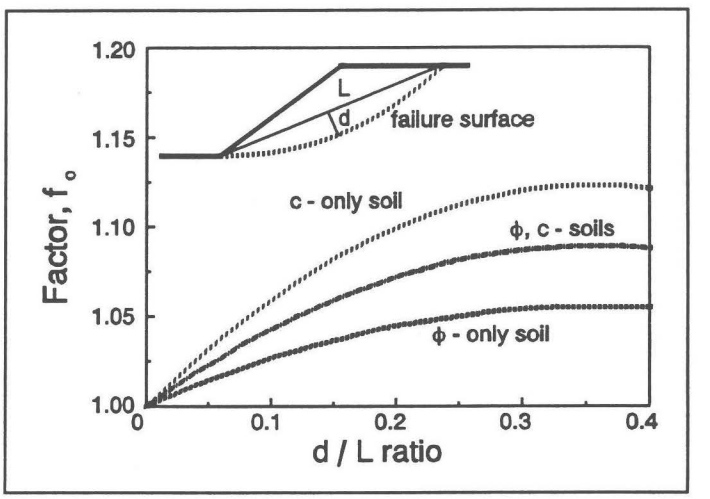

Figure 2.3. Janbu's correction factor for the simplified method

These curves were presented by Janbu in an attempt to compensate for the assumption of negligible interslice shear forces (X_i) in his formulation for the simplified method. Janbu then performed calculations using his simplified and rigorous (i.e., satisfying complete equilibrium) methods for the same slopes with homogenous soil conditions. The subsequent comparison between the simplified and rigorous FOS values was used to develop the correction curves shown in Fig. 2.3.

There is no consensus concerning the selection of the appropriate f_o value for a surface intersecting different soil types consisting of c-only, ϕ-only and c-ϕ soils. In cases where such a mixed variety of soils is present, the c-ϕ curve is generally used to correct the calculated FOS value. Within **XSTABL**, this modification factor is calculated according to the formula:

$$f_o = 1.0 + b_1 \left[\frac{d}{L} - 1.4 \left(\frac{d}{L} \right)^2 \right] \qquad \textbf{(2.11)}$$

where b_1 varies according to the soil type : c only soils: $b_1 = 0.69$

ϕ only soils: $b_1 = 0.31$

c and ϕ soils: $b_1 = 0.50$

The appropriate b_1 value is selected for use in Eq. 2.11 according to the type (i.e., c only, ϕ only or both c and ϕ) of soil encountered *along* the analyzed failure surface. If a mixed soil-type is encountered, **XSTABL** uses the c and ϕ soil relationship described by the above expression.

2.2 Simplified Bishop Method

The simplified Bishop method also uses the method of slices to discretize the soil mass for determining the factor of safety. This method satisfies vertical force equilibrium for each slice and overall moment equilibrium about the center of the *circular* trial surface. The simplified Bishop method also assumes zero inter-slice shear forces. Using the notation shown in Figure 2.2, the overall moment equilibrium of the forces acting on each slice is given by :

$$\begin{aligned} \Sigma M_o = & \sum_{i=1}^{n} \left[\Delta W \, (1 - k_v) + \Delta U_\beta \cos\beta + \Delta Q \cos\delta \right] R \sin\alpha \\ & - \sum_{i=1}^{n} \left[\Delta U_\beta \sin\beta + \Delta Q \sin\delta \right] (R \cos\alpha - h) \\ & - \sum_{i=1}^{n} [\Delta S] R + \sum_{i=1}^{n} \left[k_h \, \Delta W (R \cos\alpha - h_{eq}) \right] \\ & = 0 \end{aligned} \qquad \textbf{(2.12)}$$

where R is the radius of the circular failure surface, h is the average height of the slice and h_{eq} is the vertical height between center of the base slice and the centroid of the slice. The above equation may be simplified by dividing throughout by the radius to get:

$$\frac{\Sigma M_o}{R} = \sum_1^n [(\Delta W\ (1-k_v) + \Delta U_\beta \cos\beta + \Delta Q \cos\delta)\ ] \sin\alpha$$

$$- \sum_1^n [\Delta S\ ] - \sum_1^n [\Delta U_\beta \sin\beta + \Delta Q \sin\delta](\cos\alpha - h/R) \qquad \textbf{(2.13)}$$

$$+ \sum_1^n [k_h\ \Delta W\ (\cos\alpha - \frac{h_{eq}}{R})]$$

Please note that the effective normal and pore pressure forces, acting on the base of the slice, do not affect the moment equilibrium expression since they are directed through the center of the circle. *Thus XSTABL may not be used to compute a Factor of Safety for* ***non-circular surfaces using Bishop's method!***

If the FOS is assumed to be the same for all slices, substitute Eq. 2.3 into Eq. 2.13 to give:

$$F = \frac{\sum_{i=1}^n (\Delta C + \Delta N' \tan\phi)}{\sum_{i=1}^n A_2 - \sum_{i=1}^n A_3 + \sum_{i=1}^n A_4} \qquad \textbf{(2.14)}$$

where:

$$A_2 = (\Delta W\ (1 - k_v) + \Delta U_\beta \cos\beta + \Delta Q \cos\delta) \sin\alpha$$

$$A_3 = (\Delta U_\beta \sin\beta + \Delta Q \sin\delta)\ (\cos\alpha - h/R) \qquad \textbf{(2.15)}$$

$$A_4 = k_h\ \Delta W (\cos\alpha - \frac{h_{eq}}{R})$$

Next, forces are summed in the vertical direction for each slice to determine the effective normal force in the same manner as used for Janbu's method,

$$\Delta N' = \frac{1}{m_\alpha}\left[\Delta W(1 - k_v) - \frac{\Delta C \sin\alpha}{F} - \Delta U_\alpha \cos\alpha + \Delta U_\beta \cos\beta + \Delta Q \cos\delta\right] \quad (2.16)$$

where m_α is given by

$$m_\alpha = \cos\alpha\left[1 + \frac{\tan\alpha\tan\phi}{F}\right] \quad (2.17)$$

Equations 2.14-2.17 are the expressions that are programmed into **XSTABL**, to calculate the factor of safety for circular surfaces according to the simplified Bishop Method.

2.3 Reinforced Slope Analysis

XSTABL may be used for the analysis and design of steep soil-slopes that are to be reinforced with geogrids or geotextiles. The approach is based on the Coulomb analysis used for the assessment of lateral earth forces for design of frictionless retaining walls. The proposed methodology uses **XSTABL** to analyze the soil slope for the following three conditions :

1. Identification, via a search, of a potential failure surface that requires the greatest external force to maintain stability at a specified, post-construction FOS,

2. Minimum FOS for a critical surface in the unreinforced soil-slope,

3. Delineation of a reinforced zone to satisfy requirements of external stability.

Once the above analyses have been performed, the engineer can then select an appropriate reinforcing system that can provide the required external resistance reported by analysis performed according to item 1, above. The design is completed by ensuring that the reinforcement is adequately embedded beyond the reinforced zone (item 3, above).

If a minimum Factor of Safety (FOS), F_{min}, is specified by the user, the external force required to maintain a specified FOS may be calculated using Eqs. 2.9 (Janbu) and 2.14

(Bishop). The effective normal force, $\Delta N'$, is calculated for both the Bishop and Janbu methods using Eqs. 2.4 or 2.16 with the FOS value specified:

$$\Delta N' = \frac{1}{m_\alpha}\left[\Delta W(1 - k_v) - \frac{\Delta C \sin\alpha}{F_{min}} - \Delta U_\alpha \cos\alpha + \Delta U_\beta \cos\beta + \Delta Q \cos\delta\right] \quad (2.18)$$

where

$$m_\alpha = \cos\alpha\left[1 + \frac{\tan\alpha\tan\phi}{F_{min}}\right] \quad (2.19)$$

Once the effective normal force is calculated, the new FOS value, $F_{calculated}$, is computed using either Eqs. 2.8 or 2.14 for Janbu's or Bishop's FOS. Typically $F_{calculated}$ will be less than F_{min} if the slope requires reinforcement. Then the magnitude of the external *horizontal* resisting force or moment, **ΔF** and **ΔM**, required to maintain stability with a FOS of F_{min} may be calculated using one of the following:

For Janbu's Method:

$$\Delta F = (F_{min} - F_{calculated})\left[\sum_{i=1}^{n} A_1 + \sum_{i=1}^{n} \Delta N' \sin\alpha\right] \quad (2.20)$$

and for Bishop's Method:

$$\Delta M = (F_{min} - F_{calculated})\, R\left[\sum_{i=1}^{n} A_2 - \sum_{i=1}^{n} A_3 + \sum_{i=1}^{n} A_4\right] \quad (2.21)$$

where A_1, A_2, A_3 and A_4 are the same as defined earlier and R is the radius of the circular failure surface. If Bishop's method is used, the magnitude of the external reinforcing force may be determined for a specified elevational location of this resultant force. The analysis assumes that the reinforcing force is horizontal for both methods.

Then if the moment arm of the reinforcement force is $y_{\Delta F}$, the force will be given by:

$$\Delta F = \frac{\Delta M}{y_{\Delta F}} \qquad (2.22)$$

In **XSTABL**, the user must specify the elevation of the resultant force that simulates the expected reinforcement stress distribution. This elevation is compared to the y-coordinate of the center of the circular surface to find the moment arm, $y_{\Delta F}$ (see Fig. 2.4).

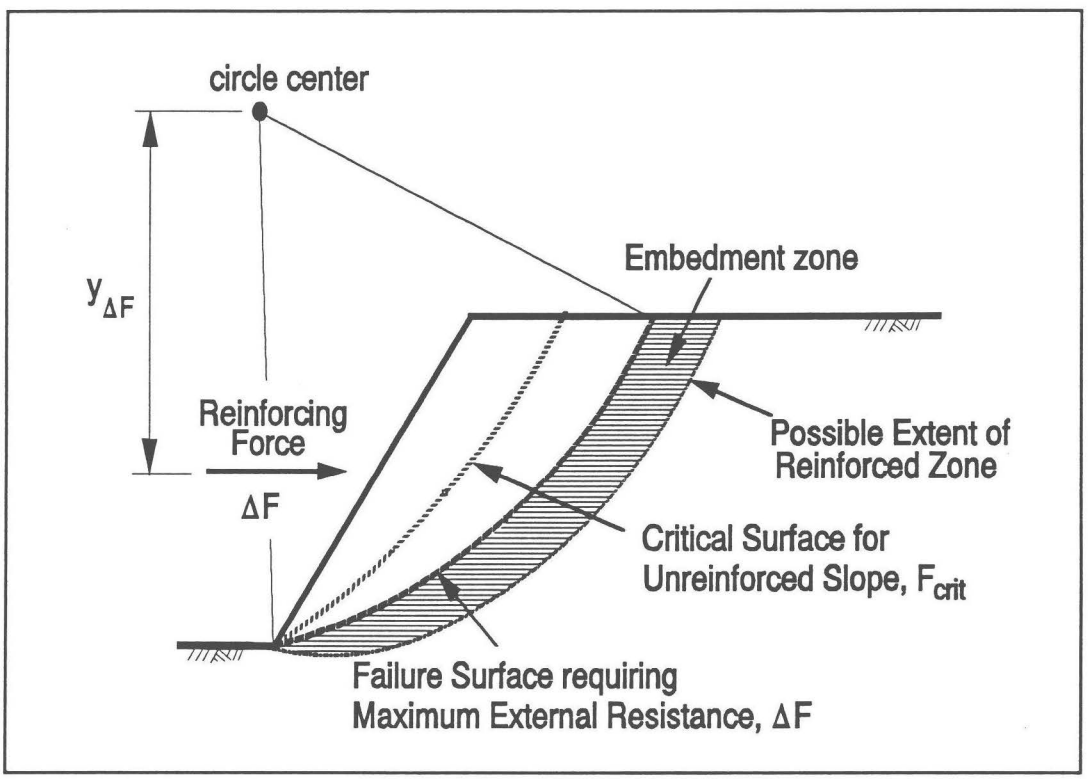

Figure 2.4. Location of critical surfaces for reinforced and unreinforced slope

In order to assess the external stability of the reinforced slope, a reinforced zone is included in the analysis. This zone is specified as consisting of "new" soil units with the strength, ϕ_{reinf} and c_{reinf}, increased to simulate the effects of the reinforcement. The increase in the shear strength parameters is based on the analysis of the unreinforced slope. If the critical FOS value for the unreinforced slope is given by F_{crit}, and the required FOS for the reinforced slope is F_{min}, then the soil strength parameters are modified according to:

$$\phi_{reinf} = \tan^{-1}\left[\frac{F_{min}}{F_{crit}} \tan\phi_{orig}\right] \qquad (2.23)$$

$$c_{reinf} = \frac{F_{min}}{F_{crit}} \left[c_{orig} \right] \qquad (2.24)$$

The user may then manipulate the size of this reinforced zone in order to satisfy the requirements for external stability.

As an initial guidance, the reinforced zone should be selected such that it is at least 3 feet (or one meter) beyond the critical surface identified during the search for the external force, as shown in Fig. 2.4. Once the extent of the required reinforced zone is identified, the user should ensure that the proposed reinforcement extends beyond these boundaries and has adequate pull-out resistance (i.e., embedment).

An example illustrating this approach is presented in Chapter 5.

2.4 Non-linear Mohr-Coulomb Envelope

Most slope stability analyses use a Mohr-Coulomb failure envelope that is linear for ***all*** effective stress ranges. This linearity is simulated by constant shear strength parameters: c' and ϕ'. However, in cases where the strength of the soil, ***in the slope***, is strongly dependent on the normal effective stress, **XSTABL** allows the user to implement a non-linear (or curved) Mohr-Coulomb shear strength envelope. The input data for this option is based on laboratory, or field, test data presented on a conventional σ - τ plot, and consists of simulating the curved envelope with a series of discrete (σ, τ) points. These data points are transformed internally to represent a series of "straight" lines, each with a constant c' and ϕ' over a particular stress range.

The factor of safety computations follow the same order as outlined earlier, but the c' and ϕ' parameters are selected according to the calculated normal effective stresses acting at the base of each slice. This process is repeated until compatibility is achieved between the calculated normal effective stresses and the selected soil strength parameters. Depending on the curved envelope data, these calculations usually require 2 or 3 additional iterations in comparison to calculations based on a linear Mohr-Coulomb envelope.

2.5 Factor of Safety Iteration

The FOS (i.e., variable, F) occurs on both sides of the Janbu (Eq. 2.9) and Bishop (Eq. 2.14) expressions and so the solution is obtained iteratively. This is achieved by assuming an initial F value that is the greater of the following two values :

1. $F = 1.5$, or
2. $F = 1.5 + \tan\alpha \tan\phi$

where α and ϕ correspond to the slice with the largest ***clockwise*** base inclination for slopes that face the positive y-axis. Such a slice is usually located close to the toe of the slope. The iteration procedure uses the initial value to calculate a new FOS value, F_{new}, using Eq. 2.9 and 2.14. For all analyses the initial FOS value is used in the right-hand-side of Eqs. 2.9 and 2.14 to calculate the "F" variable on the left-hand-side of the same equations. This newly calculated "F" value represents a better estimate of the actual FOS. This sequence of operation is repeated with the new "F" value used in the right-hand-side of the expression to calculate another "F" (FOS) value. This iteration is performed until:

(a) the absolute difference between these FOS values, $(F_{new} - F_{old})$, is less than 0.005, or

(b) the procedure has passed through ***twenty-five*** iterations.

If convergence is not achieved within the twenty-five iterations, the user will be informed by an appropriate message in the **XSTABL** output file. In such cases, the coordinates of the trial failure surface will be printed and the FOS value reported for the last iteration. For subsequent sorting of the data, this particular surface will then be purposely assigned a FOS = 500. Such erroneous FOS values are excluded for the preparation of the final summary of the ten surfaces with the lowest factor of safety.

This simple iteration method has been selected due to its robustness and reliability over other iterative methods, due to ease of implementation and overall success in consistently calculating FOS values.

2.6 Control of Negative Effective Stresses

The limit equilibrium method that has been implemented via the "simplified" procedures suggested by Bishop and Janbu can sometimes lead to numerical difficulties that are manifested by **negative** normal effective stresses calculated along the failure surface using:

$$\sigma' = \frac{\Delta N'}{b \sec\alpha} \qquad (2.25)$$

$$= \frac{\cos\alpha}{b m_\alpha} \left[\Delta W(1 - k_v) - \frac{\Delta C \sin\alpha}{F} - \Delta U_\alpha \cos\alpha + \Delta U_\beta \cos\beta + \Delta Q \cos\delta \right]$$

where

$$m_\alpha = \cos\alpha \left[1 + \frac{\tan\alpha \tan\phi}{F} \right] \qquad (2.26)$$

Negative effective stresses are usually encountered for cases that involve: (1) ***high*** pore water pressures, (2) a combination of thin slices with a low self-weight and a high "c-value", and (3) ***steep*** slice-base angles. Most of these problems are associated with the indeterminacy of the limit equilibrium analysis and the failure to adequately satisfy the conditions for complete static equilibrium.

The influence of negative effective stresses for a slice within the *last five percent of the total number of slices* near the crest of the failure surface being analyzed are neglected by **XSTABL**. This criteria has been established on the basis that the upper portion of a failure mass may pass through a potentially *cracked* zone. For such cases, **XSTABL** "ignores" the strength contribution of these last few slices (i.e., sets shear strength to zero), if calculations reveal a negative normal effective stress. An error is ***not*** reported for such cases.

If a ***negative*** effective normal stress is calculated and the slice is not within the last five percent of the total number of slices, **XSTABL** examines the scenario and attempts to correct the problem if the negative stresses are due to excessively high pore water pressures. In such cases, the *total* normal stress is computed by adding the pore water pressure to the calculated effective stress. If this results in a positive total stress, it is concluded that the pore water pressures are excessive and the effective stress is set to ***zero***. This control essentially "reduces" the calculated pore water pressure at the base of the slice, thus eliminating the

negative effective stress that had been computed initially. If such a correction is made for any potential failure surface during the analysis, an explanatory warning message is written to the output file.

If control of excessive pore water pressures fails to eliminate the computed negative effective stress, **XSTABL** concludes that the combination of a small ΔW and a relatively large ΔC component in Eq. 2.26 is the problem. In this case the user is cautioned on-screen and asked to select one of the following three options:

Option-1: Proceed with analysis, but enforce the condition that the Mohr-Coulomb shear strength, $\tau = c' + \sigma' \tan\phi$, is ***always*** greater than or equal to zero.

Option-2: Proceed with analysis without any restrictive conditions concerning the computed shear strength;

Option-3: Proceed with the analysis, but only retain and summarize the factor of safety values for surfaces that did not have any calculated negative effective stress values (i.e., within the initial 95 percent of slices). *However, the parameters of the erroneous surface (and its FOS based on unrestricted ΔS values) are written to the **XSTABL** output file for information.*

The selected option remains in effect for the current analysis only. For subsequent analyses, the user will be prompted to make a "fresh" selection. An error message, ERROR #48, is written to the output file followed by an explanatory message indicating the option that was selected for the subsequent analysis.

In selecting option (1), the assumption that all slices have the same FOS such that the shear strength, ΔS, given by

$$\Delta S = \frac{\Delta C + \Delta N' \tan \phi}{F} \geq 0 \qquad (2.27)$$

will be violated if ΔS is arbitrarily adjusted to ensure that it is not less than zero. This restriction implies that for the cases where ΔS would have been less than zero, the FOS for the slice is implicitly increased to infinity to ensure zero shear strength. This assumption implicitly contradicts the FOS value used in Eq. 2.26 to calculate $\Delta N'$ that is subsequently used in Eq. 2.28. Although this is offered as the default option for practical convenience, it is important that users recognize the implication of these assumptions. The alternative option (2) does not violate the limit equilibrium assumption of a constant FOS for all slices. Thus it will always generate the lowest factors of safety as the strength mobilized along the failure surface will be a minimum because ΔS may be calculated to be less than zero for some slices.

Please note that the FOS values resulting from the selection of options (1) or (2) will be identical if values of $\Delta S < 0$ are not computed during the analysis. For other cases where $\Delta S < 0$ is computed, the FOS values will be different depending on whether the user selects option (1) or (2). In certain circumstances where unusual geometric conditions exist, significantly different FOS values may be reported by **XSTABL**. Interestingly, it is also possible that if the ϕ-angle for the offending layer is increased, the FOS may be ***reduced*** due to the mobilization of *negative* frictional strength. Two examples illustrating this problem are presented at the end of Chapter 5.

Finally, ERROR # 50 is written to the output file if negative stresses are computed for the rare cases that m_α, calculated using Eqs. 2.5 or 2.17 or 2.27, becomes negative. This informs the user that the negative normal effective stresses were computed due to steep negative angles at the base of the slices near the toe of the slope.

Such errors were not reported in previous versions of **XSTABL** and thus it is possible that previously successful slope analyses may be affected by this additional feature. For compatibility with previous versions of **XSTABL**, users may select Option-2 for Version 3 and option-3 for Version 4.0.

2.7 Comparison of Results with Other Methods

The simplified Bishop and Janbu Methods for slope stability analysis have been used extensively since their presentation in the 1950's. Although Bishop's method fails to satisfy horizontal force equilibrium and Janbu's method does not satisfy moment equilibrium, a factor of safety (FOS) can be readily calculated for most slopes. However, these FOS values may generally differ by up to $\pm$ 15 percent upon comparison with results calculated using procedures that satisfy complete force and moment equilibrium, e.g. Spencer's Method or the Morgenstern - Price Method.

The limit equilibrium formulation leads to a statically indeterminate solution and one cannot directly compare these results with a closed-form *correct* solution. Although a direct comparison between the different methods is not always possible, the FOS value determined using Bishop's Simplified Method for circular surfaces can be expected to differ by less than 5 percent with respect to the more rigorous Spencer or Morgenstern-Price solutions. The Simplified Janbu Method, used for non-circular failure surfaces, generally *underestimates* the FOS, by as much as 15 percent, with respect to the more rigorous methods. However, for some slopes the Simplified Janbu Method may also *overestimate* the FOS value by as much as 5 percent.

A good example comparing the different limit equilibrium methods has been presented by Fredlund and Krahn (1977). The failure surface in the slope shown in Fig. 2.5 was analyzed and the results are presented in Fig. 2.6 as a function of lamda (λ), defined as the ratio of the normal and shear forces acting along the vertical slice boundaries. One can see from this figure that the Spencer and Morgenstern-Price solutions are in good agreement with the simplified Bishop result whereas the simplified and rigorous Janbu FOS values appear to be slightly lower. The two curves labeled F_m and F_f represent the loci of the points corresponding to the FOS and λ value in satisfying static moment or force equilibrium, respectively. The intersection of these two curves provides a unique combination of FOS and λ that satisfies *complete* static equilibrium within the context of the implied assumptions. For a more complete discussion, and comparison, of the slope analysis methods, the reader should refer to the paper by Fredlund and Krahn (1977).

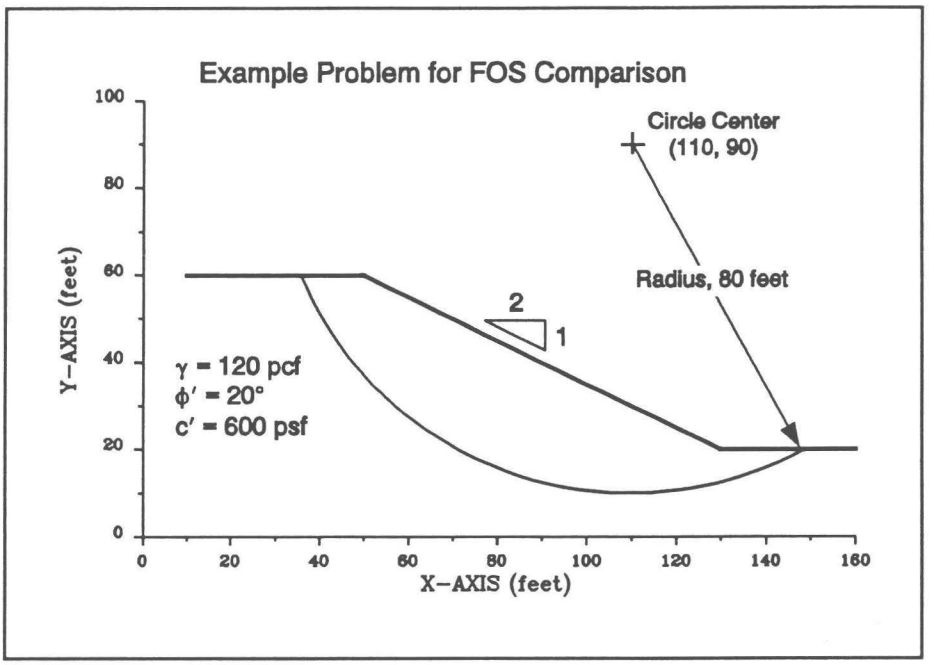

Figure 2.5. Example slope used for comparison of limit equilibrium methods (after Fredlund and Krahn, 1977)

The methods that satisfy complete equilibrium are more complex and subsequently require a ***much*** greater level of understanding for successfully assessing the stability of slopes. The user should note that the numerical difficulties experienced with the Simplified Bishop (or Janbu) methods usually lead to much more serious problems in the Spencer or Morgenstern-Price procedures. These numerical problems often intensify and may lead to unreasonable FOS values and an unrealistic thrust line. Such numerical difficulties generally limit the use of these more complex methods for the analysis of single surfaces only as these methods do not appear suitable for automatic surface generation and analysis.

Some of these problems related to the Spencer's Solution are discussed in Chapter 6.

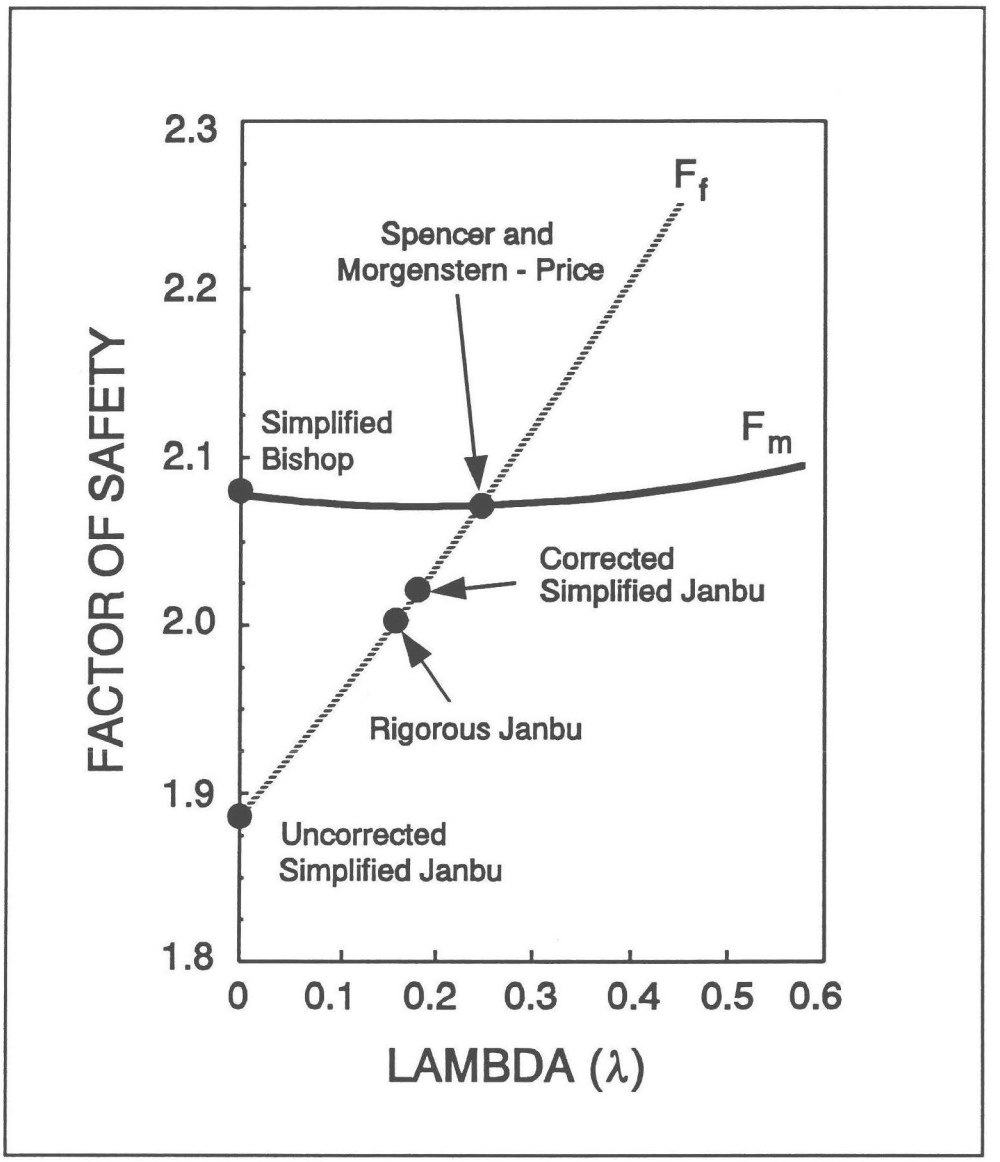

Figure 2.6. Comparison of FOS values calculated using different limit equilibrium methods. The Morgenstern-Price solution uses a uniform distribution of λ. (after Fredlund and Krahn, 1977)

CHAPTER 3

SEARCHING TECHNIQUES

XSTABL implements the three trial surface generators programmed into STABL4 with some modifications that improve their overall reliability. These automatic generators can provide: (1) circular, (2) noncircular, or (3) block shaped surfaces for analysis. These greatly facilitate the slope analysis process by automatically generating surfaces that may be subsequently examined with respect to their factor of safety. This is a necessary procedure as a closed form solution for a critical surface with a minimum factor of safety is not available for heterogenous slopes. Once a satisfactory number of surfaces have been examined, the surface with the lowest factor of safety is generally pronounced to be the critical failure surface.

3.1 Random Numbers

All three trial surface generators use a series of pseudo random numbers to develop different surfaces for the stability analysis. These random numbers are generated, in **XSTABL**, using a FORTRAN function presented by Press et al. (1986). This function generates a sequence of real numbers with magnitudes that are uniformly distributed between 0 and 1. The algorithm has been successfully tested to ensure that the random number sequence is not repeated within the first 100,000 calls to the programmed function.

A modification of the original algorithms allows the function to be initialized at the beginning of each analysis. Thus during an **XSTABL** analysis, the same sequence of random numbers will be accessed in ***every instance***, allowing the user to duplicate previous results. However, this does limit the truly "random" generation of surfaces. This is manifested during the analysis by the inability of **XSTABL** to generate additional "new" surfaces without changing the input data.

This would occur, for example, when the user generates and analyzes 200 surfaces, and then follows the same analysis by requesting the analysis of another 100 (say) trial surfaces. However in this case, the first 100 surfaces that were generated in the previous analysis of 200 surfaces would be generated again, leading to a redundant analysis. In such cases, it is recommended that the user change one of the surface generation parameters (e.g. segment length or the initiation / termination limits). With such a change, additional *new* trial surfaces can be generated successfully to supplement a previous analysis.

Within **XSTABL**, the STABL4 methodology is used to effectively generate the segments that form the trial failure surface. The rules and conditions that control the use of the random numbers for the different surface generators is described below.

3.2 Circular Surface Generation

Circular surfaces are generated by using two random numbers only. The first number defines the orientation of the initial (first) segment of the failure surface and the second random number is used to establish the orientation of the remaining segments of the circular surface.

The first random number is used to determine the angle of the initial segment of the failure surface, within user defined upper and lower angular limits, as it is generated in a left to right direction (see Fig. 3.1). Also, a bias in selecting this angle is introduced by using the square of the random number:

$$\theta_1 = \alpha_2 + (\alpha_1 - \alpha_2)\, R^2 \qquad \textbf{(3.1)}$$

where R is the random number and the angles are as defined in Fig. 3.1.

The probability of the location of the initial failure surface segment within an upper and lower angular limit range that has been subdivided into ten equal sectors is illustrated in Fig. 3.2. From this figure, one can see that the introduced bias results in the initial segment being located within the sector closest to the lower angular limit for about 32 percent of the cases. The probability for a segment close to the upper angular limit is only about 5 percent.

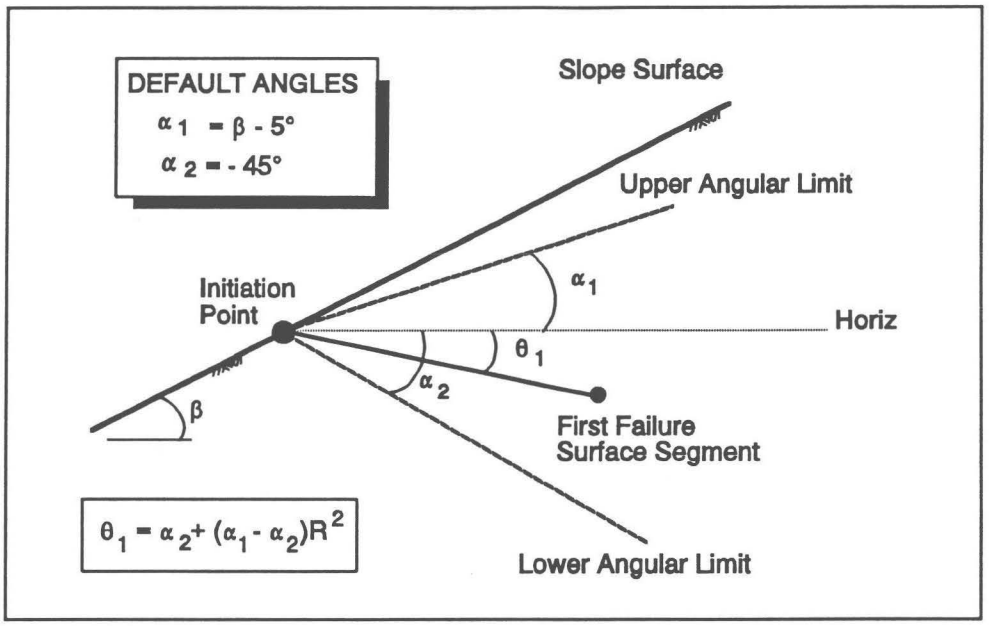

Figure 3.1. Selection of initial line segment for circular surface generation *(angles are measured positive CCW from the horizontal)*

This bias leads to initial segments that are nearer to the lower angular limit and is introduced primarily to obtain trial surfaces that are deeper. During the development of the STABL program, it was found that a poor distribution of the factor of safety values was obtained if the initial segment was given an equal likelihood of being oriented in any direction within the specified angular directional limits.

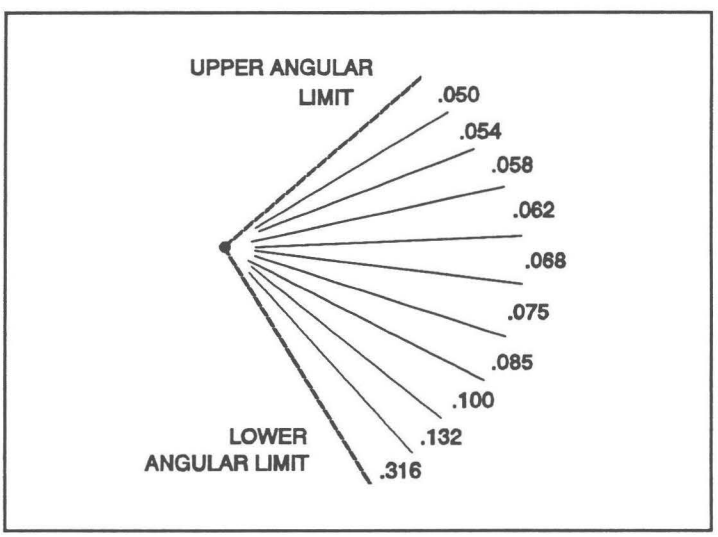

Figure 3.2. Probability of the orientation of the initial line segment for automatic generation of circular and noncircular surfaces.

Once an initial segment is selected, the remaining portion of the proposed circular surface is generated such that it intersects the ground surface within the specified termination range. These circles will all start from the initiation point (near the toe in Fig 3.3), have a common first segment and be confined within the region shown in Fig. 3.3. All such surfaces are generated so that the termination point is always *above* the elevation of the initiation point.

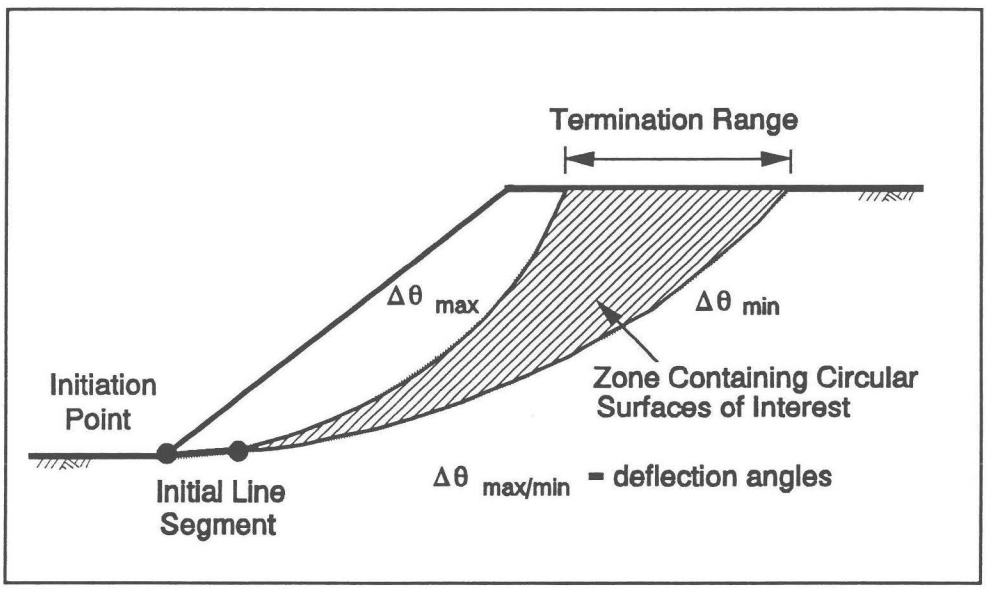

Figure 3.3. Zone of surface generation based on location of initial line segment and the user-defined termination range.

The segments that compose a circular shape have fixed lengths, T, and each successive segment is deflected by a constant angle, $\Delta\theta$, with respect to the preceding segment as shown in Fig. 3.4. The deflection angle may be calculated according to :

$$\Delta\theta = 2 \sin^{-1} \left[\frac{T}{2r} \right] \qquad (3.2)$$

where r is the radius of the circle. The STABL4 algorithms determine this deflection angle, $\Delta\theta$, required to encompass the potential range of the termination limits. In Fig. 3.3 the two angles $\Delta\theta_{max}$ and $\Delta\theta_{min}$ correspond to circular surfaces terminating at the left and right termination range, respectively. Effectively, the $\Delta\theta_{max}$ and $\Delta\theta_{min}$ range corresponds to the shaded area shown in Fig. 3.3 and allows for a random selection of the remaining segments of a circular surface.

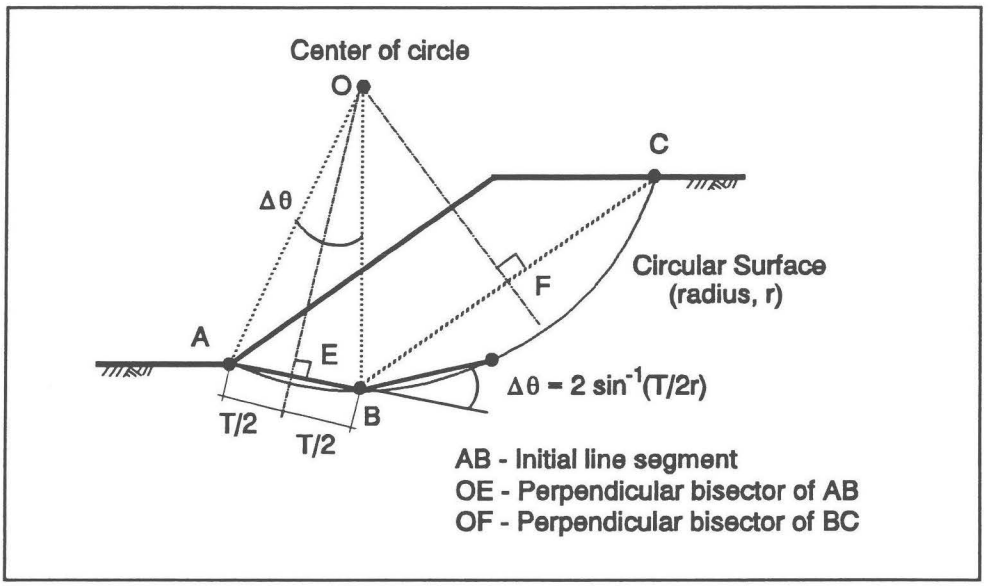

Figure 3.4. Calculation of deflection angles for circular surface generation

The fixed deflection angle, $\Delta\theta$, for the remaining segments is selected within this $\Delta\theta_{max}$ and $\Delta\theta_{min}$ range by using the expression :

$$\Delta\theta = (\Delta\theta_{max} - \Delta\theta_{min})\ R^2 \qquad \textbf{(3.3)}$$

The orientation of each successive segment will then be given by the inclination of the previous segment plus the randomly generated deflection angle,

$$\theta_i = \theta_{i-1} + \Delta\theta \qquad \textbf{(3.4)}$$

The above approach of selecting the orientation of the first segment followed by a deflection angle forms the basis of the circular surface generator in STABL4 and **XSTABL**. However, there are cases where small adjustments have to be made to accommodate the slope geometry and user defined limitation. Such examples are discussed below.

Adjustment of $\Delta\theta$:

1. If $\Delta\theta$ is calculated such that it is less than zero (suggesting a convex surface), it is changed to a minimum limiting deflection angle of 0.0. This corresponds to a planar surface that intersects the ground within the specified termination limits.

2. If $\Delta\theta_{max}$ is less than zero, only convex surfaces may be generated from the initial segment (see Fig. 3.5). In such cases, the upper angular limit is reduced to θ_1, the orientation of the currently selected initial segment, and the search is restarted with a new initial segment to seek a desirable, concave circular surface. This step is repeated until a positive $\Delta\theta_{max}$ value is obtained for the maximum deflection angle.

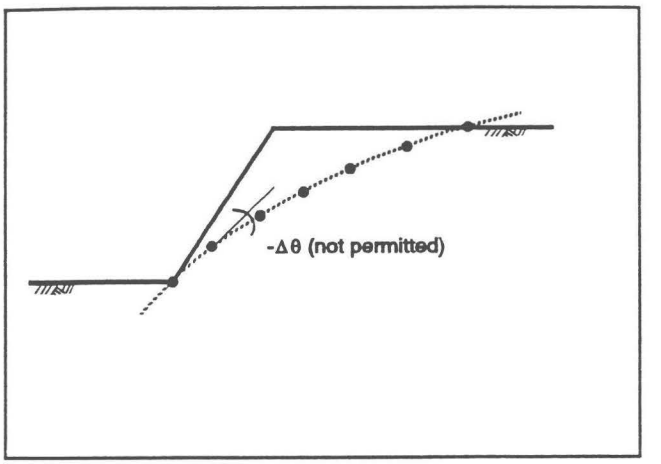

Figure 3.5. Unsuitable convex surface generated by a negative deflection angle.

3. $\Delta\theta_{max}$ is limited to an angle less than 45° as larger deflection angles will lead to a poor approximation of a circular surface (see Fig. 3.6).

4. If $\Delta\theta_{min}$ greater than 45°, the lower angular limit is changed to θ_1, similar to case 2 above, and the search is repeated with a new initial segment for an acceptable $\Delta\theta_{min}$ value.

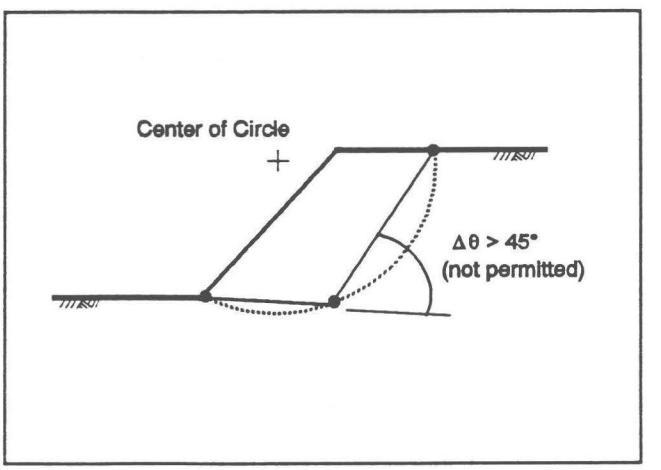

Figure 3.6. Maximum limit for deflection angle for generation of suitable circular surfaces.

5. An overturned shear surface may be generated if the center of the circle is below the elevation of the termination range, as shown in Figure 3.7. This problem is avoided by reducing $\Delta\theta_{max}$ such that a circle center corresponding to the left termination limit is at least T/2 above the elevation of the termination range (Fig. 3.8). The overall effect of this feature is to move the left termination limit to the right.

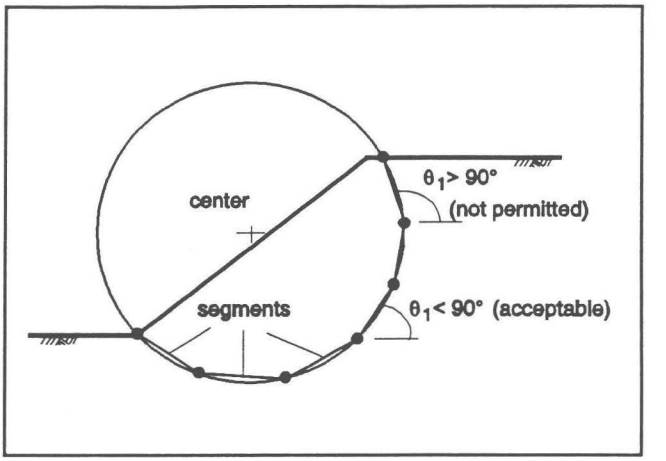

Figure 3.7. Unsuitable, reversed surface with upper line segment orientations exceeding 90°.

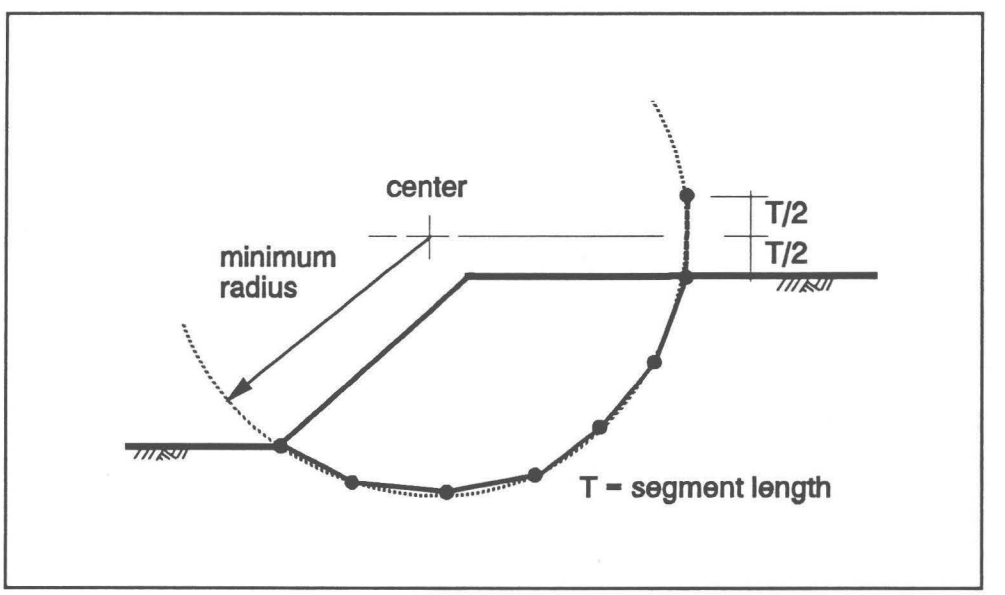

Figure 3.8. Limitation imposed on elevation of circle center for generating suitable surfaces.

6. If overturned surfaces may be generated for segments passing through the right termination limit the lower angular limit is changed to the current initial segment orientation, θ_1, and the search process repeated with a new initial segment.

7. If the assigned lower angular limit, α_2, prevents a successful generation of the initial segment (Fig. 3.9), the value of α_2 will be adjusted to allow generation, accordingly.

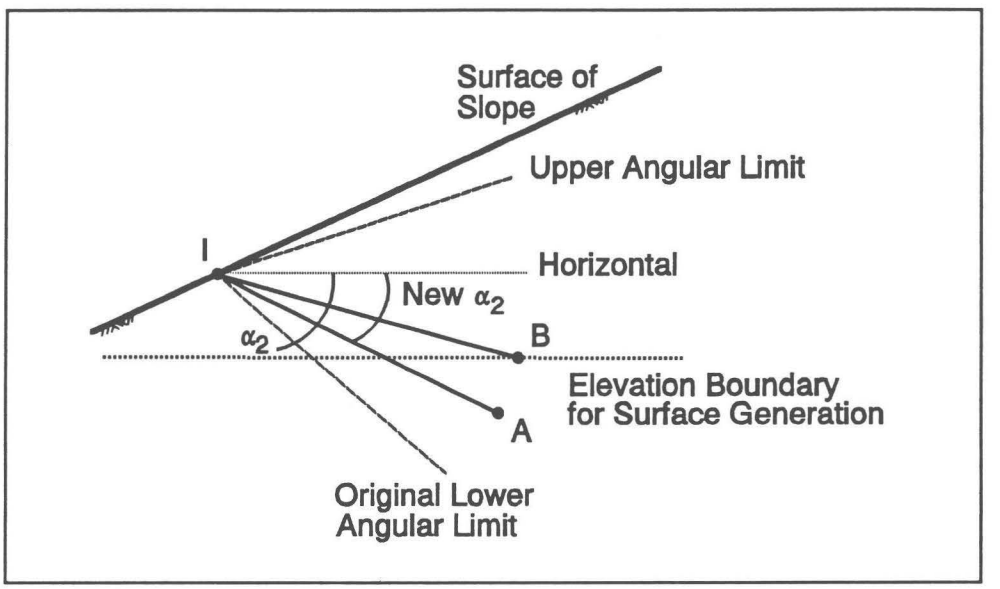

Figure 3.9. Adjustment of lower angular limit if an elevational boundary prevents successful generation of the initial line segment.

8. If a segment impinges into a user defined boundary, $\Delta\theta_{min}$ is adjusted to allow space for surface development. However, if this results in $\Delta\theta_{min} \geq \Delta\theta_{max}$, the lower angular limit, α_2, is adjusted until a satisfactory surface is generated.

9. If segments intersect a lower boundary, the algorithms check to ensure that a surface can indeed be successfully generated by using $\Delta\theta_{max}$ as the deflection angle from the initial segment. If a surface is possible, the search process is continued with a new initial line segment. However, if a surface cannot be generated with $\Delta\theta_{max}$, $\Delta\theta_{min}$ is changed to the deflection angle, $\Delta\theta$, of the surface that originally intersected the boundary. The process is then continued with the selection of a new deflection angle within the newly defined $\Delta\theta_{min}$ - $\Delta\theta_{max}$ range. This has the same effect as moving the right termination limit to the left.

10. For intersection with upper boundaries, the adjustment is similar except that the $\Delta\theta_{min}$ value is used to determine if any surfaces can be successfully generated. If an intersection does occur, the $\Delta\theta_{max}$ value is adjusted to $\Delta\theta$ in an attempt to continue generating desirable surfaces.

3.3 Irregular Surface Generation

The initial segment of an irregular surface is generated in the same manner as that employed for the circular surface. The remaining trial surface segments are generated sequentially, from left to right, using randomly generated deflection angles.

A narrow angular range is randomly determined and then a deflection angle is calculated within this range to generate the next trial surface segment. This angular range extends 45° CCW and 18 R^2 ° CW from a line produced as an extension of the previously generated trial surface segment. This is illustrated in Fig. 3.10, which shows the generation of a new segment **AB** from the end of the initial segment **IA**.

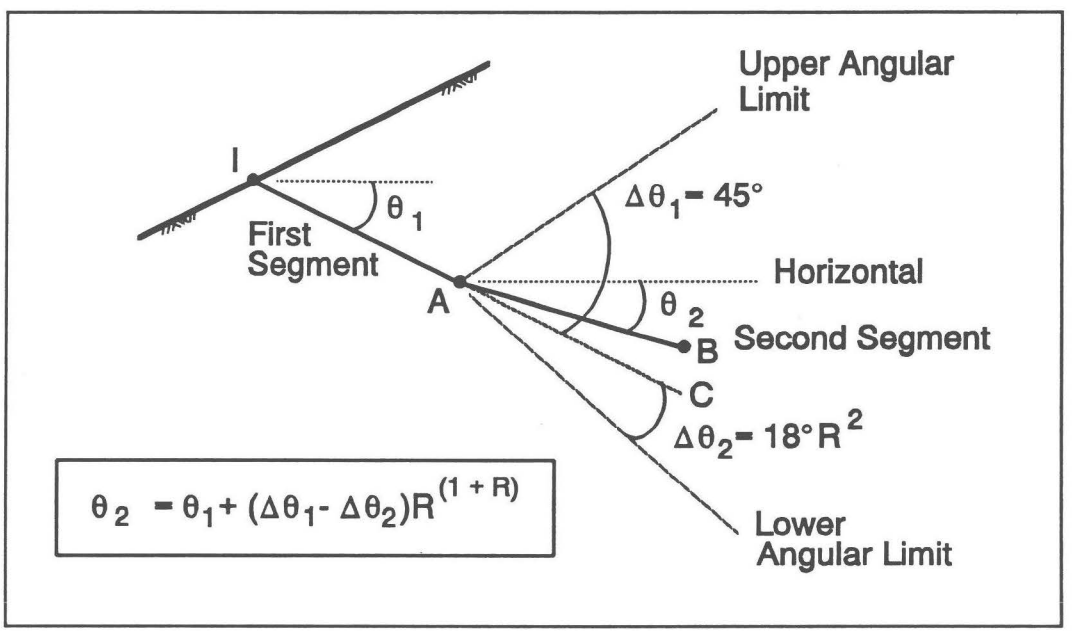

Figure 3.10. Orientation of line segments for irregular surface after generation of initial line segment.

An adjustment to the CCW angular range, $\Delta\theta_1$, is made if the inclination of the previous trial surface segment is greater than 45°. This effectively prevents the possible generation of a vertical segment by limiting the CCW range.

A random number is then used to select the orientation angle, θ, within this angular range according to:

$$\theta = \theta_2 + (\Delta\theta_1 - \Delta\theta_2)\ R^{(1+R)} \qquad (3.5)$$

This tends to favor angles that are closer to the inclination of the previous trial surface segment. The allowable CCW angular range ($\Delta\theta_1$) is 45° compared to the 0° to 18° CW range ($\Delta\theta_2$), as measured from a projection of the previous segment. Thus there is a greater probability that a majority of positive deflection angles will be generated by the algorithm. These positive angles will generate a desirable surface that is predominantly concave with a few convex "kinks".

The irregular surface generator is more computer intensive than the circular or block surface generators as there is no prior knowledge regarding whether the surface will :

(a) intersect the ground surface within the specified termination limits, or

(b) intersect an upper or lower boundary, or

(c) intersect a lower elevational boundary.

If any of the above conditions is violated, the current surface being generated is discarded for most cases and a search for a another viable surface is started with a new initial segment. Hopefully, the next sequence of random numbers will then permit a surface to be generated successfully.

Minor adjustments, similar to the circular surface generator, are also made for the irregular surfaces.

(a) If a segment extends beyond the right termination limit or intersects the specified minimum elevation (i.e. a boundary), the possibility of successfully bypassing the boundary is checked by using a deflection angle equal to $\Delta\theta_1$. If the boundary can be bypassed, the CW limit is adjusted to 0° and a new deflection angle is selected within the CCW angular range. However, if the segment still intersect the boundary, it is rejected and a new search started.

(b) If a segment intersects an upper or lower boundary, procedures similar to those listed above are used to adjust the CCW or CW angular ranges, accordingly.

In order to reduce the number of segments needed to complete a failure surface, the user should try to use large segment lengths, preferably in the range H/4 to H/3, where H is the maximum elevational difference between the initiation and termination ranges. With such lengths, the chances of generating unsuitable surfaces are reduced considerably.

Users should note that the **XSTABL** algorithms generate a smoother transition than the original STABL program by limiting the clockwise angular range to a maximum of 18° rather than the 45° used in STABL4. This effectively eliminates the overly "kinky", reversed surfaces that were generated with larger negative deflection angles.

3.4 Block Surface Generation

XSTABL offers the same two methods for generating block shaped surfaces as used in STABL4. This option is recommended for cases where the user wishes to generate trial surfaces that closely follow a relatively "weak" layer. This option is also suitable for analyzing translational slope failures which often tend to follow the soil-rock interface.

The block surfaces are developed by connecting points that have been randomly selected within user specified **search boxes** as shown in Fig. 3.11. The generated block surfaces consist of three distinct portions: (1) passive block, (2) central block and (3) active block, as shown in Fig. 3.11.

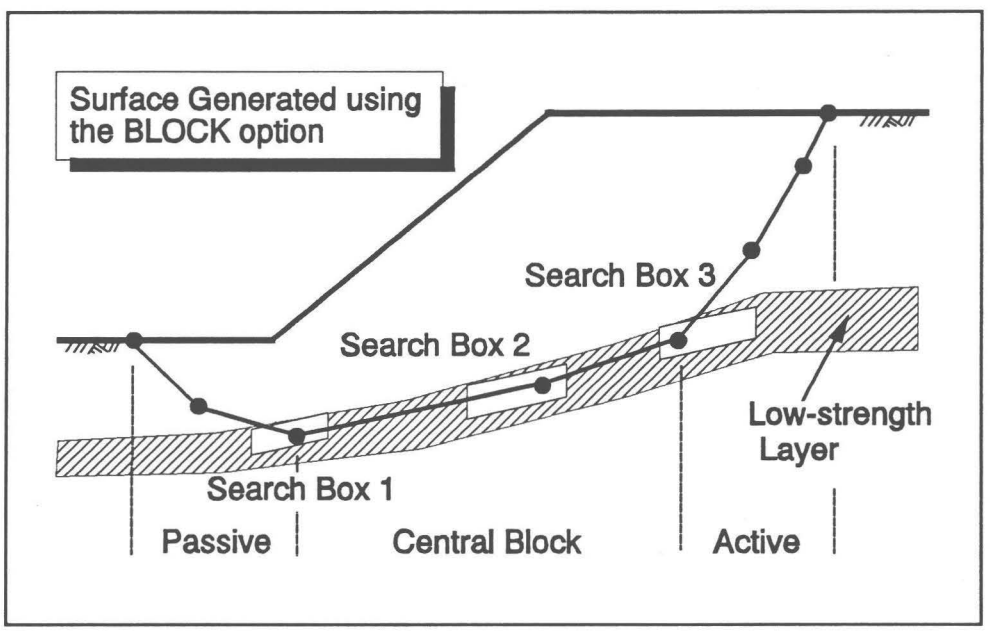

Figure 3.11. Generation of block-shaped surfaces through a low-strength soil layer using three search boxes.

For both the **Rankine** and **Block** options, the central block is generated by:

1. Randomly selecting an x-coordinate within the horizontally defined boundaries of the search box as:

$$x = x_{left} + R_1 \left[x_{right} - x_{left}\right] \tag{3.6}$$

2. Randomly selecting a y-coordinate within the specified boundaries of the search box according to :

$$y = y_{left} + R_1 \left[y_{right} - y_{left}\right] + H \left[R_2 - 0.5\right] \tag{3.7}$$

where R_1 and R_2 are random numbers and H is the height of the search box.

Although the central block for these surfaces are the same for the two options, the active and passive wedges are generated differently. The central block is generated first and is then followed by generation of the passive and active wedges. The passive wedge is generated from the leftmost search box and the active wedge extends upwards from the righmost search box.

Rankine Wedges

These are generated according to the assumption that the limiting surface will be a function of the angle of internal friction (ϕ) of the soil. Thus for the passive wedge, the failure surface segments will be inclined at (45 + ½ϕ) degrees, CCW from the vertical, as shown in Figure 3.12. Similarly, the failure surface segments for the active wedge will be inclined at (45 − ½ϕ) degrees, CW from the vertical. In slopes with multiple soil layers, the inclination of the failure surface segments for the passive and active wedges will vary according to the ϕ-values of each soil unit.

For cases where the Rankine passive or active failure surface passes through a soil layer that is defined by either anisotropic or curved Mohr−Coulomb strength parameters, the ϕ-value is selected from the value defined for the isotropic properties.

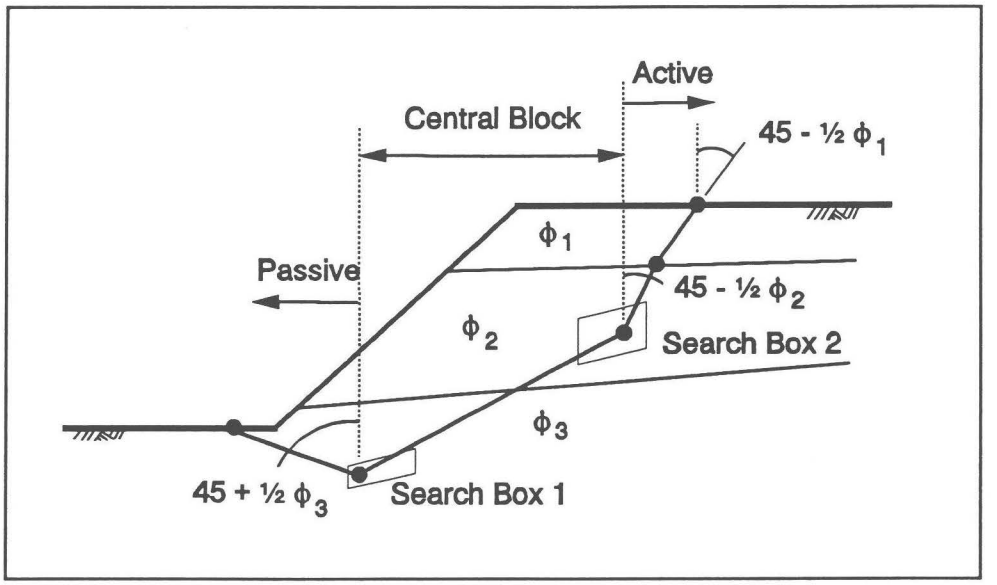

Figure 3.12. Rules used to generate the active and passive line segments for RANKINE option.

Block Wedges

This option develops the passive and active wedges of the failure surface (see Figure 3.13) using an approach that is similar to the generation of irregular surfaces. The passive portion is generated by randomly selecting a segment inclination that ranges between 0° and −45°, measured CCW from the horizontal according to the equation shown below:

$$\theta = (-45 + 45R^2)° \tag{3.8}$$

The active portion of the block surface is similarly generated using :

$$\theta = (45 + 45R^2)° \tag{3.9}$$

The user must exercise care in selecting the segment length for the **Block** option as small value may result in the generation of an admissible surface.

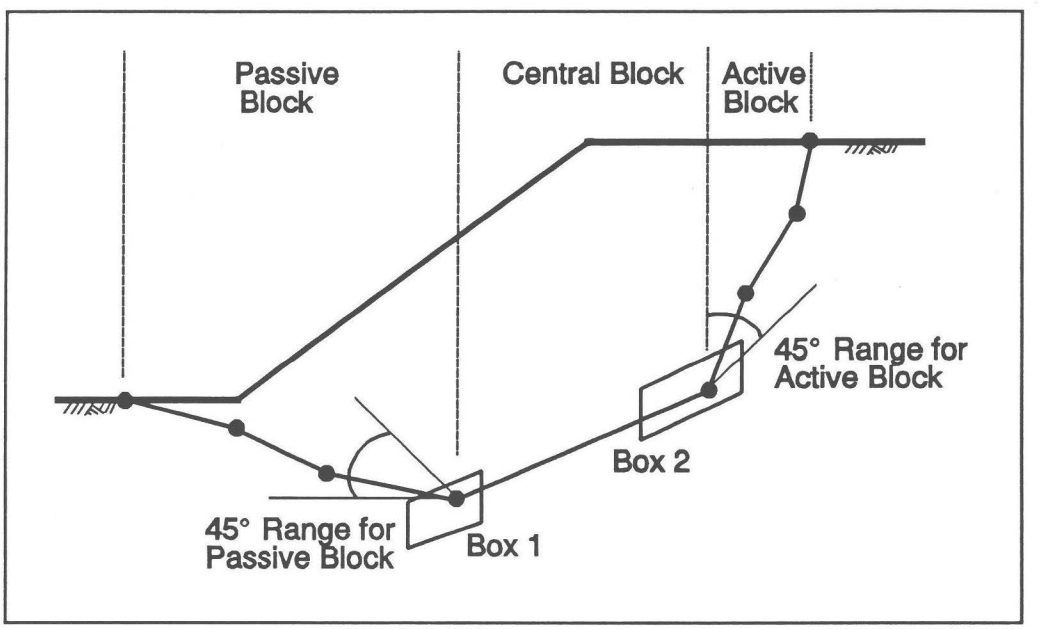

Figure 3.13. Rules used to generate the active and passive line segments for the BLOCK option.

Search Boxes

The dimensions of the search boxes may be manipulated to control the location of the search area through which **XSTABL** will generate potential failure surfaces. At first glance, it appears that the user is asked to specify trapezoidal shaped search boxes. However, the dimensions of these boxes can be specified to simulate a line or a point through which all generated surfaces must pass.

"Line Boxes": Figure 3.14 shows a search box which reduces to a line as the side length has been specified as zero. The use of this method is very effective for cases where the failure surface is expected to follow a "thin", low strength soil layer or a soil-rock interface. Appropriate use of the side length and the left and right side coordinates allow the user to generate a "line-box" of any length and at any required orientation.

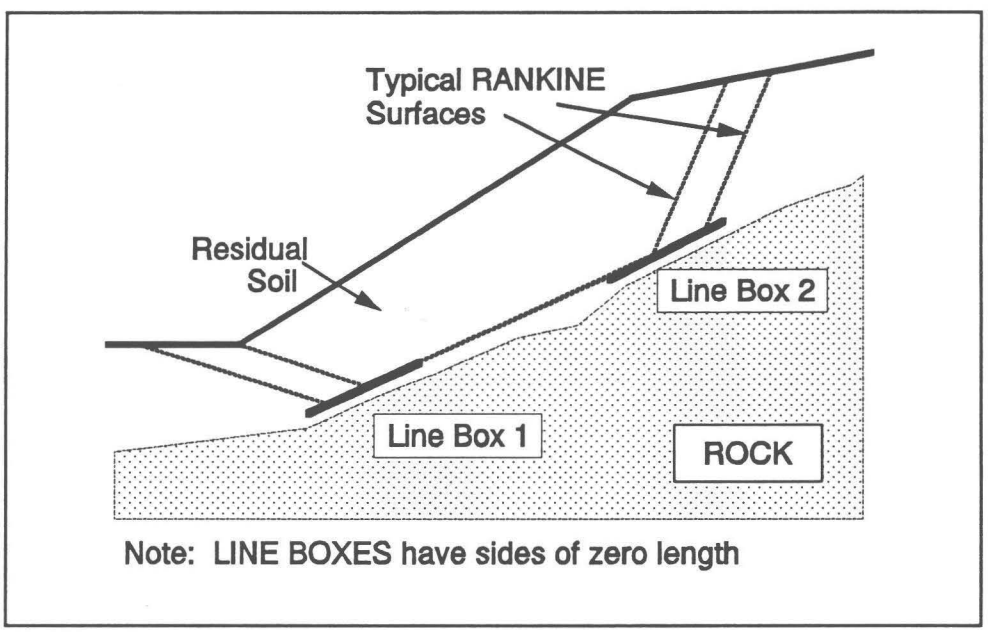

Figure 3.14. Suggested use of a "LINE" box that is simulated with a side height of zero.

"**Point Boxes**": Figure 3.15 shows a case where the coordinates of the left and right middle points of the specified search boxes are the same, and the side length has also been specified as zero. With these dimensions, the trapezium reduces to a point. This powerful technique forces all generated failure surfaces to pass through a point. In the example illustrated in Figure 3.15, "point-boxes" located near the surface boundary at two locations effectively force all failure surfaces to start and end at the same locations on the slope.

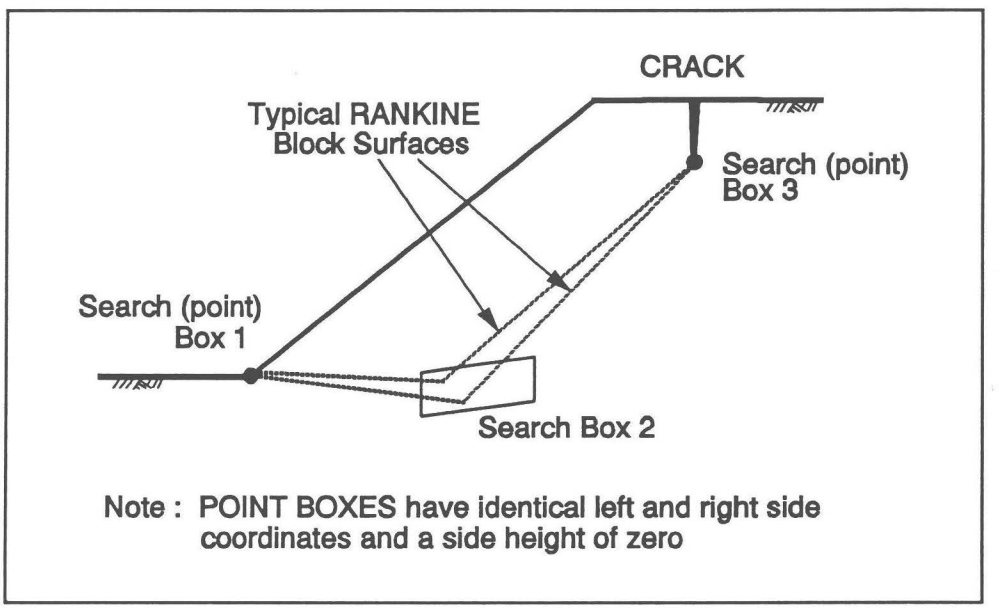

Figure 3.15. Suggested use of a "POINT" box that is simulated by specifying a side height of zero and identical (x, y) coordinates for the left and right sides.

NOTE

Please note that if a lower limiting boundary is specified along with search boxes for the Rankine-block analysis, the limiting boundary is neglected by **XSTABL**. Thus if search boxes have been established so that they overlap a lower limiting boundary, the user cannot expect **XSTABL** to implicitly only generate surfaces that do not penetrate this limiting boundary. If a limiting boundary, along with search boxes for a Rankine-block search, is specified, an explanatory warning message will be written to the output file.

CHAPTER 4

DETERMINATION OF SLICE DATA

Once a potential failure surface has been generated, or specified by the user, the method of slices may be used to determine the factor of safety. In this chapter, the various parameters that define the slices are discussed along with the approach used to discretize the slope mass into slices.

4.1 Determination of Slice Widths

The slide mass is divided into slices with vertical sides according to the specified slope geometry and the potential failure surface. The location of vertical sides will occur at:

1. each specified x-coordinate used to define the surface and subsurface boundaries located directly above the failure surface under analysis,

2. each x-coordinate of the specified water surfaces that are likely to affect the slide mass,

3. each intersection of a water surface and subsurface boundary,

4. each intersection of the failure surface segments with a subsurface boundary or water surface,

5. each lateral boundary used to define a surface surcharge load.

The above criteria will result in slices that have straight sides, and may include several soil types and the effects of different water surfaces. All these specific effects will be simulated by boundaries that are straight lines between the left and right hand sides of each slice.

Thus if a user wishes to have many slices generated (within an overall maximum of 100 slices), a small failure segment length and many slope geometry coordinates will result in the use of a large number of slices. However, this will also directly affect the time required for performing the computations. On the basis of the author's experience, a slide mass discretized into more than twelve slices is likely to lead to reliable results for most soil conditions.

4.2 Calculation of Slice Weight

The program determines the soil types that are contained within any slice mass and determines the total weight according to the specified unit weights. These weights are selected according to the following:

1. Soil Unit completely above its associated water surface -- use the moist unit weight,

2. Soil Unit completely below its associated water surface -- use the saturated unit weight,

3. Soil Unit intersected by a water surface -- the weight of the material above the phreatic surface will be based on the "moist" unit weight while the weight of the material below the intersecting water surface will be calculated according to the "saturated" weight.

The user should note that a piezometric line is NOT the same as a phreatic line. The use of saturated and moist unit weights with a specifiied piezometric line has been implemented into **XSTABL** for the convenience of the user. For typical cases, the saturation line, corresponding to the phreatic line, will be slightly above the piezometric surface.

4.3 Pore Pressure Calculations

The forces at the base of a slice due to pore water pressures may be simulated in **XSTABL** by employing one of the following methods:

1. ***Phreatic Surface***: This surface, or line in two dimensions, is defined by the free groundwater level. This surface may be delineated, in the field, by using open standpipes as monitoring wells. This is the most commonly programmed method available.

2. ***Piezometric Data***: Specification of pore pressures at discrete points, within the slope, and use of an interpolation scheme to estimate the required pore water pressures at any location. The piezometric pressures may be determined from :

   (1) field piezometers,
   (2) a manually prepared flow net, or
   (3) a numerical solution using finite differences or finite elements.

   Although, this approach is only available in a few slope stability programs, it is the best method for describing the pore water pressure distribution.

3. ***Pore pressure ratio***: This is a popular and simple method for normalizing pore water pressures measured in a slope according to the definition:

$$r_u = \frac{u}{\sigma_v} \qquad \textbf{(4.1)}$$

   where u is the pore pressure and σ_v is the vertical subsurface soil stress at depth z. Effectively, the r_u value is the ratio between the pore pressure and the total vertical stress at the same depth. The normalized data is then available for developing correlations, e.g. see Sherman and Clough, 1968; Leonards and Humphrey, 1984 for a summary of pore pressure data from earth dams during construction.

   This factor is easily programmed, but the major difficulty is associated with the assignment of the parameter to different parts of the slope. Often, the slope will require an extensive subdivision into many regions with different r_u values. This method, if used correctly, will permit a search for the most critical surface. However, it is usually reserved for estimating the FOS value from slope stability charts or for assessing the stability of a single surface, as presented in the example problem.

4. ***Piezometric Surface***: This surface is defined for the analysis of a unique, single failure surface. This approach is often used for the back-analysis of failed slopes. Because the combination of a piezometric and a failure surface is unique, a search for the critical surface is not possible. The user should note that a piezometric surface is NOT the same as a phreatic surface, as the calculated pore water pressures will be different for the two cases.

5. *Constant Pore Water Pressure*: This option is available if the user wishes to specify a constant pore water pressure in any particular soil layer. This may be used to examine the stability of fills placed on soft-soils during construction where excess pore water pressures are generated according to the consolidation theory.

Phreatic Surface

If a phreatic surface is defined, the pore water pressures are calculated for the steady state seepage conditions according to the sketch shown in Fig. 4.1. This concept is based on the assumption that *all* equipotential lines are straight and perpendicular to the segment of the phreatic surface passing through the discretized slice.

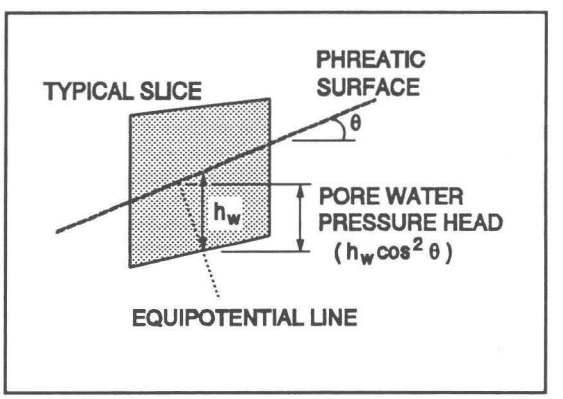

Figure 4.1, Calculation of pore water pressure head from defined phreatic surface

Thus if the inclination of the phreatic surface segment is θ, and the vertical distance between the base of the slice and the phreatic surface is h_w, the pore pressure is given by:

$$u = \gamma_w (h_w \cos^2\theta) \qquad (4.2)$$

where γ_w is the unit weight of water. This is the easiest approach that can be readily programmed and the phreatic surface may be defined with minimal data.

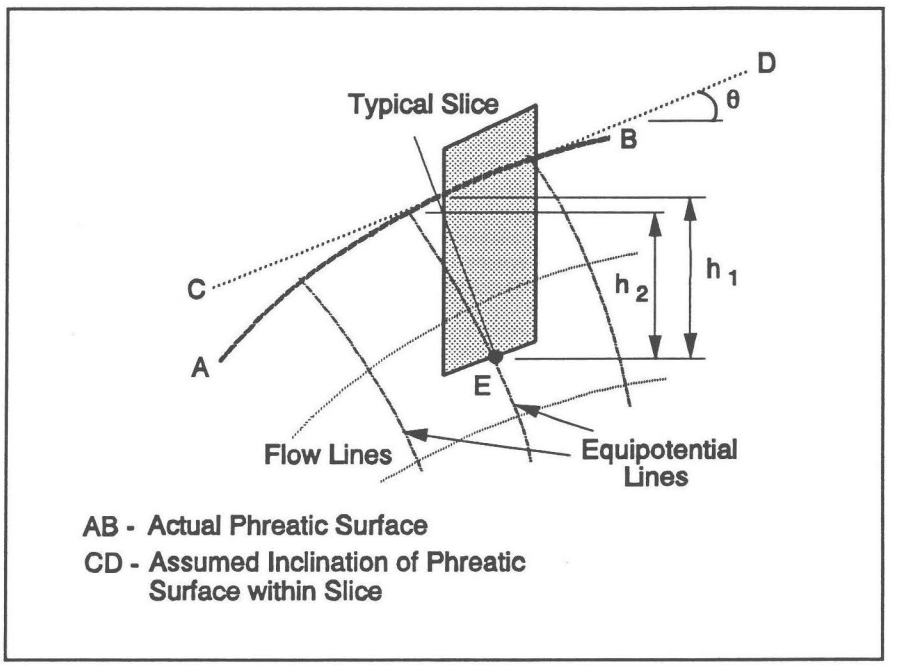

Figure 4.2, Phreatic surface and curved equipotential lines

This is a reasonable assumption for a sloping *straight-line* phreatic surface, but will provide ***higher*** or ***lower*** estimates of pore water pressure for a curved (convex) phreatic surface. For the steeply sloping phreatic surface, a convex-shaped phreatic surface (as shown in Fig. 4.2) generates an overestimate of the pore water pressures whereas a concave-shaped surface may lead to an underestimation. This feature is shown in Figure 4.2. This over estimation is entirely due to the assumption of straight equipotential lines intersecting the projected phreatic surface line, CD. If the actual phreatic surface (line AB) is steeply curved, the equipotential lines must also curve, as shown. In this example, **XSTABL** would use the *greater* pore water pressure head $\mathbf{h_1}$ rather than the true head, $\mathbf{h_2}$. However, this over-estimation is small and will only affect a few slices within the sliding mass. Also, this conservatism is not expected to significantly affect the Factor of Safety.

In cases where the user is concerned about this problem, the pore water pressure grid option may be used to simulate the pore water pressure distribution more accurately.

Piezometric Surface

A piezometric surface may be specified to correspond to a single, ***unique*** failure surface in the slope. This feature is typically used to back-analyze slope failures where the pore water pressures may have been determined from insitu measurements. Fig. 4.3 shows the approach taken to calculate the pore water pressure for a piezometric surface.

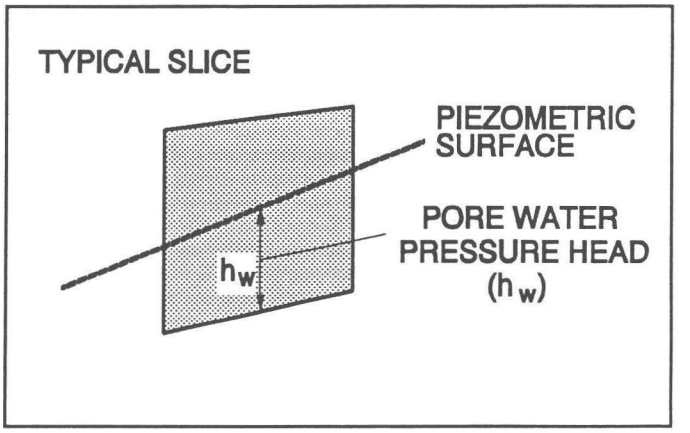

Figure 4.3, Calculation of pore water pressure head for specified piezometric surface

The user should note that the vertical distance (elevational head) is taken to represent the pressure. Also, if a piezometric surface is located above the slope surface, a water surcharge is ***not*** included in the analysis. If the user wishes to include such a surcharge, boundary loads may be specified to simulate these external loads. If a phreatic (water) surface has been specified for the surficial soils, a hydrostatic surcharge is automatically included in the analysis.

There are some computer programs that over simplify the problem by incorrectly assuming the phreatic surface as a piezometric surface. With this erroneous assumption, the over estimated pore water pressure head is incorrectly taken as the vertical distance between the phreatic surface and base of slice, as illustrated in Fig. 4.2, rather than the correct approach presented in Fig. 4.1. An example displaying the effects of this error is given in Chapter 5.

Pore Pressure Grid

If the pore water pressures are specified at discrete points within a slope, an interpolation scheme is required to estimate the pressures at the required locations. The method proposed by Chugh (1981) provides realistic results and is sufficiently robust to be used within a search procedure for locating the critical failure surface. Other methods based on a weighting scheme may fail to realize consistent results and may, in some circumstances, calculate unrealistic pore pressures.

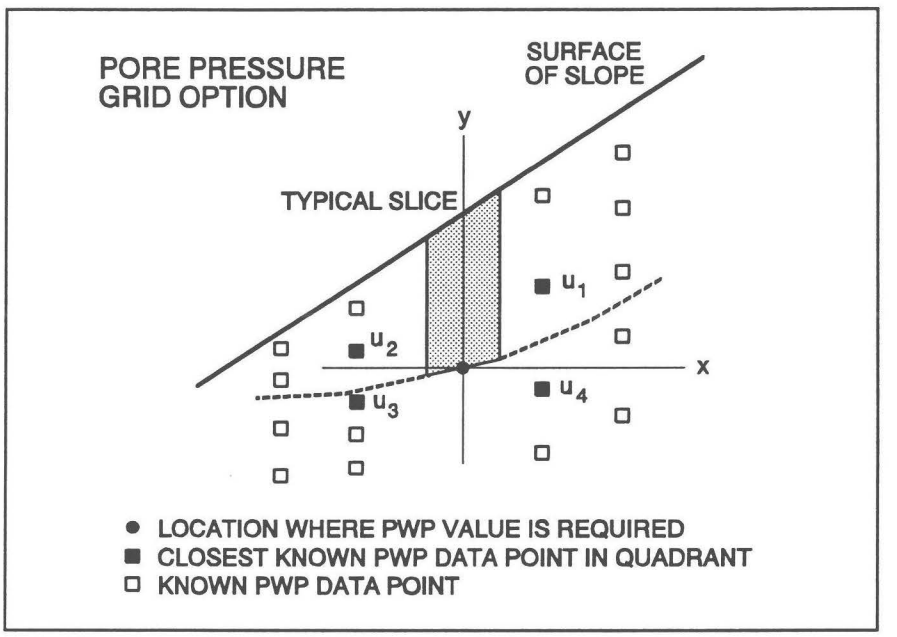

Figure 4.4. Pore water pressure based on interpolation

In Chugh's method, the pore pressures at the required points along the potential failure surface are estimated using an interpolation scheme that uses the "closest" values in each of the surrounding four quadrants. The approach is illustrated in Fig. 4.4. The origin, in this figure, represents the location of the point where the pore water pressure is required and which typically would be at the center of the base of each discretized slice. The closest data points in each of the four quadrants (U_1, U_2, U_3, and U_4) are extracted from the input data and the transformed coordinate locations: (x_1, y_1), (x_2, y_2), (x_3, y_3) and (x_4, y_4) computed using the center of the slice base as the origin, i.e. $x_i = x - x_c$, where x_i is the transformed coordinate and x and x_c are global coordinates of the known pore water pressure point and base center, respectively.

The interpolation scheme fits a flat surface to three of the known values, and then estimates the pore pressure at the origin (0, 0). The fitted surface is used to estimate the pore pressure and will take the form:

$$U = a_1 + a_2 x_1 + a_3 y_1 \qquad (4.3)$$

The three coefficients, a_1, a_2 and a_3 ,be evaluated for three known points and the pore water pressure at the unknown point (origin) will be equal to a_1. This calculation is repeated four times, each time using a different combination of a set of three known values. The pore pressure value used in the calculations is the average of the four estimated values.

Some similar interpolation schemes may use a *warped* surface, fitted through four known points, to estimate the pore water pressure. This higher order surface takes the form :

$$U = a_1 + a_2 x_1 + a_3 y + a_4 xy \qquad (4.4)$$

where the coefficients, a_1 , a_2 , a_3 and a_4 , may be calculated on the basis of the four known values of pore pressure and their transformed locations relative to the center of the slice base. Unfortunately, this expression does not behave consistently and incorrect pore pressures, either larger or smaller than the surrounding known values, may be calculated with this approach. However, Chugh's method will calculate pore pressure values within the range defined by the surrounding known values: (U_1, U_2, U_3, U_4).

4.4 Submerged Slopes

If part of a slope is submerged, the effect of the surficial water is simulated by a water force acting normal to the inclination of the top of the slice ***only if a water surface is defined as a phreatic surface for the uppermost soil unit within the slice.*** The magnitude of this force is based on the weight of water located directly above the slice in question.

For cases where only a piezometric surface is employed, submerged water forces will have to be implicitly simulated with surface boundary loads. **XSTABL** does not generate such hydrostatic forces for the case where a piezometric line is located *above* the top of the slice. For such conditions, the user can define a thin surface layer, under the submerged water, and then assign a *phreatic* water surface to the soil unit within this layer.

4.5 Earthquake Loads

Once the slices have been discretized according to the slope geometry, the pseudo-static earthquake loads are applied using the specified seismic coefficients. These loads are applied at the centroid of the slice, in the vertical and horizontal directions. The applied loads are a function of the weight of the slice (ΔW) and the seismic coefficients, k_v and k_h, for the vertical and horizontal directions, respectively. The loads are calculated according to:

1. Horizontal Load: $\Delta H = k_h \Delta W$

2. Vertical Load: $\Delta V = k_v \Delta W$

If a seismic coefficient is specified for calculating a pseudo-static factor of safety, it will not include the inertial effects of the weight of the water above the slice and the direction of the imposed water force on the surface of the slope.

4.6 Boundary Surcharge Loads

The applied surface loads are partitioned directly to the underlying slices. Because the slices are divided according to the geometry of the slope and loads, a search and allocation procedure is used to develop the loads for each slice.

The user should note that in the development of the algorithms in Chapter 2 (Eqs. 2.1, 2.6 and 2.12), the surcharge load (ΔQ), applied at the surface of the slice, is included in the calculation of the normal stress at the base of the slice. The entire magnitude of the force is transferred from the surface to the failure surface, without any dissipation of the load with increased depth. This external load will directly increase the mobilized shear strength in ϕ-soils and so the user should be careful in specifying the magnitude of the surcharge load. Fortunately, the analysis is not overly affected by such loads as the greater driving moments/forces are partially offset by the increase in shear resistance.

CHAPTER 5

SLOPE STABILITY EXAMPLES

Several examples are presented in this chapter to illustrate the use of **XSTABL** for evaluating the stability of slopes. These examples cover pore water pressures variations, side-hill embankments, foundations on slopes and other interesting aspects concerning reinforced slopes and control of negative effective stresses. Considerable effort has been expended by the author (and reviewers) to ensure the practicality of the examples and the presented solutions. It is possible that *slightly* different solutions may be generated for different search limits or other failure surfaces. Thus it is important that the reader maintain some objectivity as unique design solutions in geotechnical engineering practice are rare. A total of thirty-one analyses are discussed in this chapter with complete listings of all input datafiles provided in the Appendix. Hopefully, these examples will provide an opportunity to understand the analytical intricacies of slope analysis.

5.1 PORE WATER PRESSURES

Slopes are conventionally analyzed using two dimensional, limit equilibrium methods. However, as a unique solution is not available, a trial and error search procedure is used to determine the factor of safety (FOS) for a number of surfaces to locate the potentially critical failure surface. In performing this search and analysis, the engineer has an option to use effective or total strength parameters for the subsoils. If an effective strength analysis is contemplated, the pore water pressures in the slope will have to be adequately defined so that the effective stresses can be computed along each trial failure surface.

This section describes an example where several methods are used to assign the estimated pore water pressures for an effective stress analysis using **XSTABL**. Results between the different methods are also compared to illustrate the significant differences between the

methods. Also, this information will allow the reader to critically examine the approach necessary to adequately define the pore water pressures within a slope.

EXAMPLE

An example of an effective stress analysis of a slope affected by seepage will be presented to show the advantages and disadvantages of using the various procedures for specifying pore water pressures within **XSTABL**. The example slope is presented in Fig. 5.1 and consists of an earth embankment (γ = 125 pcf, ϕ' = 32° and c' = 90 psf) founded on firm stratum (Lambe and Whitman, 1969). A phreatic surface and the relevant flow net, for steady state conditions, is also shown in the same Fig. 5.1.

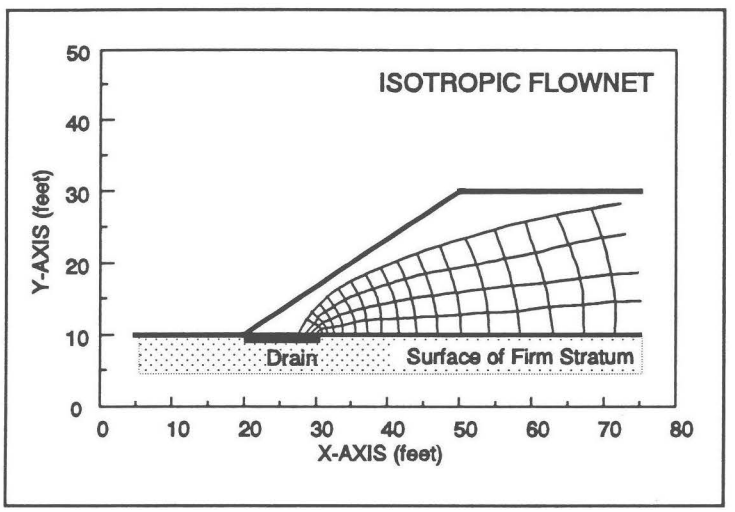

Figure 5.1. Example embankment with flownet

Search for Critical Surface

The critical circular surface was located using **XSTABL**, with the pore water pressures assigned through the use of: (1) a phreatic surface and (2) pore pressure grid. The phreatic surface was defined by twenty points along the upper line shown in Fig. 5.1. The three most critical circles, out of a possible 100 examined, are presented in Fig. 5.2. A minimum FOS value of 1.300 was determined for this analysis.

The pore pressure grid was specified by 90 discrete values that correspond to the intersection points of the flow and equipotential lines shown in Fig. 5.1. **XSTABL** uses the method proposed by Chugh (1981) to calculate the pore pressure values at the base of the slices. The same critical circle, but with a FOS value of 1.299, was located after analyzing 100 generated surfaces. The discrepancy with the FOS values is attributed to the calculated pore water pressures along the critical surface, as shown in Fig. 5.3. This figure indicates that pore pressures estimated from the phreatic surface were generally ***lower*** in the upper half

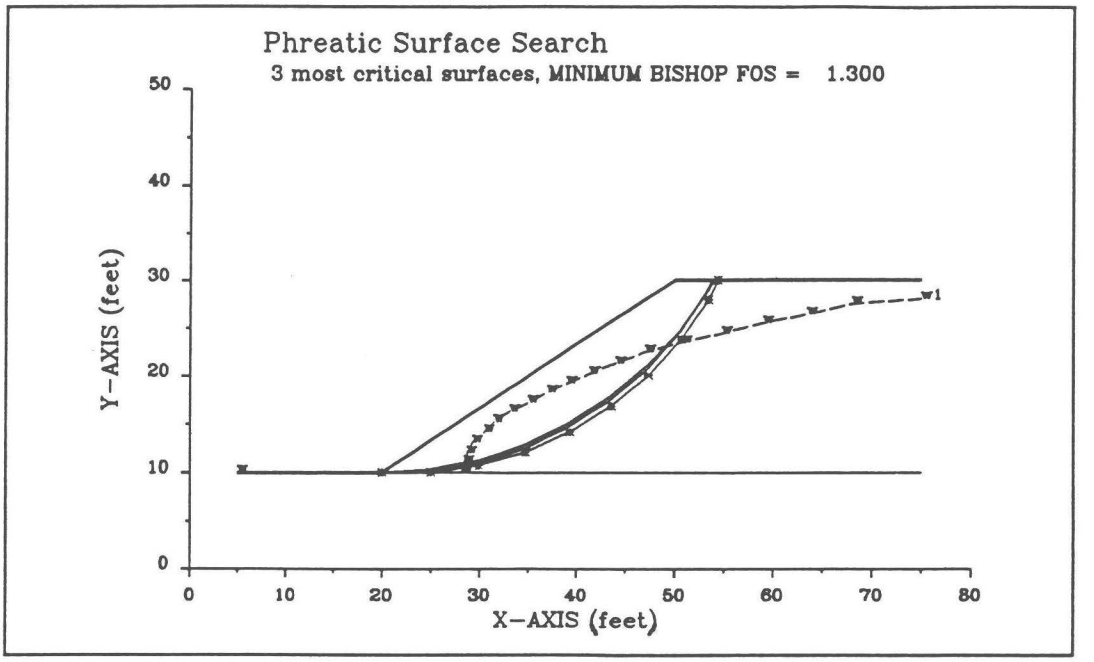

Figure 5.2. The three most critical surface identified by **XSTABL**

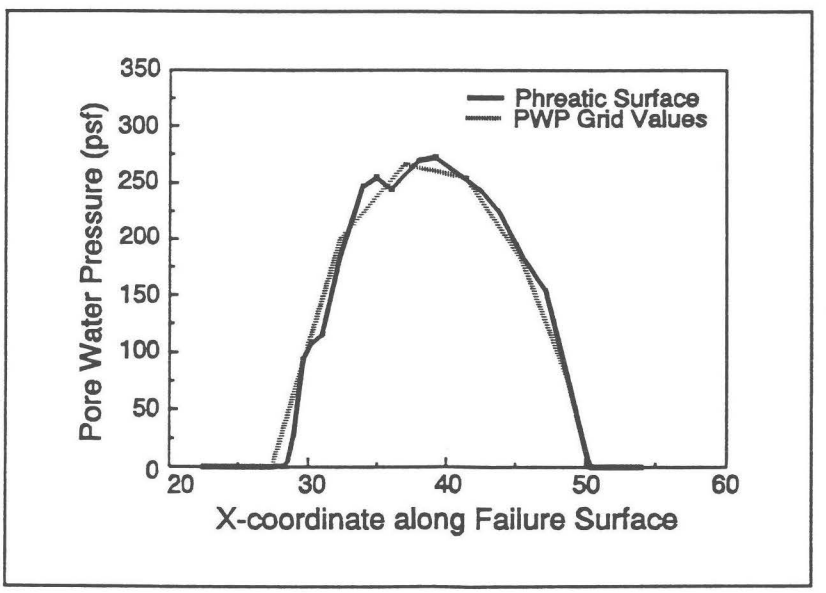

Figure 5.3. Comparison of computed pore water pressures for critical failure surface

of the slope than the values calculated from the specified grid. This variation is as expected because the phreatic surface has a convex shape and pore pressures are likely to be over estimated for the analysis.

Analysis of Critical Surface

The critical surface located in search analysis is shown in Fig. 5.4 along with the phreatic and corresponding ***piezometric*** surface. The piezometric surface, determined from the flow net presented earlier in Fig. 5.1, suggests that pore water pressures exist only between points A and B on the failure surface. A comparison between pore pressures calculated along the circular surface using the phreatic and piezometric surfaces is presented in Fig. 5.5. There are some small discrepancies, but the computed FOS for the piezometric surface was slightly lower. A summary of the FOS values for the different methods is presented in Table 5.1.

Table 5.1. Summary of FOS Values

Type	FOS
Phreatic Surface	1.300
Pore Pressure Grid	1.299
Piezometric Surface	1.291
Ratio, r_u = 0. 157	1.300
Incorrect Piez. Surface	1.233

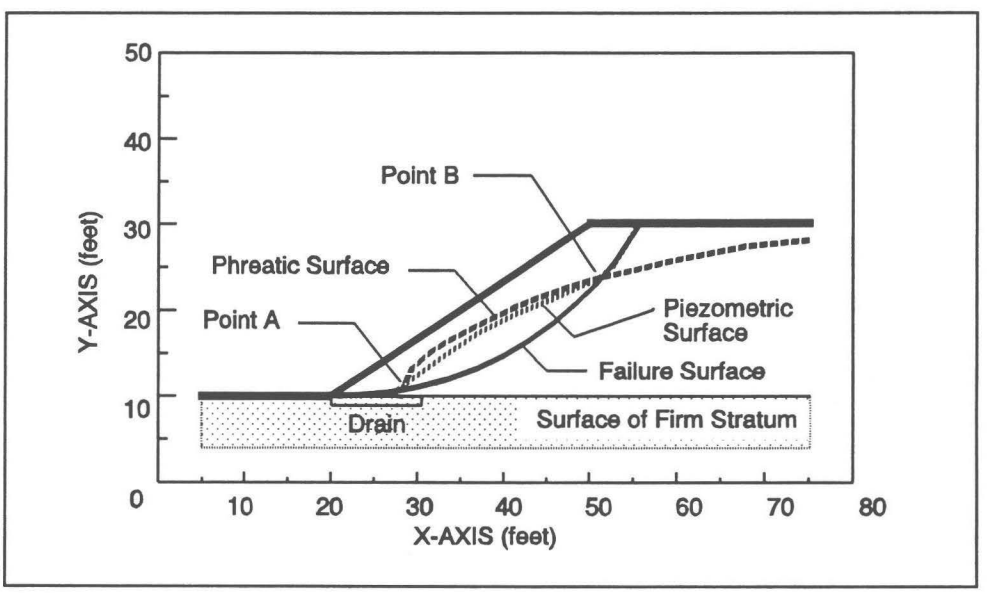

Figure 5.4. Comparison of piezometric and phreatic surfaces applicable for the re-analysis of the critical surface

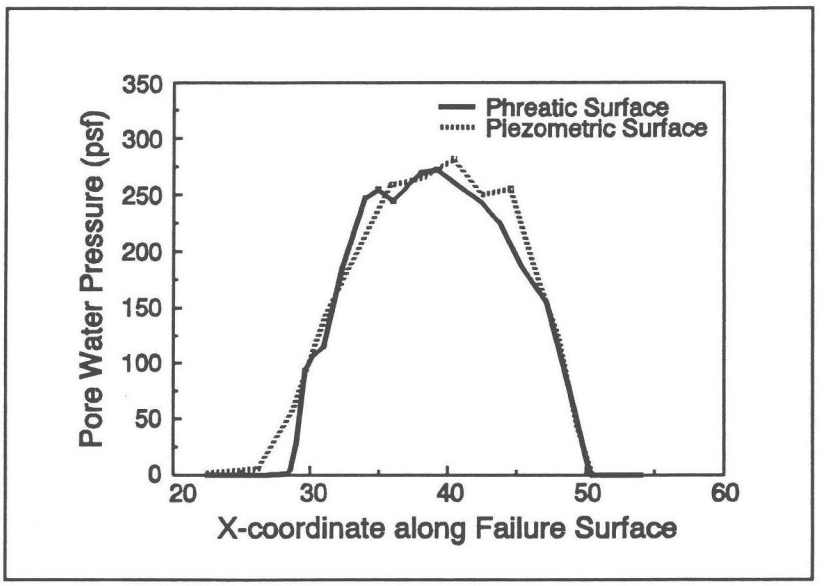

Figure 5.5. Comparison of pore water pressures computed using specified phreatic and piezometric surfaces

The approach adopted for calculating the r_u value for the slope is presented in Fig. 5.6. The failure surface is represented by the arc AFEDC and the piezometric surface by the line FGD. For this example, the pore pressure ratio will be a function of the ratio between the shaded area FGDEF and the failed mass, ABCDEFA, and is given by:

$$r_u = \frac{\text{Area FGDEF}}{\text{Area ABCDEFA}} \times \frac{\gamma_w}{\gamma_s}$$

where γ_s and γ_w are the unit weights of soil and water. As expected, the computed FOS value is almost identical to the FOS for the piezometric surface.

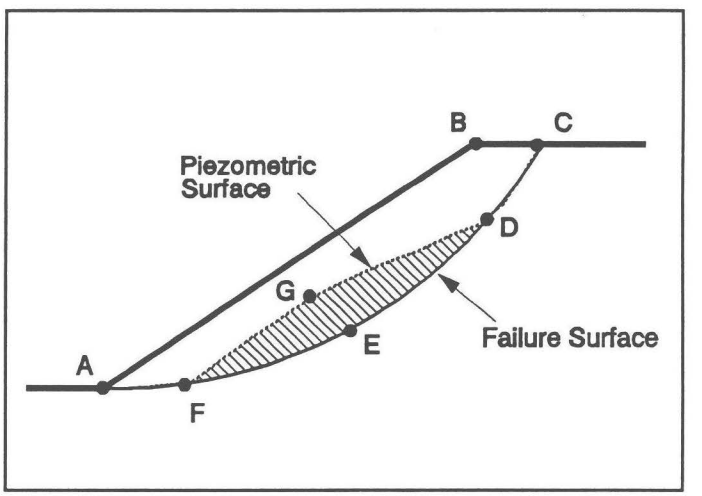

Figure 5.6. Use of piezometric surface to determine pore pressure coefficient, r_u

Finally, if the slope analysis program had *incorrectly* used the phreatic surface to simulate the piezometric surface, a FOS value for the selected circular surface would have been calculated as a conservative value of 1.233. This reduction is directly attributable to the over

estimation of the pore water pressures along about 85% of the failure surface, as shown in Fig. 5.7.

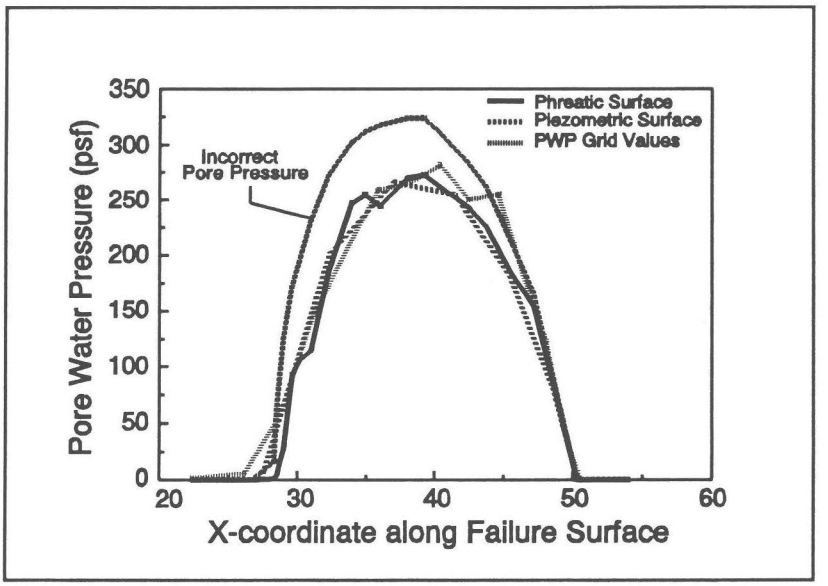

Figure 5.7. Comparison of computed pore water pressure variation for four cases

Summary and Conclusions

This example showed the use of four methods that may be used to assign pore water pressures for slope stability analysis. Of these, three are suitable for problems where **XSTABL** is used to determine the critical surface with the lowest factor of safety using the automatic search options. The input datafiles for these five examples are listed in Tables A1-A5 in the Appendix.

The analysis of a circular surface using the program **XSTABL** revealed that the factors of safety (FOS) were consistent for each of the methods employed and varied within a very small range of 1.294 to 1.301. This range is small enough to have been influenced by minor uncertainties concerning the manual development of a flow net and the determination of the piezometric surface for the circular failure surface. The small FOS range strongly suggests that a phreatic surface may be used to effectively model the pore water pressures within a slope. However, the engineer should not use **XSTABL** to search for a critical surface if the phreatic surface is erroneously used as a piezometric surface. In such cases, the pore water pressure will be overestimated and an unrealistically low FOS value will be calculated by the program.

5.2 Typical USDA-Forest Service Examples

Three general problems concerning slope analysis are presented in this section. These problems illustrate the use of automatically generated block and circular surfaces for typical problems encountered in the assessment of stability of steep slopes. Additionally, an interesting analysis that includes external surcharge loads is presented to show the effects upon the location of the critical surface and the factor of safety.

Example 1

This problem is used to illustrate the functionality of the RANKINE or BLOCK options in **XSTABL** for automatically generating block-shaped surfaces. If block-shaped surfaces are considered, the location of generated surfaces may be closely controlled by the location of the required search boxes. The slope profile for this example is presented in Fig. 5.8 along with the location of the specified search boxes. The roadway is to be widened by the construction of a retaining wall. This retaining wall structure will be built using the *Hilfiker Retaining Wall*® system that uses backfilled welded-wire boxes. The subsoils consist of a single soil unit overlying bedrock.

The material in the proposed retaining wall has been given a relatively high strength to ensure that potential failure surfaces passing through this material will have higher factors of safety in comparison with surfaces that pass around the wall area. Thus block shaped failure surfaces are considered most likely for this site. In order to control the surface generation procedure, suitably located search boxes are used to "guide" the surface generation process around the fill-zone. Because the soil unit is relatively thin, circular surfaces could not have been successfully generated around the fill-zone within the required initiation and termination ranges.

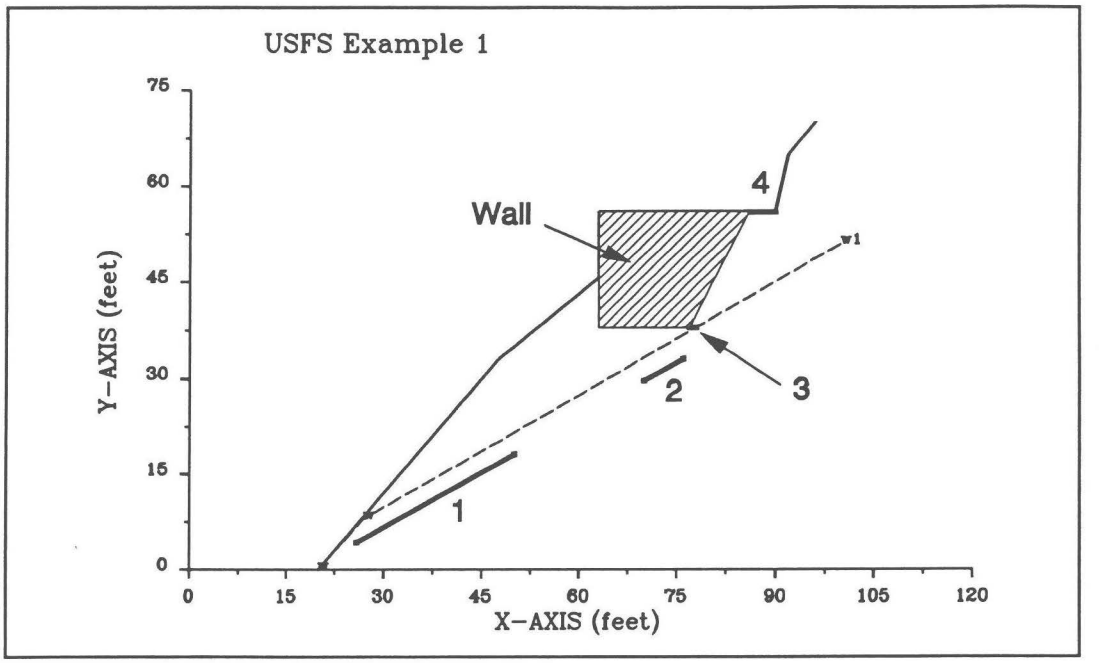

Figure 5.8. Slope geometry data for example 1

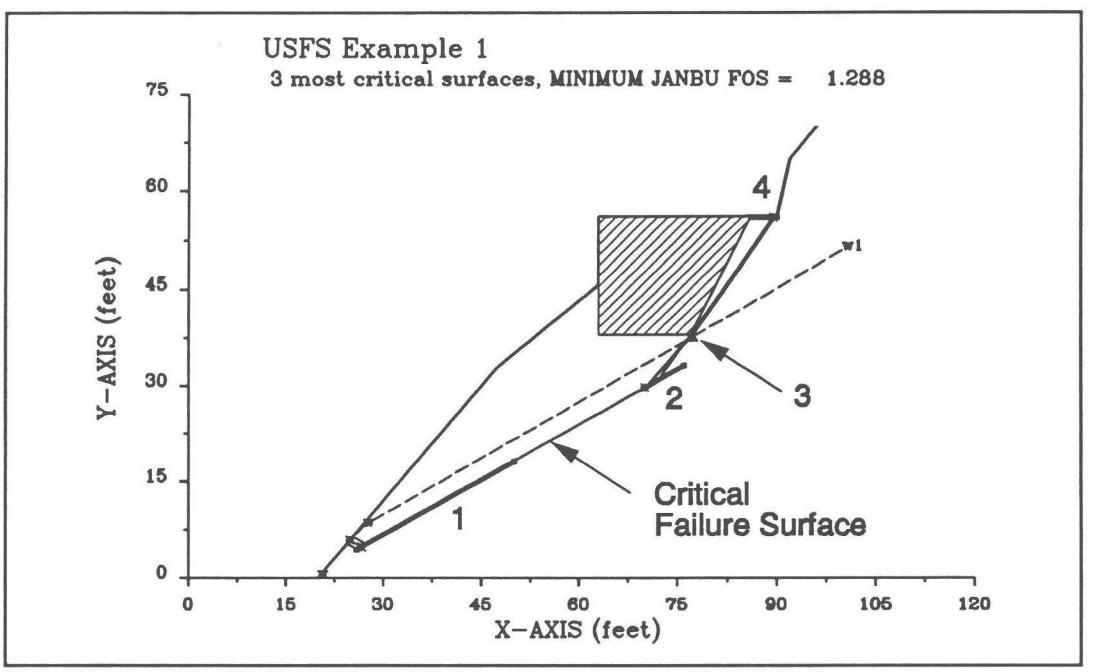

Figure 5.9. Location of critical surface identified by **XSTABL**

The block surfaces are generated to follow the four search boxes (marked 1 to 4) shown in Fig. 5.8. Four search boxes are specified as "line" boxes and one "point" box is located outside the lower right-hand corner of the fill-zone. Search box 4 will limit the termination range between x = 66.0 and 70.0 feet. The intermediate search boxes, numbered 1 to 3, force the generation of the central portion of the block surface to follow the soil-rock interface. As all surfaces must pass through box-3, it effectively acts as a control point and ensures that generated surfaces do not pass through the fill. The data for this case was assembled using **XSTABL**, and a listing of the final data file is given in Table A6 in the Appendix.

The results of the block analysis, presented in Fig. 5.9, show that the most critical block surface, based on 300 trial surfaces, has an upper boundary that just passes around the fill material before exiting the slope. For this critical surface, the corrected Janbu factor of safety was calculated as 1.288.

Example 2

A slope with multiple water surfaces is selected for this example to show use of piezometric and phreatic surfaces for a slope analysis. The soil profile for example 2 is shown in Fig. 5.10. The subsoil profile is defined by four soil units. Soil units 1-3 are the natural soils at the site and soil unit 4 is a constructed fill material. Also, soil unit 1 is the surficial layer and can be expected to include organic materials. The uppermost layers identified by soil unit 1 and 4 are influenced by the phreatic surface, labeled w1, and the other two soil layers are affected by artesian water pressures that are closely simulated by the piezometric surface, p2.

Please note that a piezometric surface should be based on the pore water pressures acting on a ***single*** potential failure surface. The **XSTABL** analytical procedure then calculates the pore water pressure as a function of the ***vertical*** distance between the failure surface and the piezometric line. However, it is used in this example as it provides a relatively "good" estimate of the anticipated pore water pressures in soil units 2 and 3. The complete data file used for this example is presented in Table A7 in the Appendix.

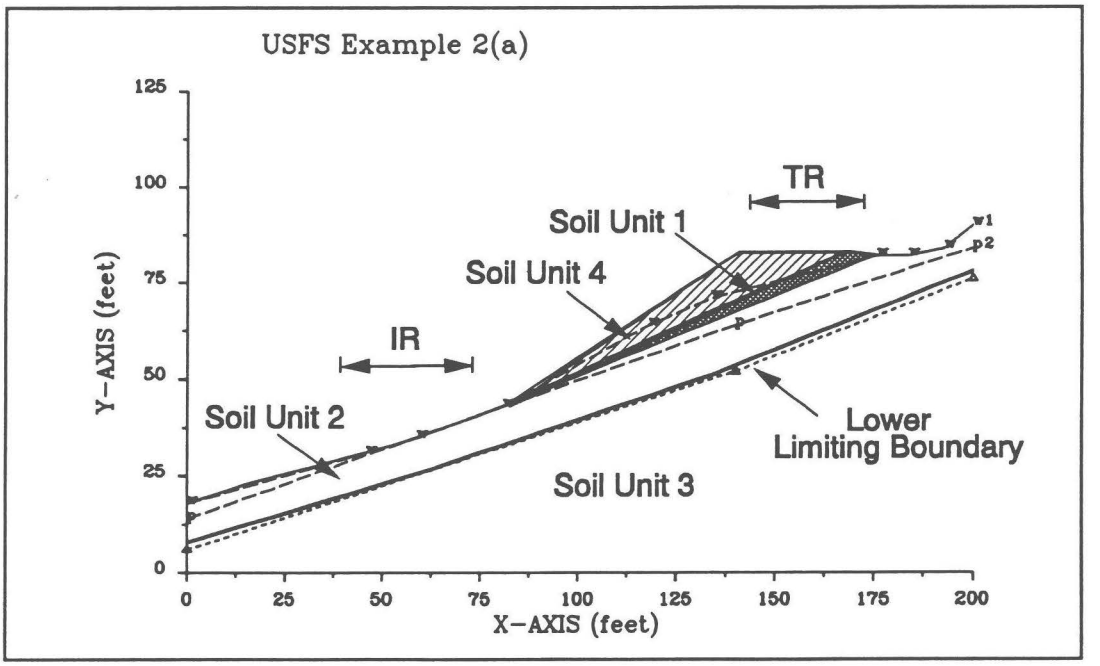

Figure 5.10. Slope data used for Example 2

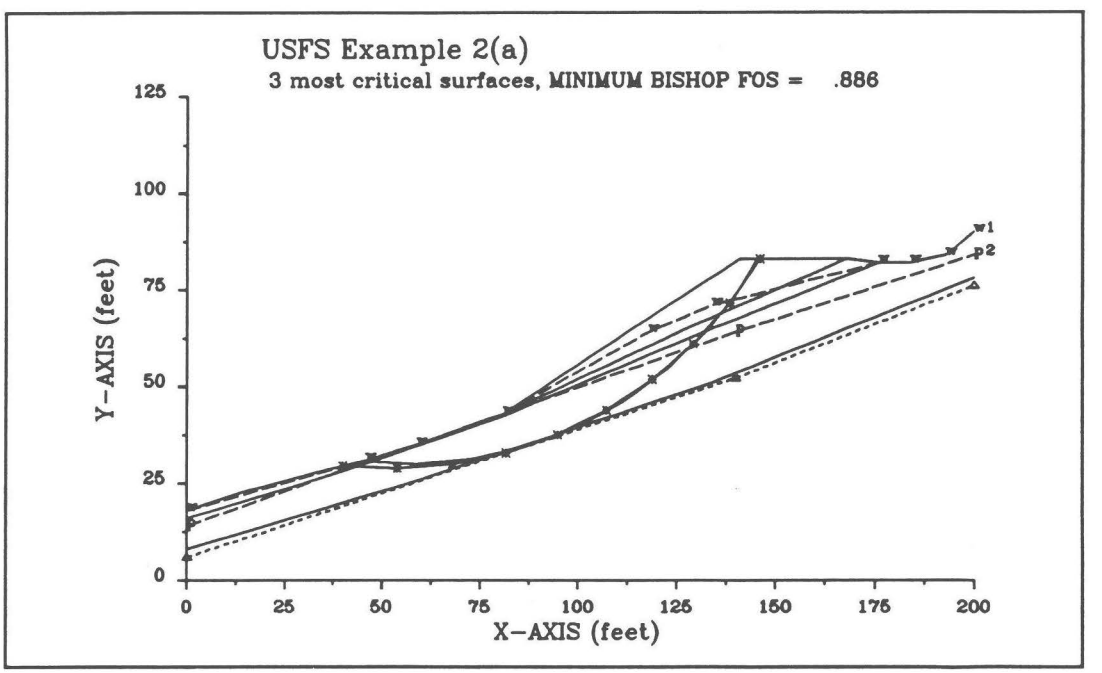

Figure 5.11. Location of critical circular surface

The stability of this slope is expected to be controlled by either a deep circular surface that passes through soil unit 2 or a shallow block-shaped surface confined to soil units 1 and 4. For circular surfaces, the generation of potential failure surfaces through soil unit 3 will be prevented by specifying a lower limiting boundary just below the interface between soil unit 2 and 3. In order to locate the critical failure surface, 50 surfaces will be generated from seven initiation points equally spaced within the initiation range (IR), x = 40 to 70 feet. The 350 generated surfaces will be forced to exit at the embankment crest between a termination range (TR) of x = 145 to 185 feet.

The five most critical surfaces, out of 350 examined, are shown in Fig. 5.11. From this analysis, the minimum factor of safety was calculated as 0.886. In completing this analysis, **XSTABL** reported the computation of negative effective stresses at the base of some of the slices for 52 surfaces from the total 350 examined during the search. In this case, a FOS of 0.886 was calculated irrespective of the option selected to control the effects of calculated negative effective stresses. Such results indicate that negative stresses were not calculated for the most critical failure surfaces.

Additionally, the stability of the highway embankment must also be assessed to ensure that a critical failure surface does not exist within soil unit 1. The shallow failure mode is assessed using block-shaped failure surfaces connecting points located within four "line" (search) boxes shown in Fig. 5.12. These search boxes, with a side length of zero , are suitable placed to confine the surface generation between well defined initiation and termination ranges. The central portion of the block-surface is limited to the layer defined by soil unit 1. For this analysis, 300 surfaces are generated to follow the zones specified by the four search boxes. The complete data file for this problem is presented in Table A8.

The five most critical surfaces are presented in Fig. 5.13. A minimum factor of safety of 0.793 was calculated for the shallow failure surface mode. Thus if a shallow failure surface can pass through the organic, surficial soil layer, a ***lower*** factor of safety can be expected for the analysis. Conversely, if this "weaker" material was removed, the FOS may be improved accordingly. For this analysis, negative stresses were reported for only *three* surfaces.

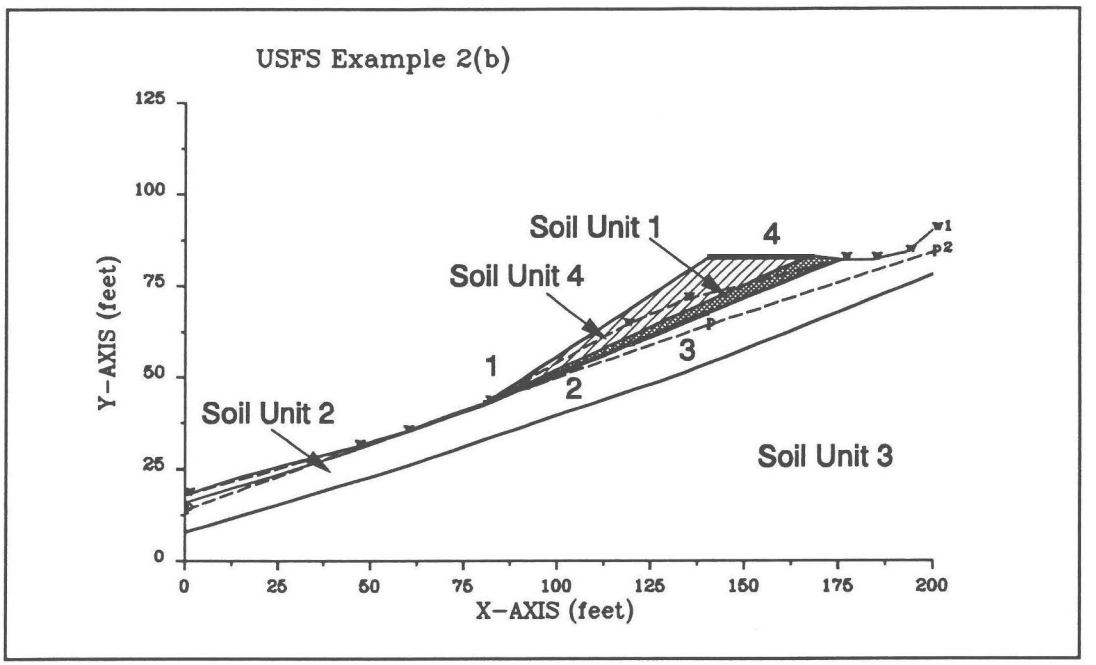

Figure 5.12. Slope geometry showing search "lines" used for block analysis

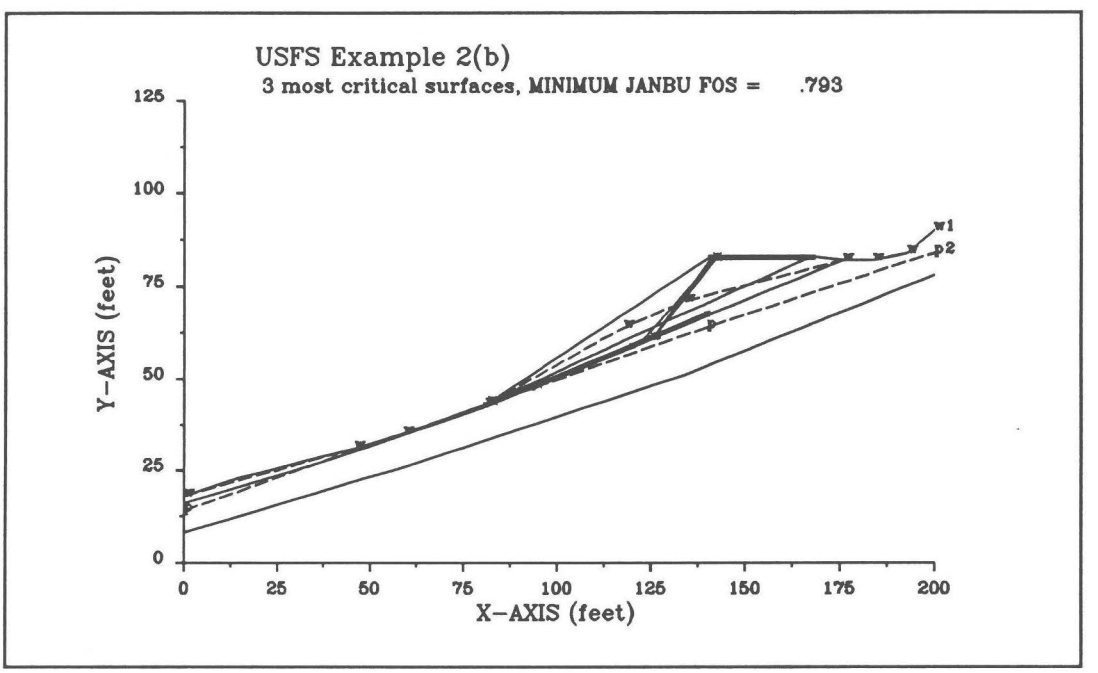

Figure 5.13. Location of critical block surface

Example 3

The third example is used to illustrate the Surcharge Load option available in **XSTABL**. This example will also be used to provide a comparison between formal bearing capacity analysis and the limit equilibrium method of slices. For relatively shallow failure surfaces, the calculated factors of safety would then correspond to *bearing capacity* and deeper surfaces would allow an assessment of the overall slope. In general, for relatively flat slopes, the shallow Terzaghi-Prandtl surfaces would be critical, whereas the overall stability would be more critical for steeper slopes.

This example, consisting of a retaining structure on a slope, has been selected from the R1 Foundation Engineering Handbook (R1 Transportation Engineering Handbook Supplement No. 11, February 1981) and is illustrated in Fig. 5.14. The general slope profile, presented in Fig. 5.14, consists of a thin layer of soil overlying bedrock. Foundation loads are due to active earth pressures, soil surcharge and live wheel loads acting above the wall. The stability of the retaining structure needs to be evaluated against a possible bearing capacity failure as well as an overall failure of the slope due to the increased loads.

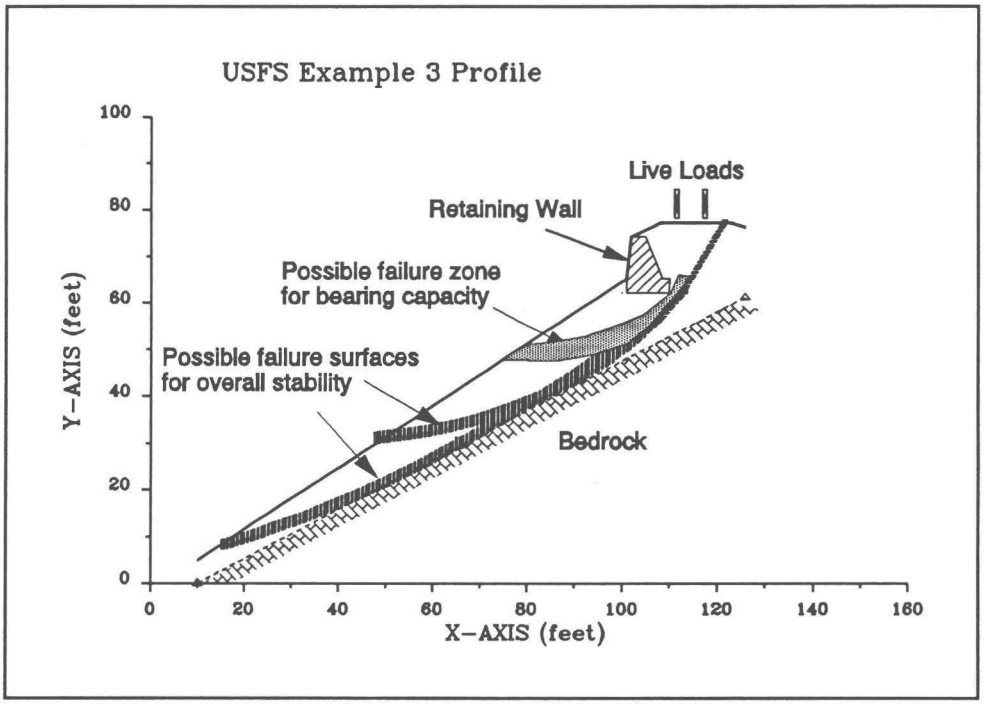

Figure 5.14 Slope geometry data for example 3

Bearing Capacity

The bearing capacity of the 9-foot-wide foundation was evaluated for a vertical eccentric load of 15.5 kips/ft and a horizontal load of 4.14 kips/ft. This loading arrangement may be simplified by replacing the horizontal and vertical loads with a resultant load of 16.04 kips/ft inclined at an angle of about 15 degrees, clockwise from the vertical, and at an eccentricity of 1.18 feet from the centerline of the foundation. The bearing pressure, under this load, varies between 3078 and 367 psf.

An ultimate bearing capacity of 10,100 psf was calculated for a vertically loaded foundation, with a modified width of 6.64 feet, using the procedures outlined in NAVFAC DM7 (1982). This calculated capacity is based on $\phi = 35°$, slope angle $\beta = 33.7°$ and an embedment ratio, D/B = 0.45. A correction to account for the inclined load reduced the final ultimate bearing capacity to about 4,240 psf.

A FOS of 1.816 may be calculated by comparing the 4,240 psf capacity and the actual imposed uniform pressure of 2,335 psf. This is a *load-based* Factor of Safety. Alternatively, using back-calculations, a minimum value of $\phi = 32°$ for the foundation soils would provide a bearing capacity of approximately 2,335 psf for the same foundation and slope. As the foundation soil has a ϕ value of 36°, a *strength-based* FOS of 1.163 can be determined by taking the ratio of the tangents of the available and required angles of internal friction.

The above calculations for the FOS are based on the classical Terzaghi-Prandtl failure shape consisting of two straight lines joined by a log-spiral, as shown in Fig. 5.15. A similar failure shape may also be analyzed with **XSTABL** and a FOS determined for the case where the foundation bearing pressure can be simulated by boundary surcharge loads inclined at 15 degrees. Figs. 5.15 and 5.16 present the results of assuming two slightly different failure surfaces. The failure surface used in Fig. 5.15 gives a FOS of 1.081 and is based on the Rankine assumption that the passive plane will intersect the surface boundary (slope) at an angle of (45 - ½ϕ) degrees. The surface used in Fig. 5.16 yields a FOS of 1.215 and is based on the assumed shape employed by the chart solution given in NAVFAC DM7 (1982). Both of these failure surfaces generate reliable values for practical design, however the surface used in Fig. 5.15 is perhaps slightly superior due to its compliance with the kinematics of the problem.

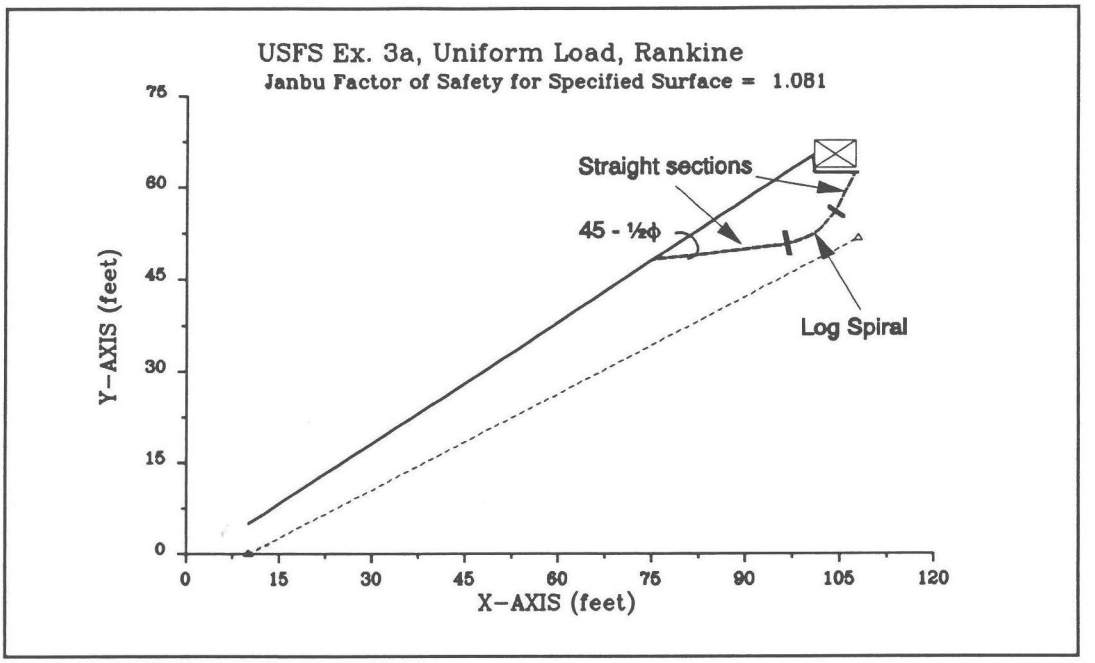

Figure 5.15 Critical surface for example 3(a)

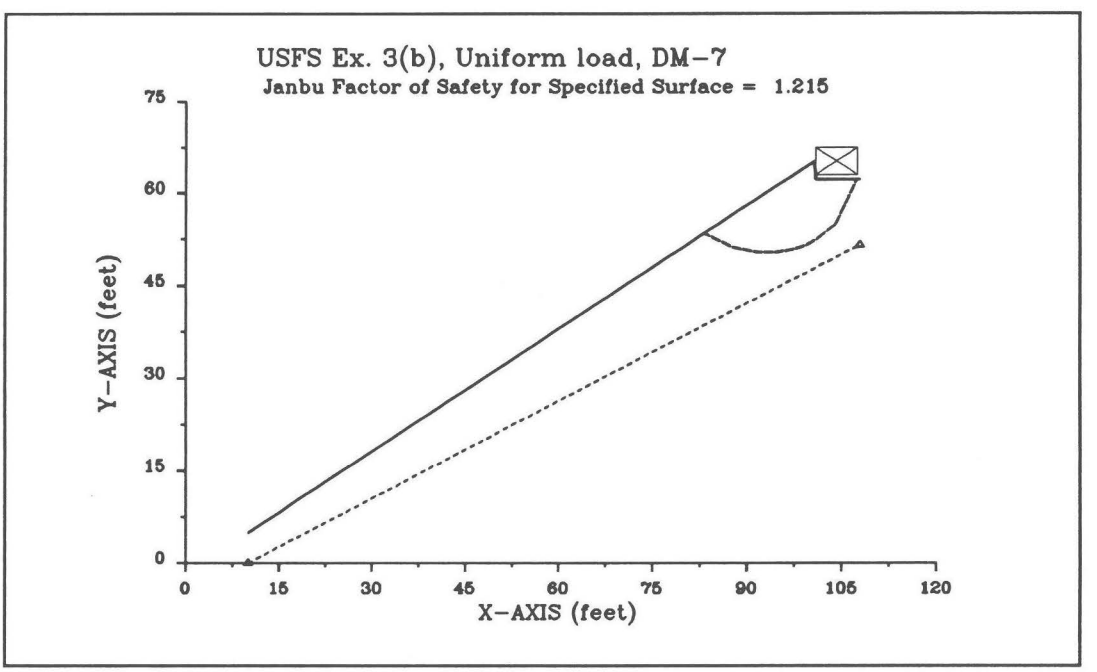

Figure 5.16 Critical surface for example 3(b)

The same analysis may also be performed using the *nonuniform* bearing pressure distribution acting on the full nine foot wide foundation. For this case, the linearly varying distribution is simulated by uniform loads applied over one-foot-wide strips to simulate the effects of the vertical and horizontal loads of 15.5 and 4.14 kips/ft. The failure surfaces, shown in Fig. 5.17 and 5.18 were developed according to the same rules as used for the solution with the uniform pressures. This analysis revealed a FOS of 1.333 for the surface that satisfies Rankine's criteria.

Table 5.2 summarizes the results from the different bearing capacity analyses. In comparing the strength-based FOS values, the use of a uniform pressure distribution resulted in FOS values ranging between 1.081 and 1.215. The FOS values for the nonuniform bearing pressure distribution extended the range, with a significantly higher FOS value of 1.473 being calculated for the surface defined according to the NAVFAC DM7 procedures. These higher FOS values are essentially generated as a larger portion of the greater surcharge loads are supported by slices with a *flatter* base, which reduces the driving forces and also increases the frictional strength. The surface shown in Fig. 5.18 also curves upwards substantially, thus mobilizing additional resistance.

Table 5.2. Summary of bearing capacity FOS values

Method	Bearing pressure distribution	Failure surface	Factor of Safety
NAVFAC DM7: Load Based FOS	uniform	DM7	1.817
NAVFAC DM7: Strength based FOS	uniform	DM7	1.163
Limit Equilibrium	uniform	Rankine	1.081
Limit Equilibrium	uniform	DM7	1.215
Limit Equilibrium	nonuniform	Rankine	1.333
Limit Equilibrium	nonuniform	DM7	1.473

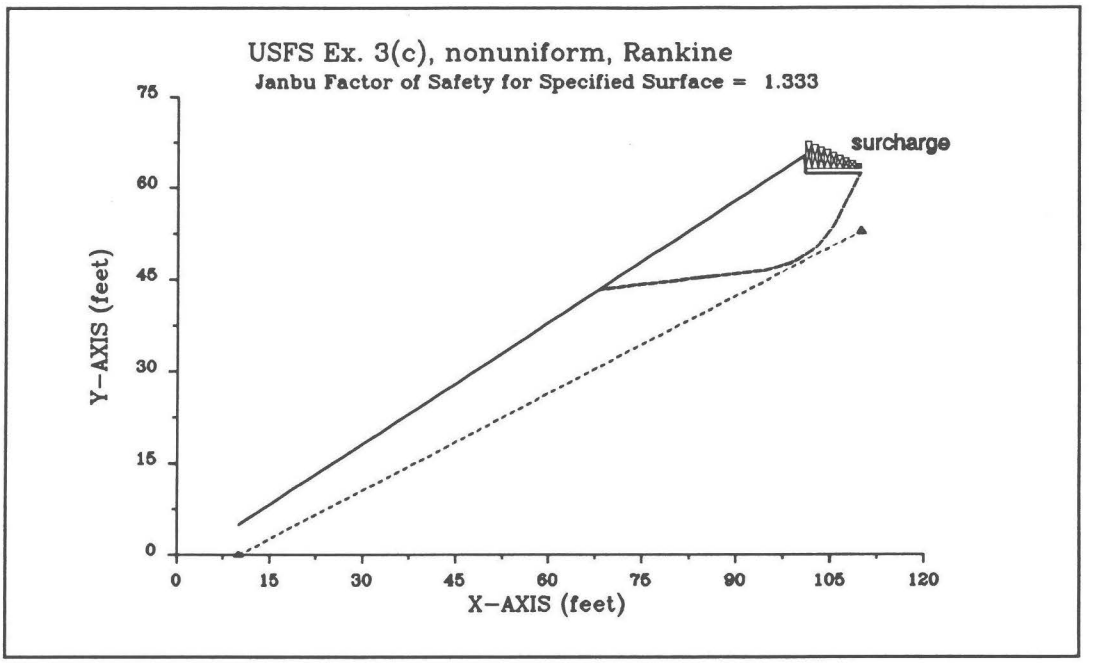

Figure 5.17 Critical surface for example 3(c)

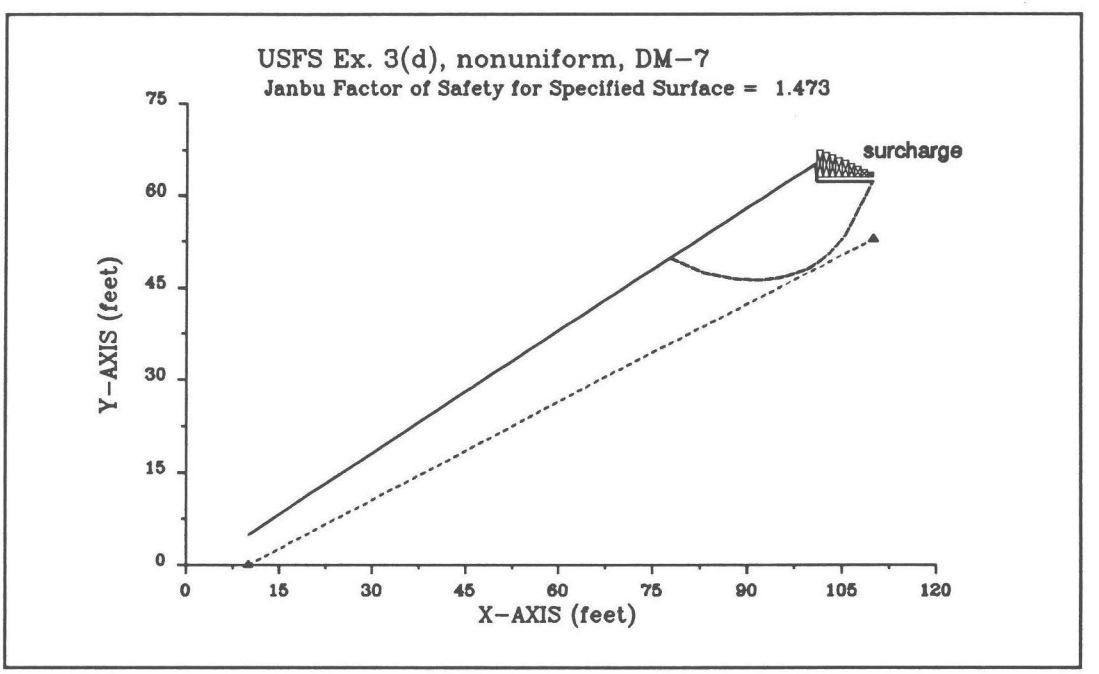

Figure 5.18 Critical surface for example 3(d)

Overall Stability

The overall stability of the slope, as affected by any changes in the loading conditions, must also be evaluated even if calculations show a satisfactory FOS against a bearing capacity failure. The potential failure zones for bearing capacity and overall stability have been shown in Fig. 5.14. The overall stability of the slope can be readily evaluated using **XSTABL**.

The critical surface can be expected to be confined to the soil overlying bedrock and should terminate just beyond the loaded foundation area. In order to limit the search area, the soil-rock interface is simulated with a lower limiting boundary that will confine the generation of failure surfaces to the relatively weaker soil layer. For this analysis, 250 circular shaped surfaces are examined for the two presumed bearing pressure distributions. The most critical circular failure surfaces, on the basis of 250 surfaces analyzed, are presented in Figs. 5.19 and 5.20. The calculated FOS values are 1.053 and 1.099 for the uniform and nonuniform pressure distributions, respectively.

A further analysis of the entire wall and backfill system should also be made as part of the overall stability analysis. For this case, a block search was selected to properly search the narrow potential failure zone. A FOS of 1.106 was calculated on the basis of analyzing 250 surfaces that passed just beyond the *heel* of the retaining structure as shown in Fig. 5.21. Two point boxes (labeled "1" and "3" in Fig. 5.22), a line box ("4") and a search box ("2") were specified to generate suitable trial failure surfaces. Finally, the live loads were introduced as a uniform surcharge of 2,000 psf and minimum FOS value of 1.056 was calculated using the same search boxes. The critical failure surface corresponding to the minimum FOS is shown in Fig. 5.22.

Thus limit equilibrium slope programs may be reliably used to determine the minimum factor of safety for a foundation placed on a slope. In this example, a minimum FOS of 1.05 was calculated for the retaining wall and live wheel loads after considering six separate analytical models. The input datafiles for these analyses is listed in Tables A9-A16 in the Appendix.

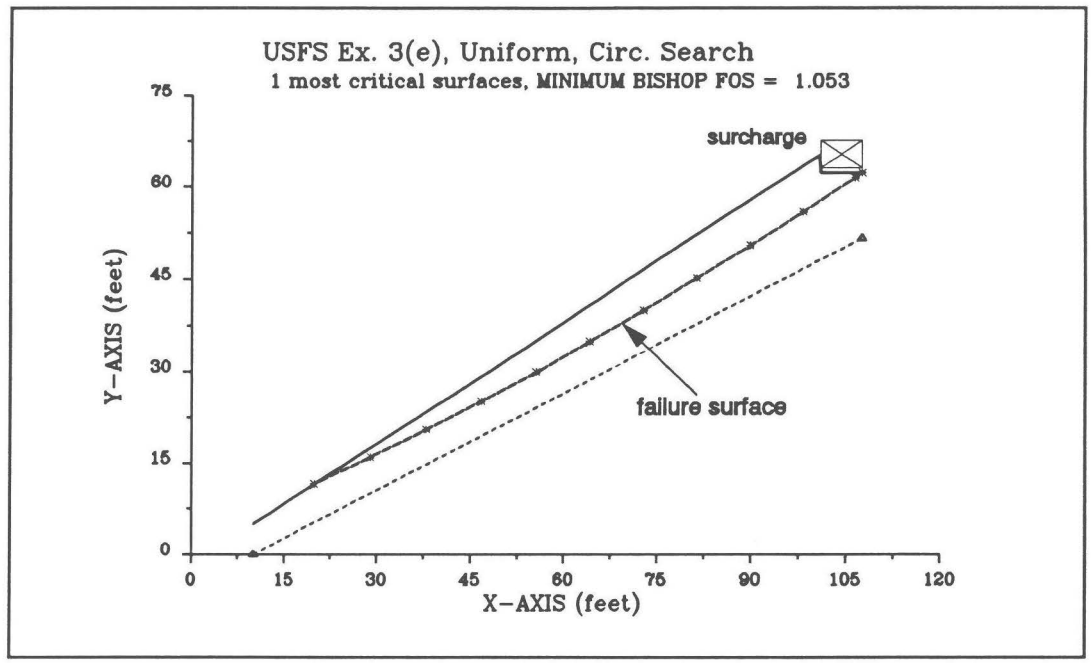

Figure 5.19 Critical surface for example 3(e)

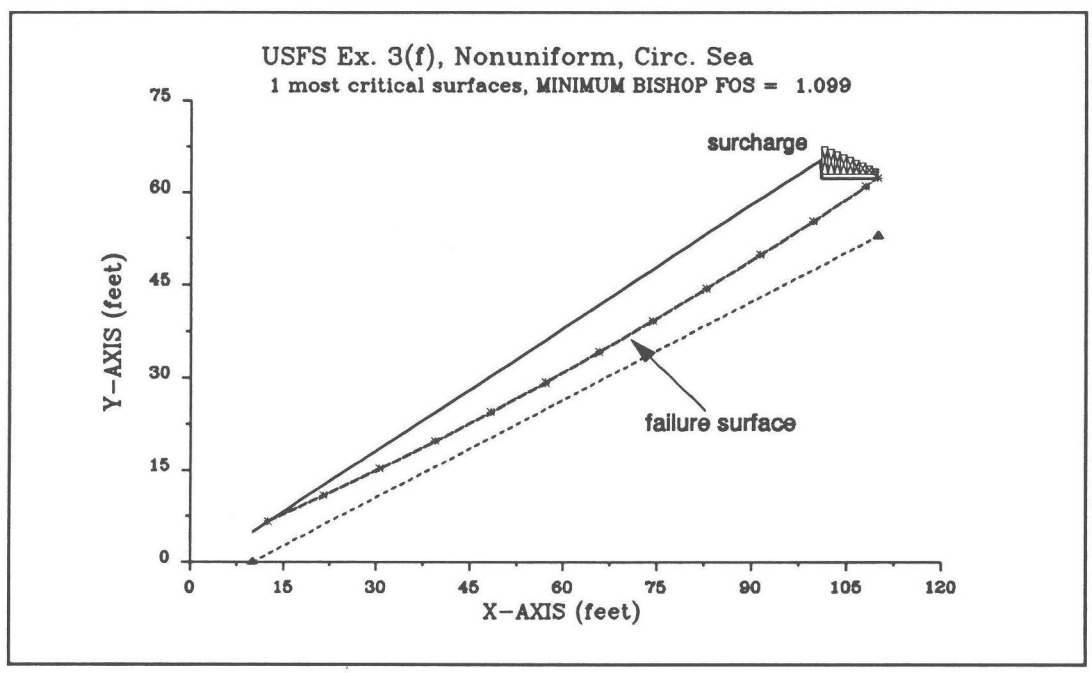

Figure 5.20 Critical surface for example 3(f)

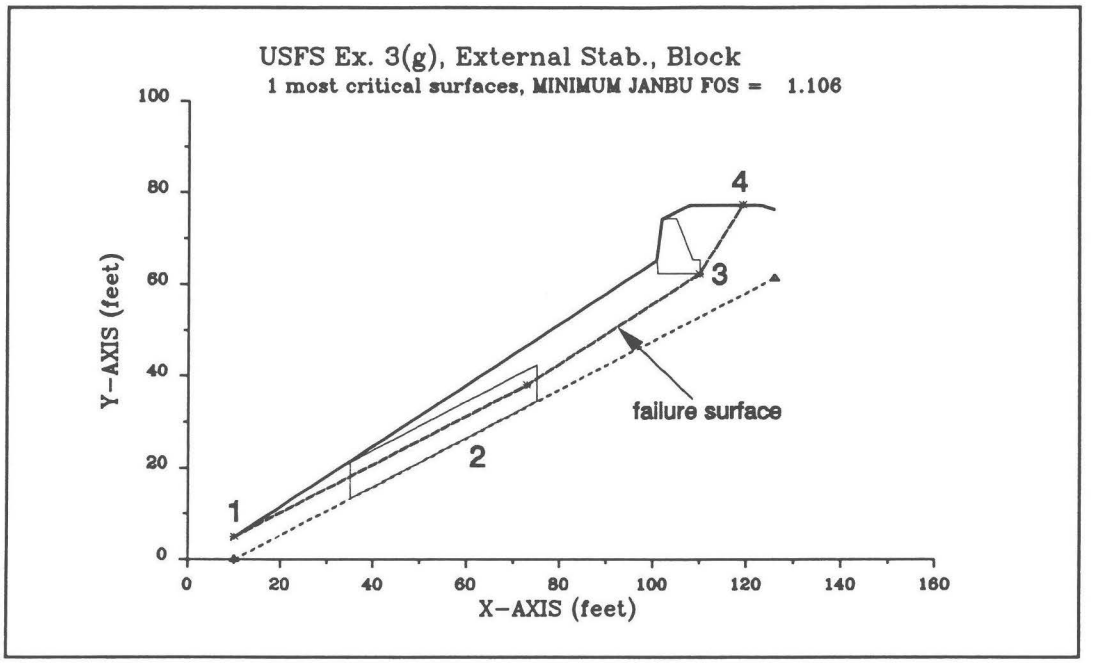

Figure 5.21 Critical surface for example 3(g)

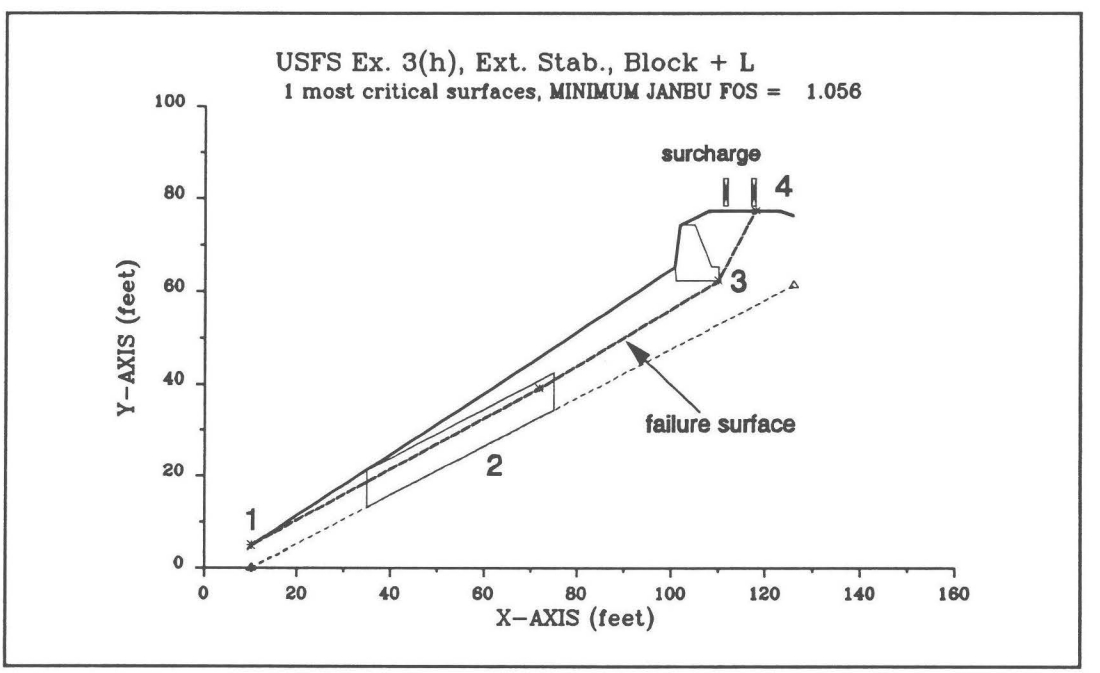

Figure 5.22 Critical surface for example 3(h)

5.3 Anisotropic Subsoils

Most natural soil deposits exhibit anisotropic soil behavior. For slope stability analyses, this anisotropy affects the shear strength of the soil, as used for the calculation of the factor of safety. In a limit equilibrium analysis, (1) the original consolidation stresses and (2) orientation of the failure plane with respect to the principal insitu stress are found to be the most significant parameters. The overall concept of this anisotropy is presented in Fig. 5.23. In this figure, three soil elements (A - C) are shown along with orientation of the principal stresses at failure and the failure plane itself. In general, the shear strength varies as a function of the angle between the principal planes and the failure plane. For San Francisco Bay Mud (Duncan and Seed, 1966), the strength along the failure plane for element C was about 75 percent of the tested undrained strength for element A. The drained strength, as estimated from effective stresses, was tested as $\phi=38°$ and 35° for elements A and C, respectively. Interestingly, for the same San Francisco Bay Mud samples that were isotropically consolidated, the angle of internal friction (ϕ') was calculated as 34.5°.

Most triaxial tests are performed on isotropically consolidated samples and the orientation of the failure plane would most likely correspond to element A in Fig. 5.23. Thus the effective strength for the San Francisco Bay Mud can be expected to range between 34.5° and 38°, depending on whether the sample was consolidated isotropically or anisotropically. Fortunately for most slope analyses, the shear strength values from isotropically consolidated tests are used to model the slope materials. This effectively under-estimates the strength and thus leads to a conservative estimate of the Factor of Safety.

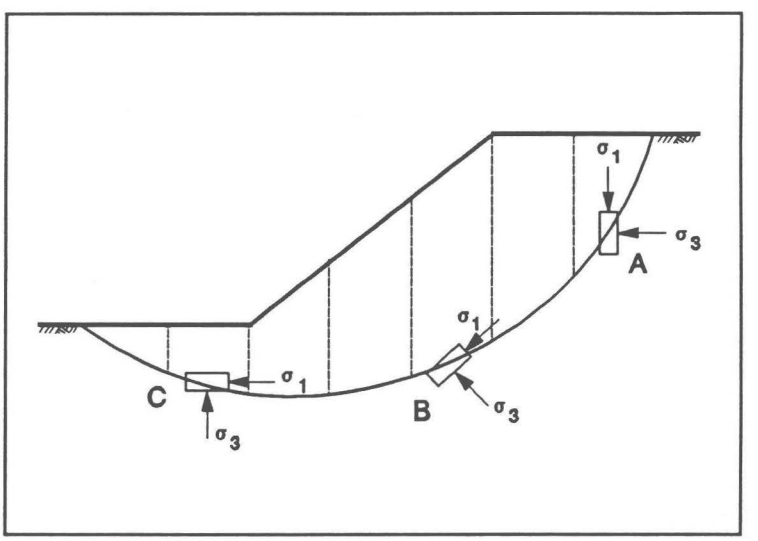

Figure 5.23, Directional Strength Anisotropy

However, if sufficient data from anisotropic tests is available to define the variation of shear strength according to the orientation of the failure plane, the anisotropic option in **XSTABL** may be used for the slope analysis. In **XSTABL**, the soil strengths may be defined along specific directional ranges to simulate angular anisotropy. Then, according to the orientation of the base of the discretized slice, the appropriate strength can be selected accordingly. An example, based on laboratory results reported by Duncan and Seed (1966) for the San Francisco Bay Mud is presented in the next section.

Example of Anisotropic Strength

A simple 2H:1V slope has been selected to illustrate the effects of angular anisotropy. The slope, shown in Fig. 5.24, was analyzed using **XSTABL** and the factor of safety determined according to the following three soil conditions:

(a) anisotropic soil, with strength data determined using anisotropic consolidation and different orientations of the failure plane. For this case the selected angular ranges and their associated strength parameters are presented in Table 5.3.

(b) isotropic soil, $\phi' = 34.5°$, to simulate strength values determined from an isotropic triaxial test;

(c) isotropic soil, $\phi' = 35°$, to simulate the laboratory results determined from an anisotropically consolidated sample failed according to the failure plane orientation indicated by element A in Fig. 5.23.

Table 5.3. Directional Anisotropic Strengths

Angular Range	ϕ'	c'
-90.0 -- -45.0	35.0	0.0
-45.0 -- -22.5	35.0	0.0
-22.5 -- 0.0	36.0	0.0
0.0 -- 22.5	37.0	0.0
22.5 -- 45.0	38.0	0.0
45.0 -- 90.0	35.0	0.0

(d) isotropic soil, $\phi' = 38°$, to simulate the laboratory results determined from an anisotropically consolidated sample failed according to the failure plane orientation indicated by element C in Fig. 5.23.

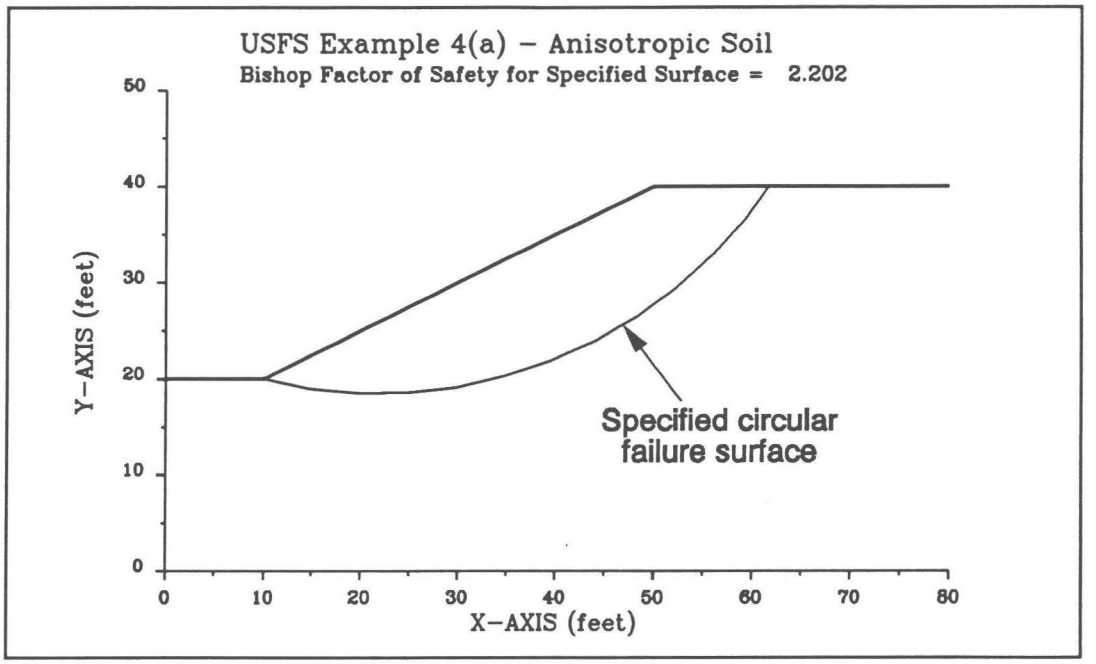

Figure 5.24 Specific circular failure surface used to illustrate the advantages of specifying anisotropic soil strengths

A search for the critical failure surface was made for the anisotropic soil strength parameters. This critical surface was subsequently used to evaluate the significance of using anisotropic or isotropic strength values. In reanalyzing the critical surface for the anisotropic data, the slice data shown in Table 5.3 was output by **XSTABL** using the input datafile listed in Table A17 in the Appendix. From Table 5.4, one can see that the program successfully selected the appropriate ϕ angle according to base angle of each slice, as specified in Table 5.3, above. For the four soil condition discussed above and the same failure surface, calculations revealed the following factors of safety:

Case (a) ..... 2.202 (ϕ ranges from 35° to 38°)
Case (b) ..... 1.992 (ϕ = 34.5°)
Case (c) ..... 2.029 (ϕ = 35.0°)
Case (d) ..... 2.264 (ϕ = 38.0°)

The input datafiles for cases (b) - (d) are given in Tables A18-A20 in the Appendix.

Table 5.4. Strength Selection for Anisotropic Analysis by **XSTABL.**

Slice #	Height (feet)	Width (feet)	Base Angle (degrees)	ϕ Used (degrees)
1	1.72	4.90	-11.32	36.0
2	4.91	4.98	-5.34	36.0
3	7.61	5.00	0.65	37.0
4	9.78	4.97	6.63	37.0
5	11.41	4.88	12.62	37.0
6	12.47	4.74	18.61	37.0
7	12.95	4.55	24.59	38.0
8	12.85	4.30	30.58	38.0
9	12.45	1.68	36.57	38.0
10	11.39	2.33	36.57	38.0
11	8.83	3.68	42.55	38.0
12	5.27	3.31	48.54	35.0
13	1.70	2.42	54.52	35.0

If the analysis had been performed using the upper and lower bound ϕ-values of 38° and 35° determined from anisotropic tests, **XSTABL** would have calculated the factors of safety (FOS) as 2.264 and 2.029. Thus one can see that the FOS determined using the upper and lower bound values will effectively envelope the results of the FOS value determined using directional strength anisotropy.

5.4 Seismic Analysis

The same slope and failure surface shown in Fig. 5.24, with anisotropic soil strength parameters, will be examined with a view to assessing its ability to resist seismic loads. Generally, the results of a seismic analysis should be presented in the form shown in Fig. 5.25. This plot shows the variation of the FOS as a function of the horizontal seismic coefficient. There is considerable uncertainty concerning the exact magnitude of seismic loads and such a plot conveys significant information regarding the stability of the slope during an earthquake.

In general engineering practice, ***only*** the critical failure surface determined for the static analysis is analyzed for seismic loads. This surface is expected to have the highest mobilization of shear strength, prior to the earthquake, and thus can be expected to "suffer" the most. Although a search for a critical surface is possible, different critical surfaces may be identified for each seismic coefficient.

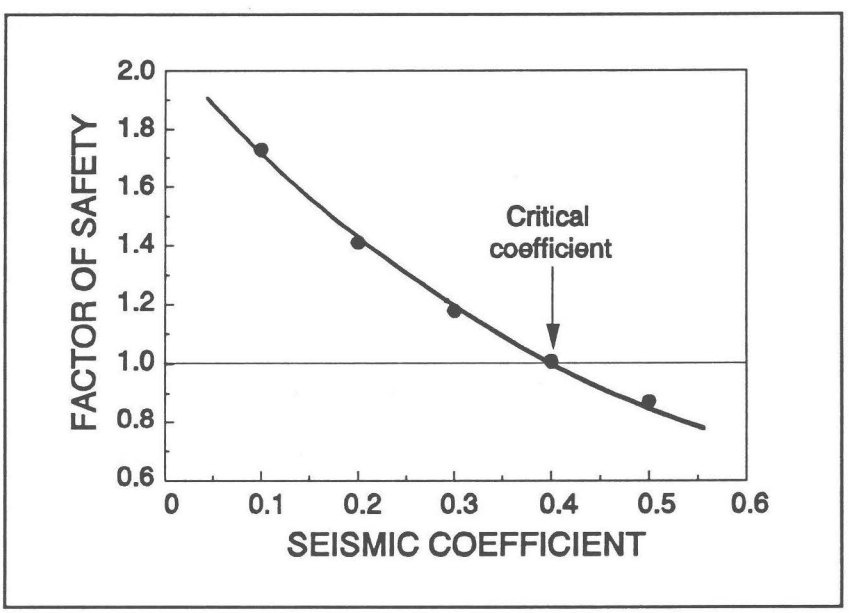

Figure 5.25. Variation of factor of safety with horizontal seismic coefficient, k_h, for example slope.

In examining Fig. 5.25, one can determine the critical seismic coefficient (or yield acceleration) that generates a factor of safety equal to one. Alternatively, the factor of safety

for any selected seismic coefficient within the k_h = 0 - 0.5 range can be readily determined from the data presented in Fig. 5.25.

For the slope analyzed, the critical coefficient (k_{hc}) is about 0.4. Table A21 in the Appendix list the input datafile for this example. This result may be interpreted such that if the expected seismic coefficient at the site is less than 0.4, the slope can be expected to remain stable during ground shaking. Conversely, the slope may be overly stressed if the seismic coefficient at the site happens to exceed 0.4. However, the slope may perform satisfactorily if the site seismic coefficient does not exceed the critical value of k_{hc} = 0.4.

In such cases, a Newmark Sliding Block Method (Newmark, 1965, and Hynes-Griffin and Franklin, 1984) may be adopted to link the critical and site specific seismic coefficients with a view to relating stability to the amount of expected displacement. This approach is based on using the computed k_{hc} coefficient as a site specific, average peak ground acceleration within the slope and comparing it with recorded accelerograms.

Franklin and Chang (1977) presented Fig. 5.26 that shows the variation between a normalized coefficient and the displacements for 354 available records. The data is presented in the form of three curves: (1) mean, (2) mean + σ and (3) an upper bound envelope to all results. The mean and the mean+σ curves were developed using regression methods. ***Please note that the displacements estimated by this methods are for qualitative use only and cannot be directly related to deformations of the embankment under analysis.***

For this example, if the expected site seismic coefficient corresponds to a peak ground acceleration (PGA) of 0.5g, the ratio k_{hc} / PGA = 0.80. Then by using the data presented in Fig. 5.26, the upper bound for the maximum amount of deformation may be estimated as approximately 20 cm. The mean and the mean+σ values will be considerably less than the 20 cm upper bound value.

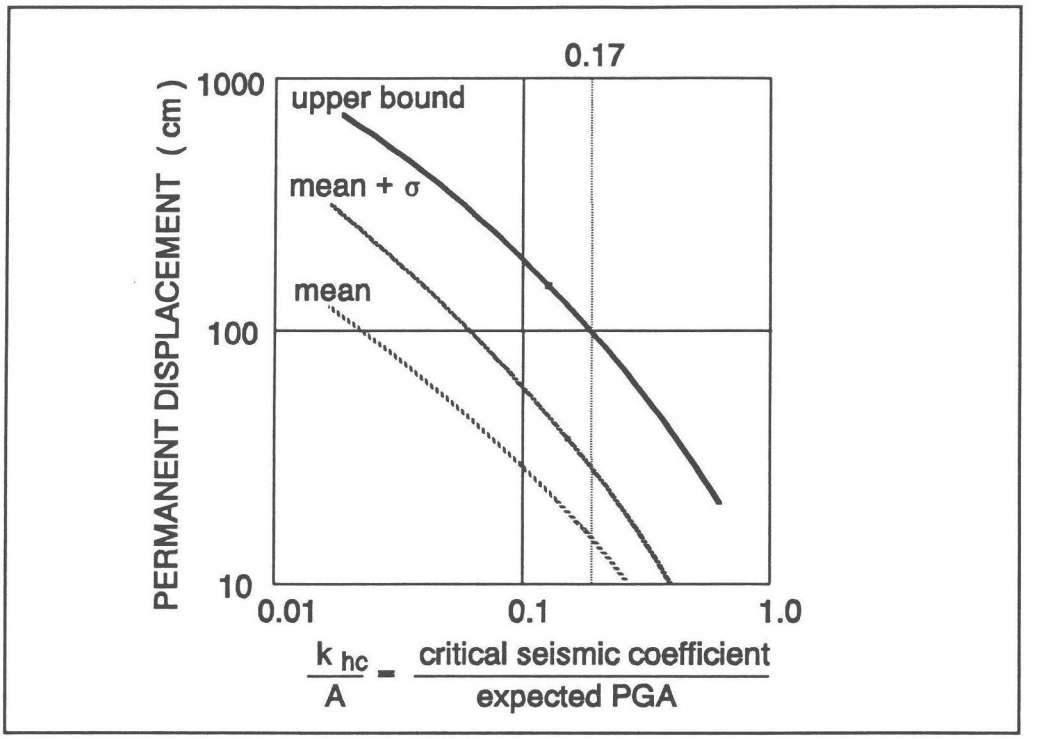

Figure 5.26. Permanent displacement as a function of N/A based on 354 horizontal accelerograms (Hynes-Griffin and Franklin, 1984).

Generally, embankment dam slopes can be expected to perform reliably for computed deformations that do not exceed 100 cm. Thus our example slope can be expected to perform satisfactorily during an earthquake that may generate a PGA that exceeds the critical seismic coefficient.

5.5 Curved Mohr-Coulomb Envelope

This example has been selected to illustrate the use of the nonlinear Mohr-Coulomb shear strength envelope option that is available in **XSTABL**. In this example, two rock-fill embankments will be analyzed with data from a publication by Charles & Soares (1984). The proposed embankment dams are to be constructed with rock-fill that has a curved Mohr-Coulomb envelope defined by:

$$\tau_f = 5(\sigma')^{0.75} \tag{5.2}$$

where τ_f is the shear strength and σ' is the effective normal stress. The curve, corresponding to the above equation, is shown in Fig. 5.27 along with the ten points used to simulate the nonlinear behavior using **XSTABL**.

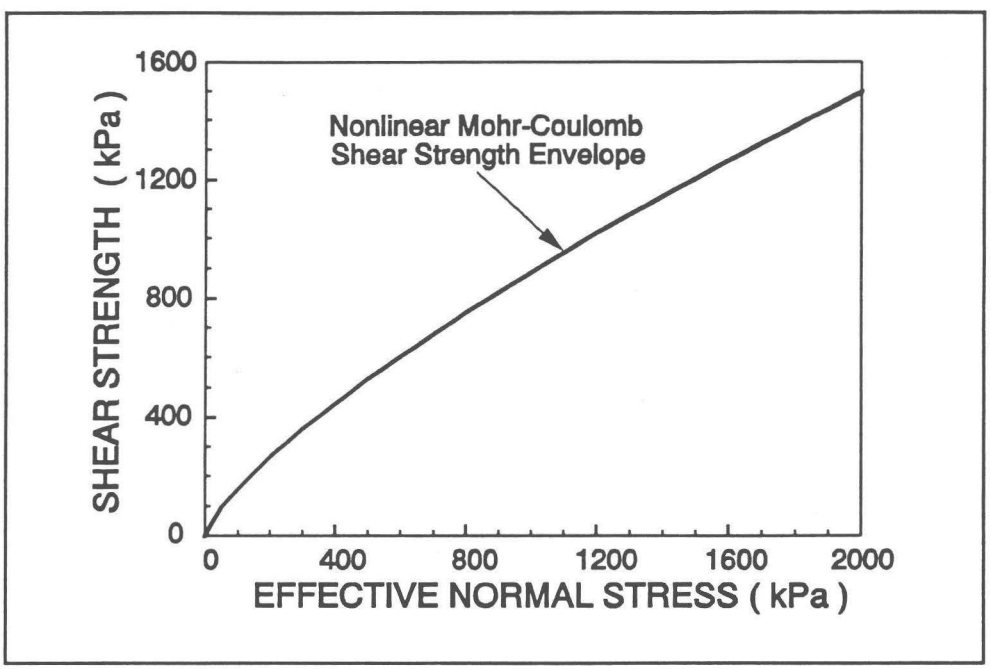

Figure 5.27. Shear strength as a function of effective normal stress

A 100-meter-high slope, inclined at 132H:100V was analyzed using the nonlinear Mohr-Coulomb envelope shown in Fig. 5.27. The discrete values of normal stress and shear strength for the rockfill are presented in Table 5.5 for stresses ranging up to 1200 kPa. The calculated c′ and ϕ' values for the specified ranges are also included in Table 5.5. One should note that ϕ' and c′ values range between 70.41° and 34.55° and 0.0 and 193 kPa, with the material displaying its greatest frictional strength at low effective stresses. The input data for the 100-meter slope is given in Table A22 in the Appendix.

Table 5.5. Nonlinear soil data for 100-meter-high slope

Normal Stress (kPa)	Shear Strength (kPa)	Assumed Parameters	
		ϕ'	c′ (kPa)
0.0	0.0		
		70.41	0.0
10.0	28.1		
		61.65	9.6
25.0	55.9		
		56.73	17.8
50.0	94.0		
		52.04	29.9
100.0	158.1		
		47.15	50.3
200.0	265.9		
		43.38	76.9
300.0	360.4		
		40.96	100.0
400.0	447.2		
		38.48	129.2
600.0	606.2		
		34.55	193.0
1200.0	1019.4		

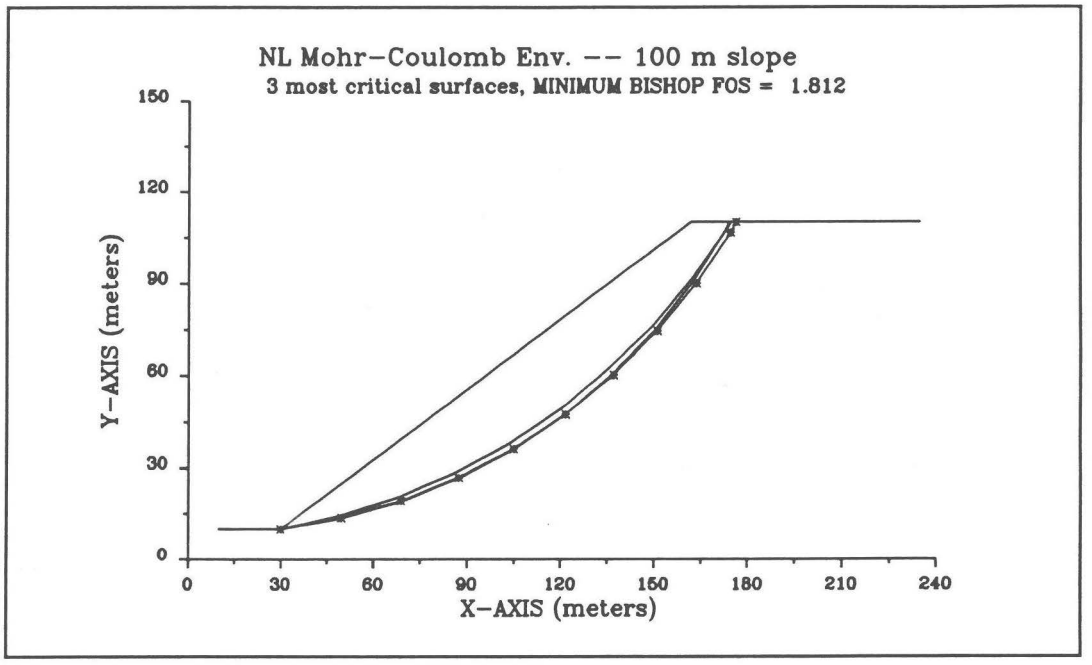

Figure 5.28. Critical failure surface for a 100-meter-high embankment using a nonlinear Mohr-Coulomb strength envelope

On the basis of 300 circular trial failure surfaces, the minimum factor of safety was calculated as 1.812. The three most critical surfaces are shown in Fig. 5.28.

In order to show the advantages of this method for cases where low normal stresses tend to dominate, a 10 meter high embankment with 1H:2V slopes was also examined using the input data listed in Table A23 in the Appendix. Using the nonlinear soil properties given in Table 5.6, and analyzing 300 circular trial failure surfaces revealed a FOS of 1.686. Results of this analysis, along with the three most critical surfaces, is shown in Fig. 5.29. From this figure, one can see that although a shallow critical surface was identified, a relatively high FOS value was computed due to the low effective stresses.

These calculated values are in good agreement with the FOS results of 1.8, presented by Charles and Soares (1984), for these two embankments.

Table 5.6. Nonlinear soil data for 10-meter-high slope

Normal Stress (kPa)	Shear Strength (kPa)	Assumed Parameters	
		ϕ'	c′ (kPa)
0.0	0.0		
		75.83	0.0
2.5	9.9		
		69.81	3.1
5.0	16.7		
		66.32	5.3
10.0	28.1		
		63.43	8.1
15.0	38.1		
		61.48	10.5
20.0	47.3		
		59.24	13.7
30.0	64.1		
		56.22	19.2
50.0	94.0		
		52.04	29.9
100.0	158.1		
		47.15	50.3
200.0	265.9		

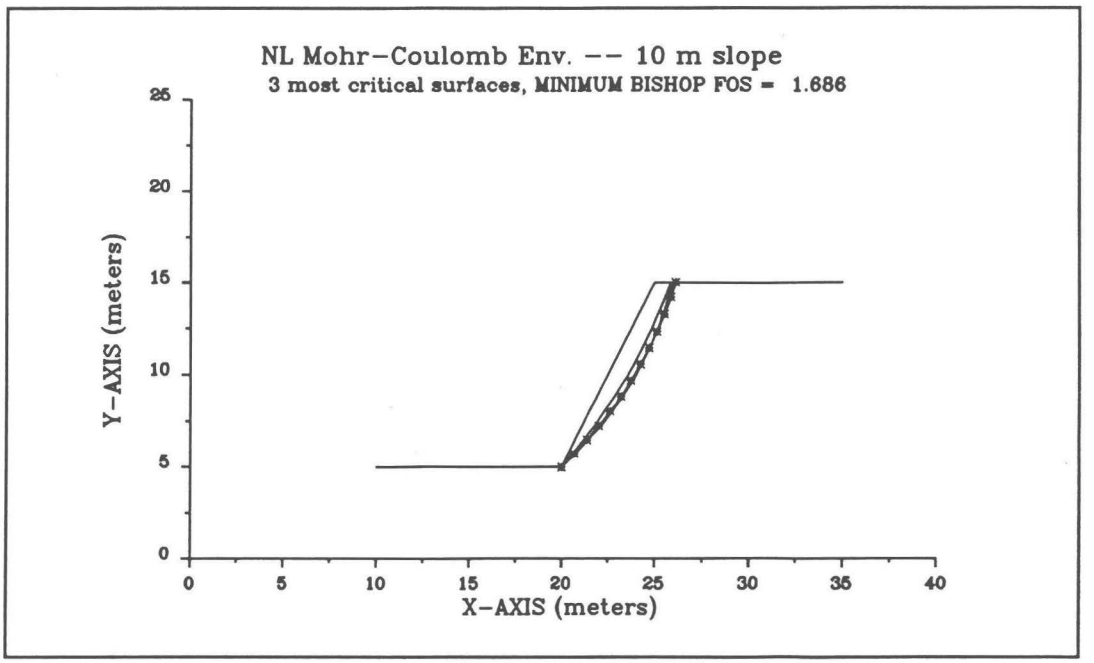

Figure 5.29. Critical failure surface for a smaller 10 meter embankment using nonlinear Mohr-Coulomb strength envelope

If the non-linear option had not been available, these slopes would have been analyzed on the basis of an *average* ϕ based on the average vertical effective stress. In this case, if the average effective stresses had been estimated as 600 kPa and 60 kPa for the 100 meter and 10 meter embankment, respectively, the appropriate angles of internal friction would be about 45.3° and 60.9°. If a similar stability analysis is performed with these single ϕ' values, a factor of safety of 1.344 and 0.923 is calculated for the 100 meter and 10 meter slope, respectively. Although these values are significantly lower than the FOS values computed for the nonlinear envelope, the critical failure surfaces were relatively shallow. The input data for these equivalent analyses is listed in Tables A24 and A25 in the Appendix.

These two examples have illustrated the use of the nonlinear Mohr-Coulomb for specifying the shear strength parameters. Charles and Soares (1984) used these examples to illustrate how very high rockfill dams can be safely constructed at angles that approach the angle of repose of loose uncompacted rockfill. The second case showed the 10 meter embankment may be safely constructed at angles that ***exceed*** the angle of repose of loose rockfill.

5.6 Geotextile Reinforcement

In principle, limit equilibrium analyses should ***not*** be used to determine the factor of safety for a failure surface that intersects geotextile reinforcement. In most cases, the strain required to mobilize the soil strength is substantially greater than the strain required to fail the geotextile material. With such (obvious) strain incompatibility, the limit equilibrium approach with its assumption that all slices have the same FOS, is unlikely to provide a reasonable answer and may also cause numerical difficulties. Any such FOS calculated for a geotextile reinforced slope is not a quantitative measure of the stability of the slope.

However, limit equilibrium programs, such as **XSTABL**, may be successfully used to investigate the overall stability of the slope and possibly identify zones that may require reinforcement. The following example presents a solution for a 12 meter high, 45° slope with a 40 kPa surcharge. This slope, shown in Fig. 5.30, has been presented as an example problem by Koerner (1991).

The reinforced slope analysis allows the user to determine the magnitude of external force necessary to maintain a specified factor of safety (FOS). In this example, the slope is designed for a FOS = 1.5 and reinforcement will be provided for the entire 12 meter height of the slope. In using the reinforcement option, the critical surface shown in Fig. 5.31, was found to require a horizontal external force of 345 kN, per lineal meter, to maintain the necessary design FOS > 1.5. This force may be simulated by a triangular stress distribution that varies from zero to 57.5 kPa. The input data for this case is listed in Table A26 in the Appendix.

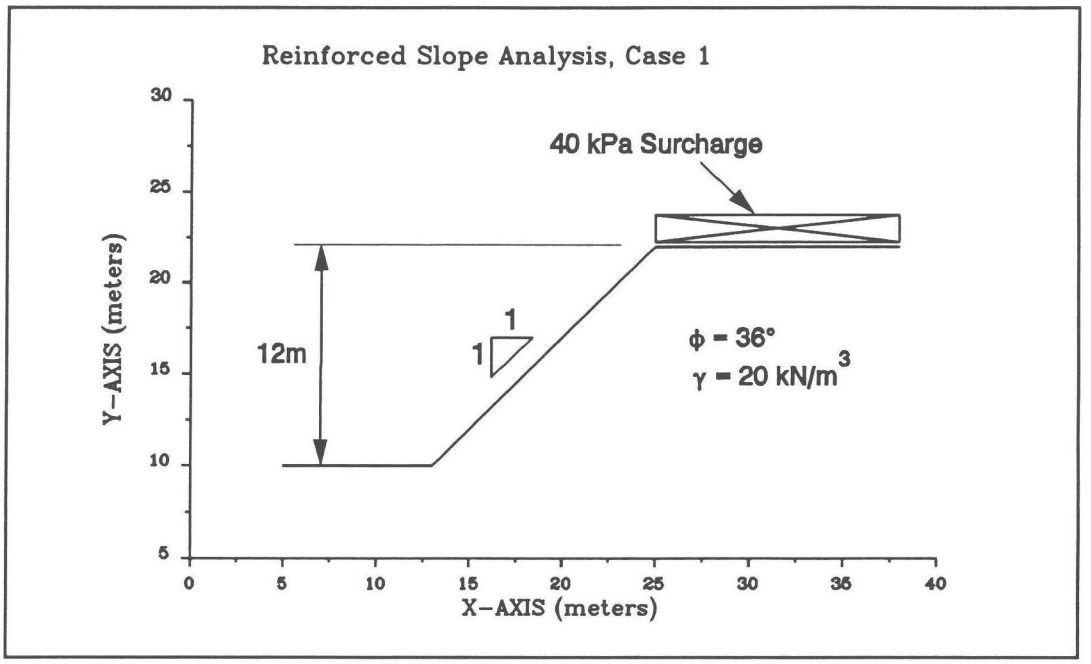

Figure 5.30. Slope for reinforced soil example

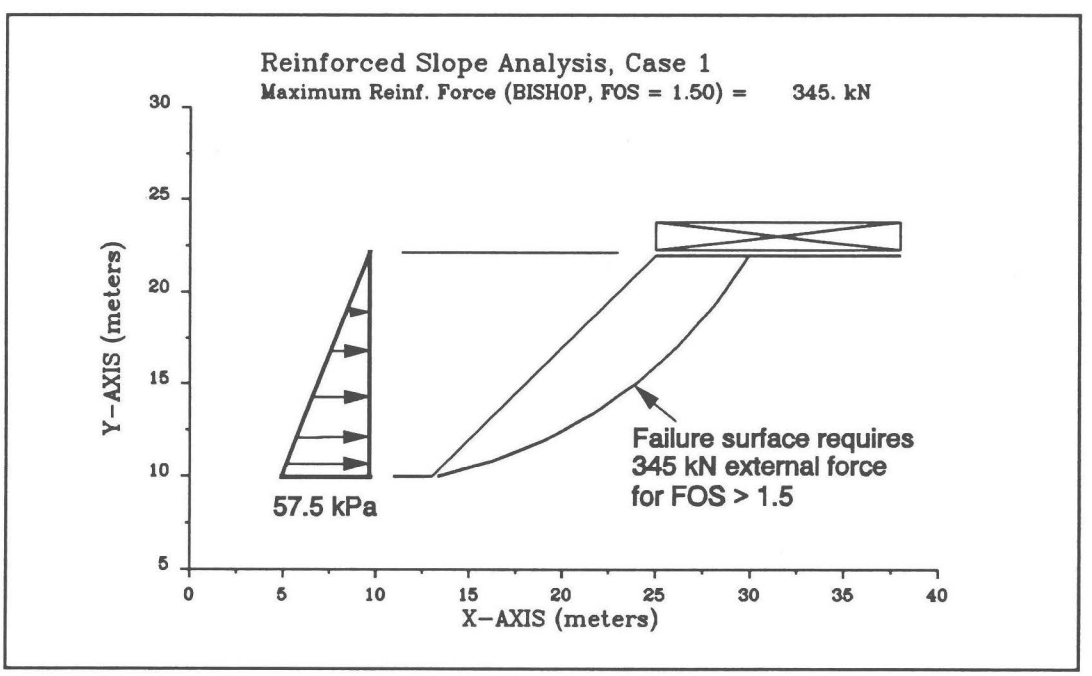

Figure 5.31. **XSTABL** results showing location of critical failure surface requiring an external force of 345 kN to maintain FOS = 1.5.

Following the reinforced analysis, **XSTABL** is used to assess the stability of the unreinforced 45° slope, using the input data from Table A27. The analysis reveals that the slope has a minimum FOS, $F_{crit} = 0.734$ for the critical surface shown in Fig. 5.32. The surface, requiring the 345 kN of external support is also shown in the same figure for comparison. If the reinforced slope must maintain a minimum FOS > 1.5, the strength parameters of a reinforced zone are determined according to Eqs. 2.23 and 2.24:

$$F_r = \frac{F_{min}}{F_{crit}} = \frac{1.5}{0.734} = 2.044$$

$$\phi_{reinf} = \tan^{-1}\left[2.044 \tan (36°)\right] = 56.04°$$

Next the analysis is repeated by including a reinforced zone, with $\phi = 56.04°$, as shown in Fig. 5.33. The critical surface, with a FOS > 1.5, is determined using an iterative process, which varies the lateral extent of the reinforced zone manually. The required reinforced region should correspond to the case where the critical surface has a FOS > 1.5. The reinforcing zone specified for this analysis is used to satisfy the criteria for ***external*** stability. The results of the above analysis, based on input data from Table A28 and A29, may be summarized as:

1. Required reinforcement force = 345 kN,
2. Reinforced zone extends *at least* 7.5 meters into the slope.
   (The FOS for a 6 meter reinforced zone was 1.412)

Please note that the reinforcement must be longer than 7.5 meters to ensure that adequate embedment is available to resist the anticipated tensile forces. This embedment length depends on the reinforcement type, spacing and the magnitude of the design force and cannot be determined using **XSTABL**. A ***minimum*** embedment length of 1 meter, or 3 feet, is generally recommended for the design of steep reinforced slopes.

For the same problem, Koerner (1991) calculated an external force of 294 kN and a reinforcement length that ranges from 8 meters at the crest to 11 meters at the toe of the slope. Koerner's solution requires 85 percent of the force calculated using **XSTABL**, but the extent of the required reinforced zone, based on a minimum 1 meter embedment, is 27 percent *larger*.

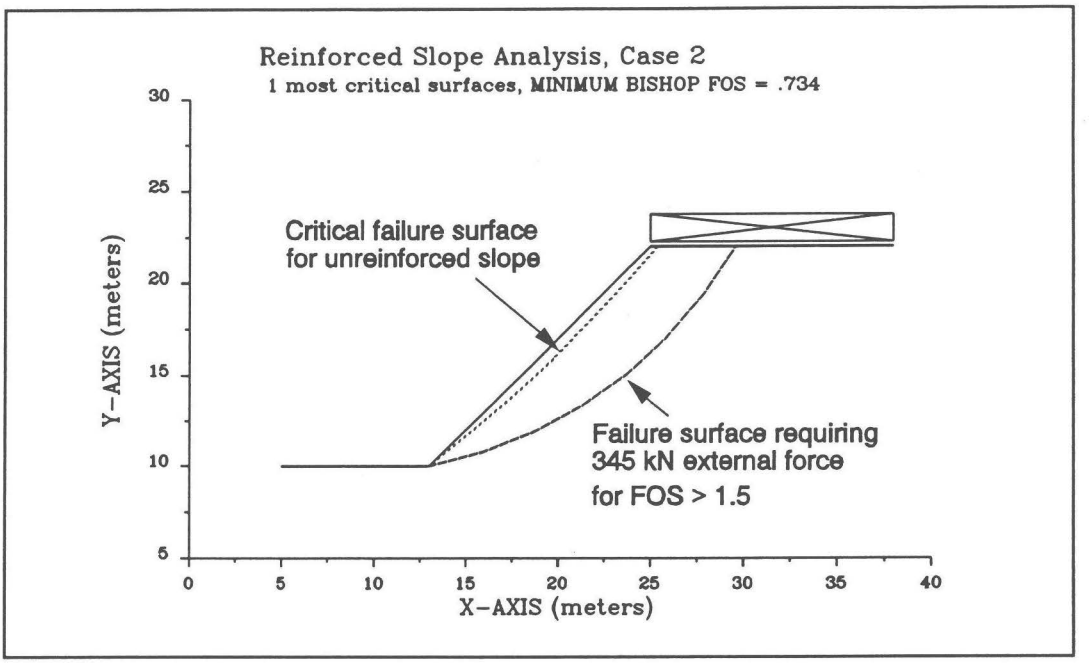

Figure 5.32. Comparison of failure surfaces for unreinforced slope and surface requiring maximum external force.

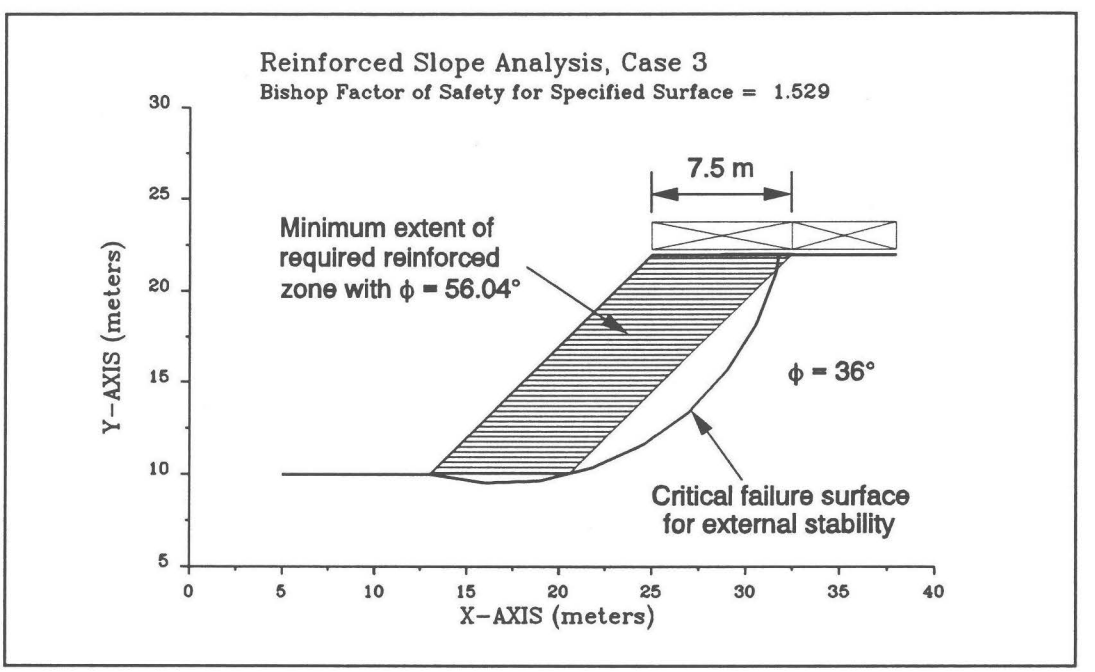

Figure 5.33. Check for external stability for a 7.5 meter reinforced zone.

5.7 Negative Effective Stresses

Two examples, one simple and one complex, are presented in this section to illustrate the effects of choosing the different options to control the influence of calculated negative effective stresses.

Example 1

The first example consists of a 45° slope with three soil units. The shear strength values and the slope profile are shown in Fig. 5.34. The data for this analysis is listed in Table A30 in the Appendix.

The critical surfaces identified by **XSTABL** on the basis of 150 trial surfaces are shown in Fig. 5.35. It is interesting that significantly different surfaces have been identified according to the control options selected for these analyses. In this figure, the selection of options 1 and 2 generated the same critical surface with a FOS of 1.362. This indicates that even though the effective stress was negative for the last four slices out of a total of 27 slices, the shear strength ($c + \sigma' \tan\phi$) was always greater than zero.

However, if the user chooses to disregard all surfaces that have negative effective stresses at the base of more than five percent of the slices (i.e., option 3), a FOS of 1.834 was reported by the program. For this analysis, 119 surfaces were rejected out of a total of 150 surfaces examined for the search for the most critical surface. Such high rates of surface rejection are usually attributed to an unrealistic selection of trial failure surfaces for the slope geometry and subsoil conditions.

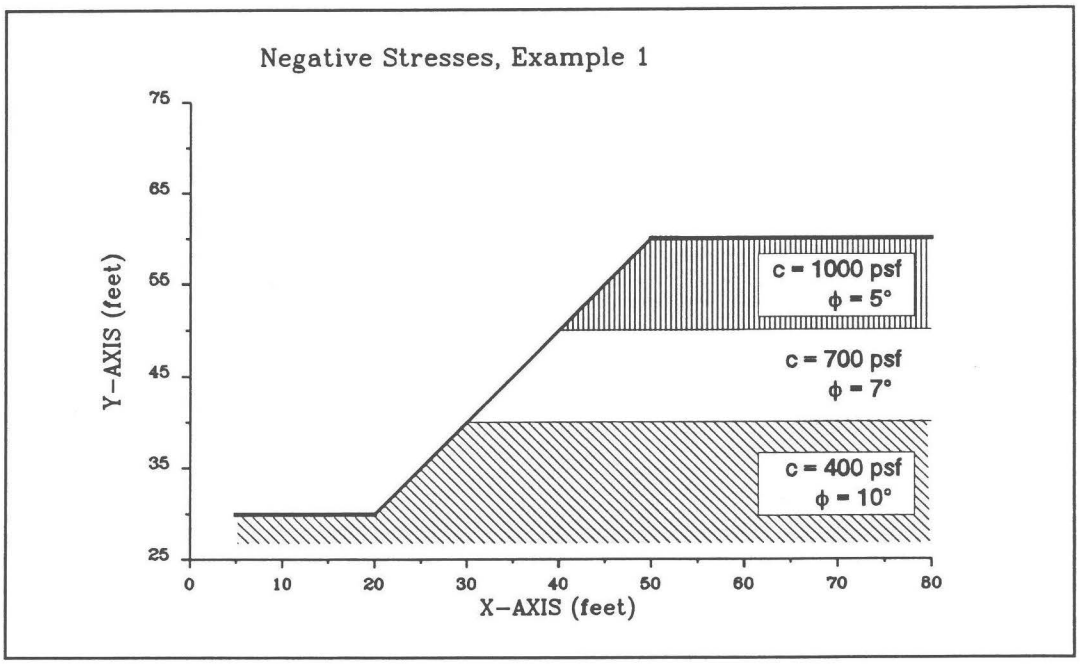

Figure 5.34. Slope geometry for illustrating influence of negative effective stresses.

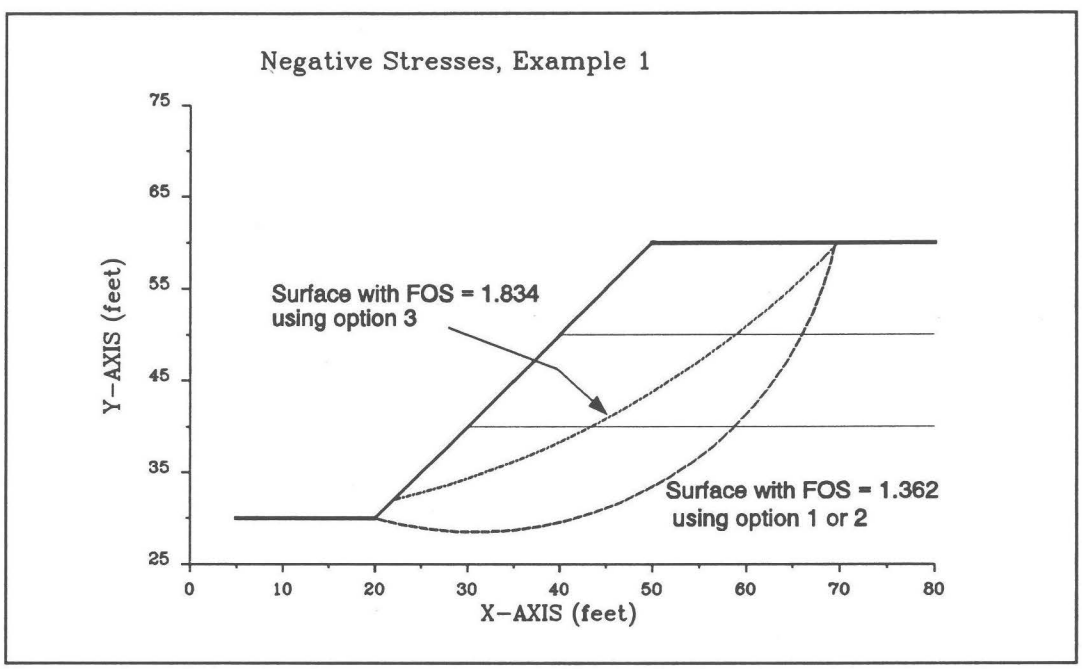

Figure 5.35. Results showing the effects of controlling negative effective stresses.

Example 2

The second example is included to further illustrate the possibility that significantly different solutions may be generated depending on the approach selected to consider the effects of calculated normal effective stresses. The data for this analysis is given in Table A31 in the appendix. The slope geometry for this reinforced-fill and the critical surfaces identified by searching with 1,500 trial surfaces using **XSTABL** are presented in Figs. 5.36 and 5.37, respectively.

From Fig. 5.37 one can readily see that the critical surfaces are very dissimilar and there is a *large* difference between the calculated FOS values. If one opts to use the negative effective stresses, negative shear strengths are not calculated and so the FOS = 1.302 is computed for both options (1) and (2). In examining the critical surface shown in Fig. 5.37, there were three slices (#1, 27 and 34) out of 49 slices that had a negative effective stress at their base due to the small self-weight and high "c" value.

In this example the geotextile reinforcement, simulated by a thin layer, has been given a relatively high "c" value of 9999 psf. This thin soil layer generates "thin" slices with small self-weight and the high "c" value, which leads to the computation of negative effective stresses (see Eq. 2.26). Thus almost all trial failure surfaces that intersect these reinforcement layers will lead to numerical problems. However in this case, one should recognize the reasons for the large discrepancy in the reported minimum values of the FOS depending on the control option selected by the user. Also, since this material has $\phi = 0°$, the shear strength calculated as a result of selecting option 1 or 2 will be the same, as indicated by identical FOS values. The 89 percent rejection rate is again very high and reflects the incompatibility associated with the high c = 9999 psf strength associated with the soil reinforcement layers.

If the user chooses to discard surfaces with a negative effective stress (as programmed into **XSTABL** version 4.0), calculations indicate a FOS of 2.982. However, in this case 1,341 surfaces out of a total of 1,500, (or 89 percent) were rejected during the search as deeper surfaces that bypassed the reinforcing layers were retained for the final summary.

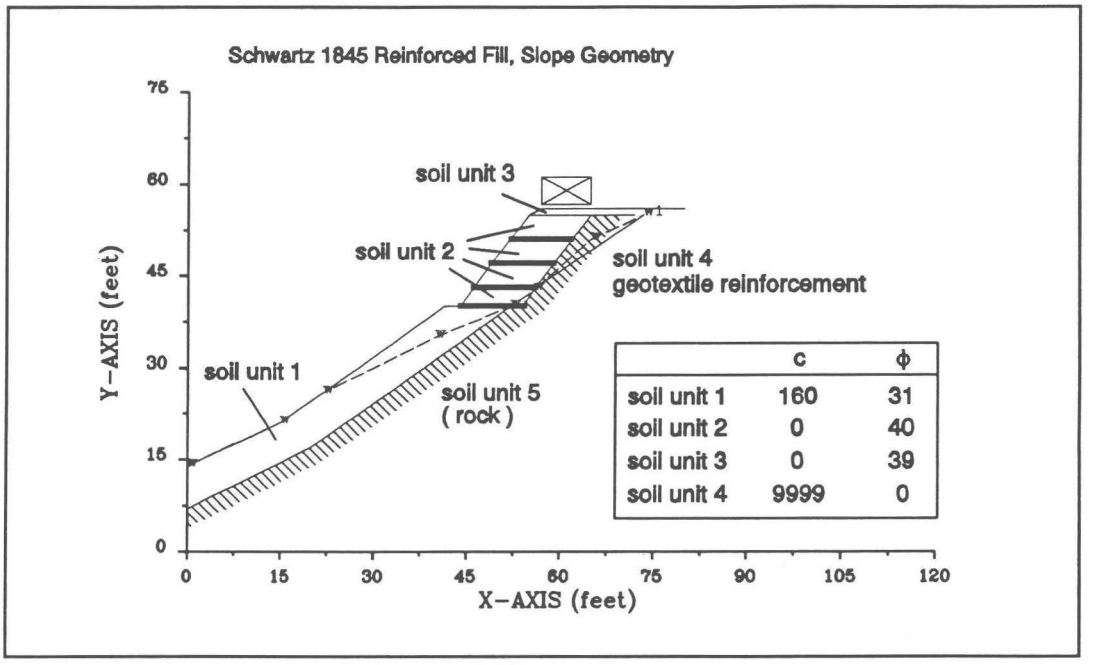

Figure 5.36. Slope geometry used to illustrate significance of options for controlling use of negative effective stresses

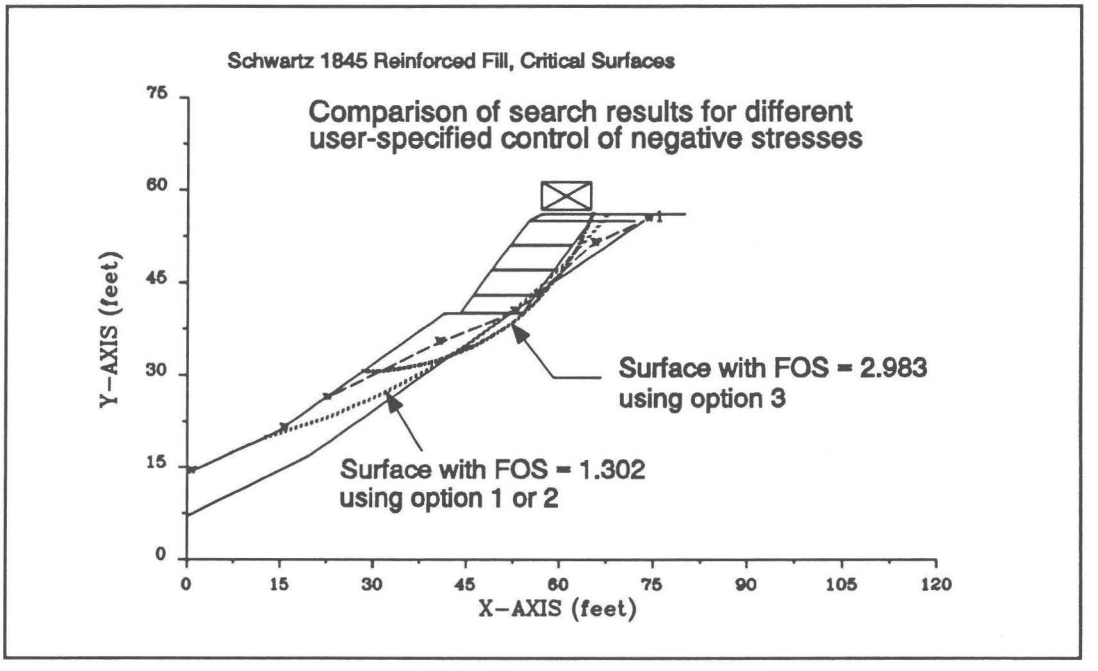

Figure 5.37. Critical failure surfaces identified using option 1 (strength $\geq$ zero), option 2 (unrestricted strength) and option 3 ($\sigma' \geq$ zero).

5.8 Random Search for Critical Surface

Some concern has been expressed about the capability of **XSTABL** to effectively identify the critical failure surface associated with the minimum FOS. In order to illustrate the effectiveness of random procedure employed by **XSTABL**, the results from the previous analysis of 1,500 surfaces will be used to provide a summary perspective of the analysis.

The centers of the 1,500 circles generated from 60 initiation points within the initiation range, x = 0 - 30 feet, occupied a region bounded by the approximate coordinates: x = -1000 and 100 feet and y = 50 and 1500 feet. Figure 5.33 presents a window of this region and shows the centers of 1,421 trial circles used to identify the critical surface.

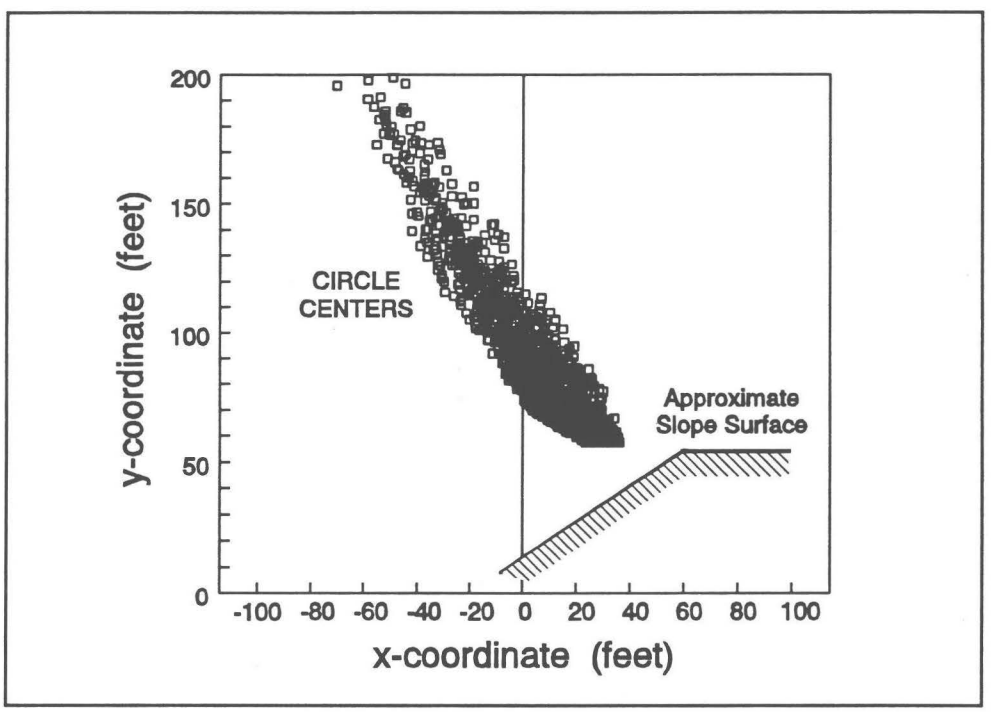

Figure 5.38. Centers of trial failure surfaces used for search of critical surface and minimum FOS

The data shown in Fig. 5.38 can also be summarized according to the location of the initial point (near the toe of the slope) for the search process. The FOS values for the 1,500 circular surfaces are presented in Fig. 5.39. This figure shows the minimum, average and maximum values of the FOS based on 25 trial circular surfaces generated from 60 initiation points. One can see that the FOS values, for the trial surfaces, range between about 1.3 and

3.6. The extent of this range appears to be large, but one can see that the minimum values for the 60 initiation points only vary between 1.3 and 1.7. Thus the search procedure has probably located the approximate minimum FOS and the critical surface.

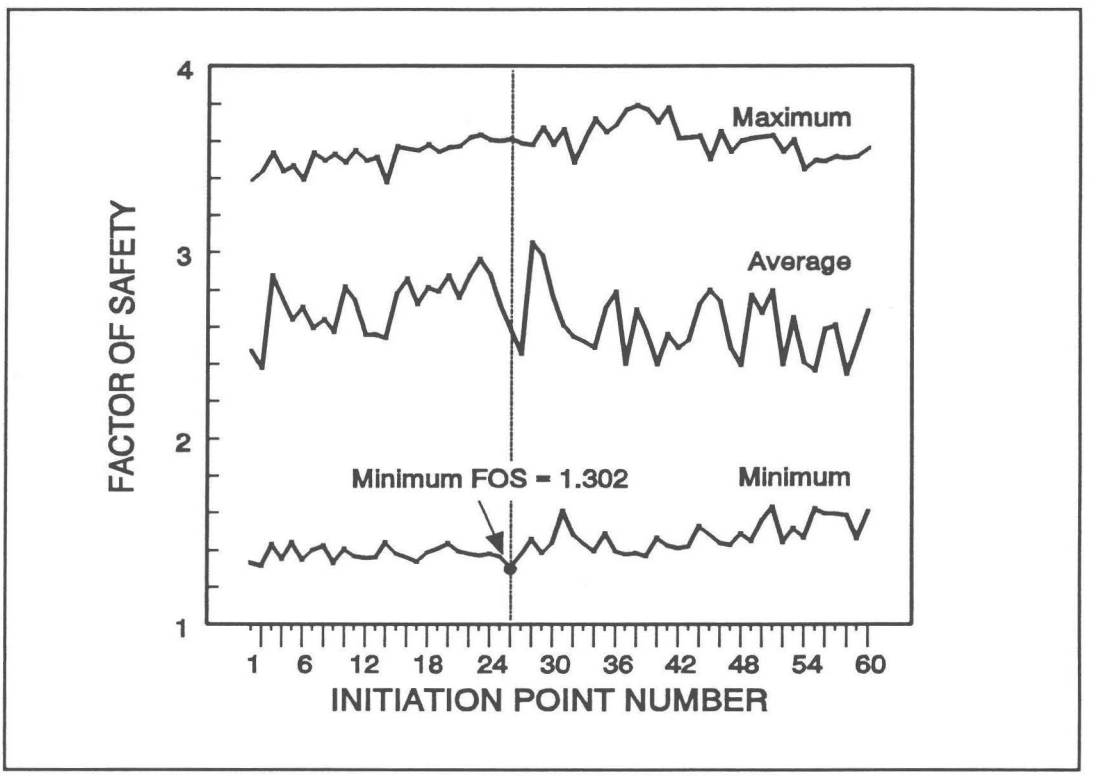

Figure 5.39. Minimum, maximum and average FOS values computed at each initiation point for 25 trial failure surfaces

If one takes the x, y and FOS values as a set, contours may be determined to investigate the spatial variation of the FOS values. Fig. 5.40 presents such a contoured diagram where the FOS values were interpolated using an inverse square method applied to the selected 1,421 data points. The minimum FOS value is located at about x = -15 and y = 123 feet.

From this figure one can readily see that the reported minimum FOS value of 1.302 is probably the critical value for the slope geometry and subsoil conditions. However, it should be noted that there are large variations in the FOS value in the "minimum" region as circles with different radii, and different soil conditions, are being analyzed for the search. This variation is much more pronounced in the three dimensional plot shown in Fig. 5.41.

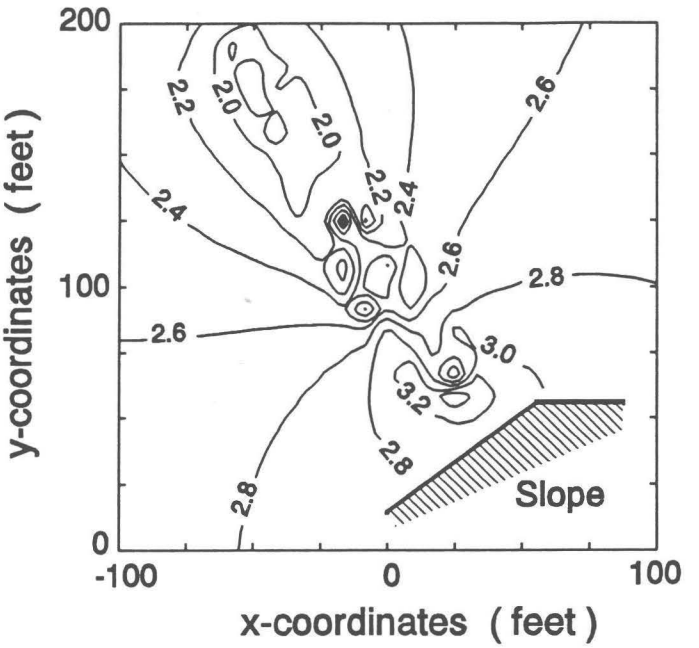

Figure 5.40. Contours showing the spatial variation of the FOS values for the trial surfaces generated for slope shown in Fig. 5.36

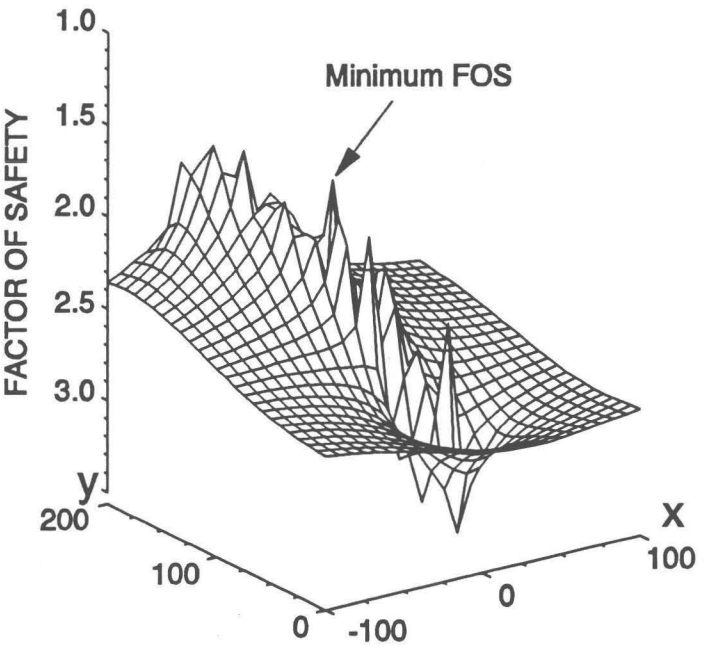

Figure 5.41. Three dimensional plot showing variation of FOS values for slope shown in Fig. 5.36 -- minimum is at (-15, 123)

CHAPTER 6

SPENCER'S ANALYSIS

The use of the Limit Equilibrium method for the assessment of slope stability has made great advances since the introduction of the Original Method of slices (Fellenius, 1936). This advancement has concentrated on developing a more robust, and precise, analytical method that can be reliably used to predict the behavior of existing and new slopes (e.g. Bishop, 1955; Janbu, 1957; Morgenstern and Price, 1965; Spencer, 1967 and 1973).

The main difference between the various methods is the implementation and inclusion of the inter-slice forces within the analytical framework. For example, the user may neglect the influence of inter-slice forces and calculate the factor of safety (FOS) using either the Modified Bishop or Janbu methods. Alternatively, the user may choose to include the effects of the inter-slice forces and select the more rigorous methods of analysis, such as the Spencer or Morgenstern and Price methods.

Analytically, the effects of the inter-slice forces must be included to satisfy complete equilibrium for the calculation of a *true* FOS. However, as the general limit equilibrium problem is indeterminate, different assumptions may be made regarding these inter-slice forces. The common assumptions usually concern the inclination of the interslice force, which may be assumed to be constant (Spencer, 1967; 1973) or a function of the slope geometry (Morgenstern and Price, 1965). Of course, if an engineer chooses to use a method that satisfies complete equilibrium, a decision has to be made regarding the underlying assumptions of the assigned inter-slice angle distribution. Also, since the more rigorous methods require a greater amount of computer time for the calculations, these have not been extensively used by practicing engineers and thus there is noticeable lack of experience that often comes through routine familiarity.

This section presents the increasingly popular Spencer's Method (1967, 1973) that satisfies complete equilibrium by implicitly including several necessary assumptions. This feature has been included in this manual to assist users of **XSTABL** gain some familiarity with a method that satisfies complete equilibrium. At this time, this analysis may be performed using the "spreadsheet" program discussed in a later section. *However, it is expected that a version of* ***XSTABL*** *capable of calculating Spencer's factor of safety will become available in 1993.*

In reviewing this section, the user will find that the method is very sensitive to the slope conditions and can also generate ambiguous FOS values (Chugh, 1981). The scope of this section is limited to reviewing the implications of the assumptions made by Spencer regarding the calculation of a "reasonable" FOS for two example slopes. Finally, recommendations are provided to guide and help the geotechnical engineer with the use of Spencer's Method for the analysis of slopes.

6.1 SPENCER'S METHOD

This method was originally presented in 1967 for calculating the FOS for circular failure surfaces. Later, Wright (1969 and 1974) and Spencer (1973) extended the method to calculate the FOS of any general, arbitrarily shaped failure surface. The method ensures force and moment equilibrium for a common interslice force angle, θ, for all slices. The formulation that is used in the interactive program uses an extension of the theoretical development presented by Chugh (1981).

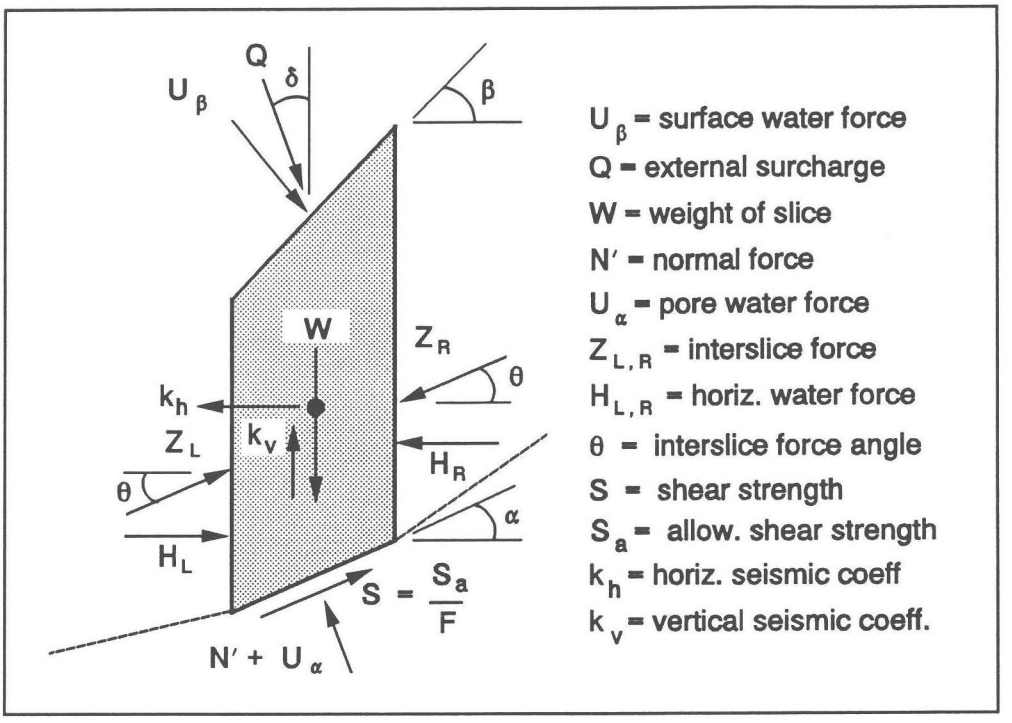

Figure 6.1. Forces acting on a typical slice

Force Equilibrium

For the typical slice shown in Fig. 6.1, by resolving forces normal and parallel to the base, the following force equilibrium equation may be formulated:

$$
\begin{aligned}
Z_R = Z_L + A_1 \Big[& W\cos\alpha\,(1 - k_v)(\tan\phi_m - \tan\alpha) \\
& + C_m - W\cos\alpha\, k_h\,(1 + \tan\phi_m\tan\alpha) - U_\alpha\tan\phi_m \\
& + (H_L - H_R)\cos\alpha\,[1 + \tan\alpha\tan\phi_m] \\
& + U_\beta\,[\cos(\alpha - \beta)\tan\phi_m - \sin(\alpha - \beta)] \\
& + Q\,[\cos(\alpha - \delta)\tan\phi_m - \sin(\alpha - \delta)]\Big]
\end{aligned}
\qquad \textbf{(6.1)}
$$

where:

$$
\tan\phi_m = \frac{1}{F}\tan\phi \qquad \text{and} \qquad C_m = \frac{C}{F} \qquad \textbf{(6.2)}
$$

and the factor A_1 is given by:

$$A_1 = \frac{1}{\cos(\alpha - \theta)\,[\,1 + \tan\phi_m \tan(\alpha - \theta)\,]} \tag{6.3}$$

Moment Equilibrium

The conditions for moment equilibrium are satisfied by taking moments of all forces about the midpoint at the base of the slice, as shown in Fig. 6.2. This formulation is used to determine the location of the interslice force on the right-hand-side of the slice according to the affected forces shown in Fig. 6.2:

$$h_2 = \frac{Z_L}{Z_R} h_1 + \frac{b}{2}[\tan\theta - \tan\alpha]\left[1 + \frac{Z_L}{Z_R}\right] - \frac{k_h}{Z_R \cos\theta} W h_5 + \frac{1}{Z_R \cos\theta}\left[(h_3 H_L - h_4 H_R) + h(U_\beta \sin\beta + Q \sin\delta)\right] \tag{6.4}$$

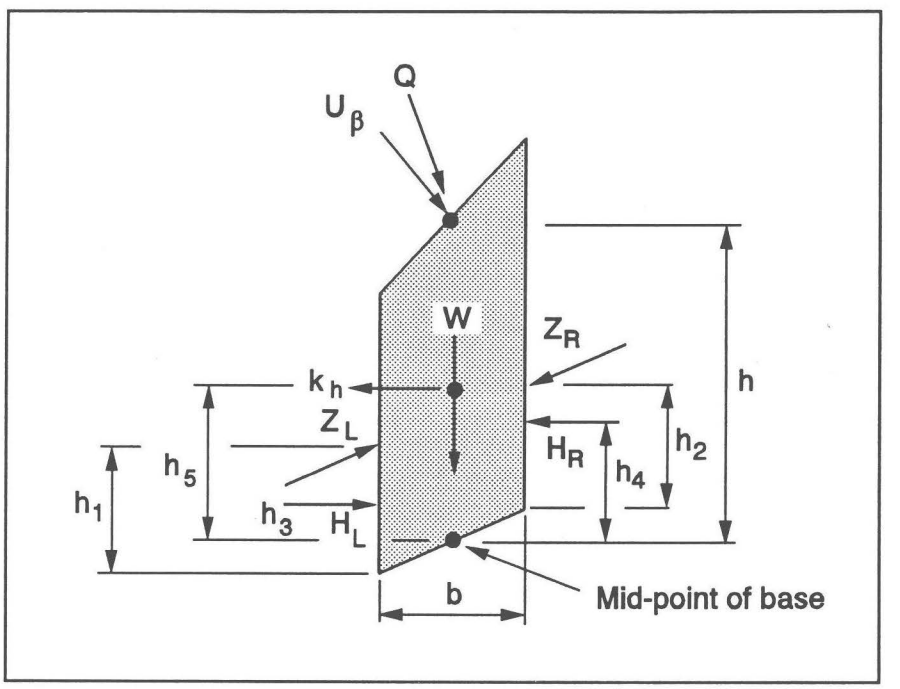

Figure 6.2. Dimensions used for moment equilibrium

6.2 Factor of Safety

The Factor of Safety (FOS) is calculated using an iterative procedure that varies F and θ until force and moment equilibrium conditions are satisfied for all slices. The solution procedure is based on the iterative procedure proposed by Spencer (1972). Alternatively, a numerical/graphical technique may also be used to obtain the final FOS value (Chugh, 1981). Users should ensure that the selected solution procedure iterate to the correct FOS or θ without generating misleading answers (Soriano, 1976; Chugh, 1981).

The FOS and the interslice angles for all examples presented in this paper were calculated using an application that has been programmed into a spreadsheet (Sharma and Moudud, 1992). This application directly reads the output file generated by the slope analysis program **XSTABL** (I.S. Designs, 1992) and calculates the FOS and θ values iteratively. This approach allows the engineer to view readily the changes in the thrust line, interslice forces and the effective normal stresses at the base of each slice.

```
22-Jun-92          SPENCER'S SOLUTION using XSTABL, 1992          Version 2.00

        Example for Spencer's FOS, Problem 1

          Modified BISHOP factor of safety =        2.000

      FORCE EQUILIBRIUM                MOMENT EQUILIBRIUM

         FOS_f =   2.000                  FOS_m =   2.0000
       THETA_f =                        THETA_m= 17.42404
       Z_R (n) =   -876.7               h_2 (n) =    -6.11

      Coeff k_v =    0.000              Tolerance =    10.00
      Coeff k_h =    0.000              (on iteration of Z_R (n) value)

      DEPTH OF CRACK  =        0.00    (feet)
      HEIGHT OF WATER =        0.00    (feet)
      WATER UNIT WT.  =       62.40    (pcf)

  F1=HELP  F3=START  F4=ITERATE  F6=VIEW  F7=QUIT  ALT=MORE  READY
```

Figure 6.3. Spreadsheet interface for Spencer's factor of safety

The interface for this application is shown in Fig. 6.3. From this interface, the user can readily perform the analysis and quickly view the changes as all the numbers are visible. After the slice data from **XSTABL** has been parsed, the user can proceed with the iteration process by pressing the "F4" key. A "pop-up" box then prompts the user to make a selection as shown in Fig. 6.4. Similar commands may be used to view the different graphs that show the thrust line, interslice force and effective normal stress distributions.

The user may start the program by pressing the F3-key and supplying the full name for a *.OPT output filename created following the analysis of a single surface with **XSTABL**. There are far too many columns of data in the spreadsheet that can be adequately described herein. Basically, the user can specify the acceptable "tolerance" for force equilibrium, with value less than 10 lb being found reliable. The analysis is started by pressing the F4-key and opting to either perform a single step or a complete iteration. Plots of the thrust line location, effective normal stresses and the interslice forces can be viewed by pressing the F6-key.

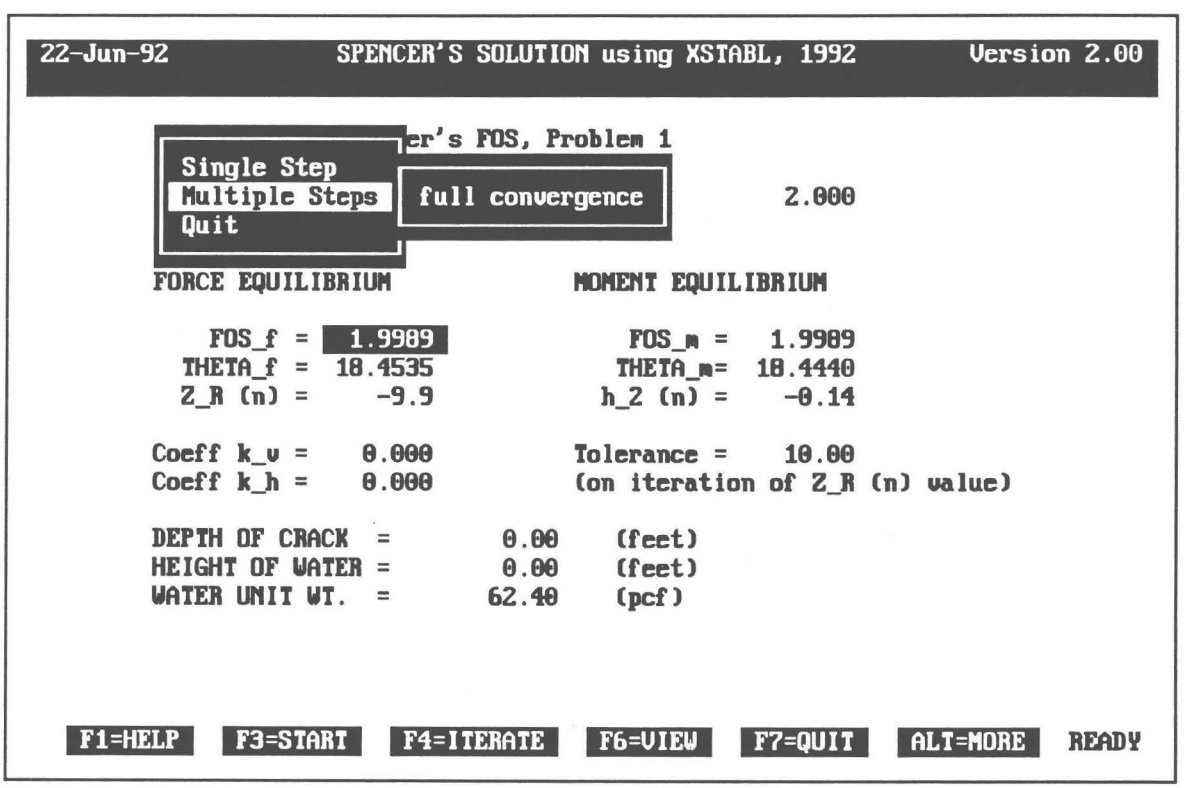

Figure 6.4. Spreadsheet interface for Spencer's factor of safety

If the reasonableness of the solution is in doubt, cracks may be incorporated into the solution by eliminating the influence of slices near the crest of the failure surface. If water is expected to infiltrate the cracks, the iteration process may be terminated once the Z_R interslice force for the last slice equals the anticipated hydrostatic force attributable to the water in the crack. The spreadsheet environment has been selected to allow the engineer to view readily the changes in the inter-slice forces and thrust line as the iteration procedure progresses towards convergence.

6.3 Example Applications

In order to illustrate Spencer's method, two slopes will be analyzed to illustrate the complexities and subtleties that may lead to difficulties in calculating a *reasonable* FOS value. The **XSTABL** data files for the five different cases presented in this section are given in the Appendix as: SPENC_1.IPT . . . . SPENC_5.IPT to allow readers an opportunity to gain some familiarity with the Spencer's solution proposed herein. The data in SPENC_5.IPT file, listed in Table A36 in the Appendix, is for use with **XSTABL**. However, it is possible to make changes to the output data from SPENC_4.IPT to arrive at similar results.

Problem 1

The first slope, shown in Fig. 6.5, is intended to show the effects of the shear strength parameters, namely the influence of the c and ϕ values. The 2H:1V slope is 40 feet high. The strength parameters for three cases, along with other properties and the calculated FOS values using the Bishop, Janbu and Spencer method are summarized in Table 6.1.

The same geometric slope is analyzed for the three isotropic soil conditions listed in Table 6.1 to show the sensitivity of Spencer's method to soils with different strength parameters. The factor of safety values calculated using Bishop's and Janbu's (both uncorrected and corrected) methods are also presented for comparison in Table 6.1. This example slope, shown in Fig. 6.4, is the same geometric slope that has been previously analyzed by Fredlund and Krahn (1977) and found to have a Spencer's FOS = 2.083 and θ = 14.81° for soil parameters corresponding to case 1(c). The assumed failure surface is simulated by a circular arc centered at x_c = 70.0 feet and y_c = 91.14 feet and a radius of 80 feet. Thirty one slices were used to simulate the effects of the sliding mass above the failure surface.

Table 6.1. Summary of data and results for Example Problem 1

Case #	c (psf)	ϕ	FACTOR OF SAFETY				Spencer's θ
			Bishop	Janbu		Spencer	
				Uncorr.	Corr.		
1(a)	0.0	33°	2.000	1.738	1.822	1.999	18.446°
1(b)	1400.0	0°	2.233	2.147	2.375	2.233	8.159°
1(c)	600.0	20°	2.077	1.877	2.022	2.073	14.479°

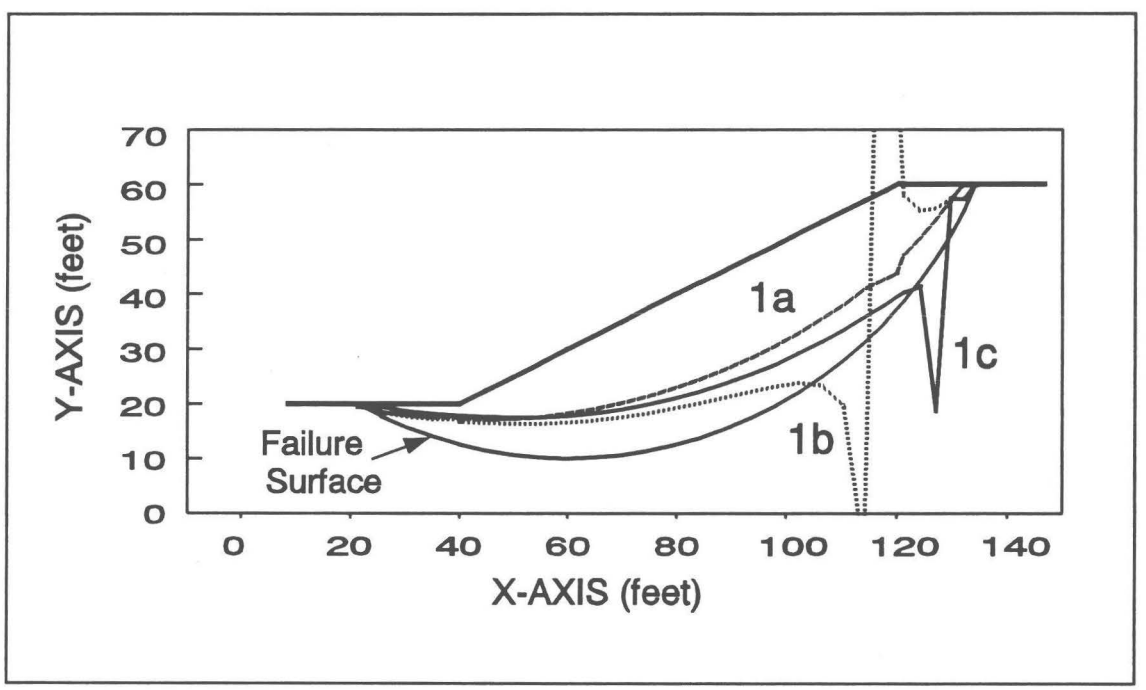

Figure 6.5. Thrust line location for example problems 1a, 1b and 1c.

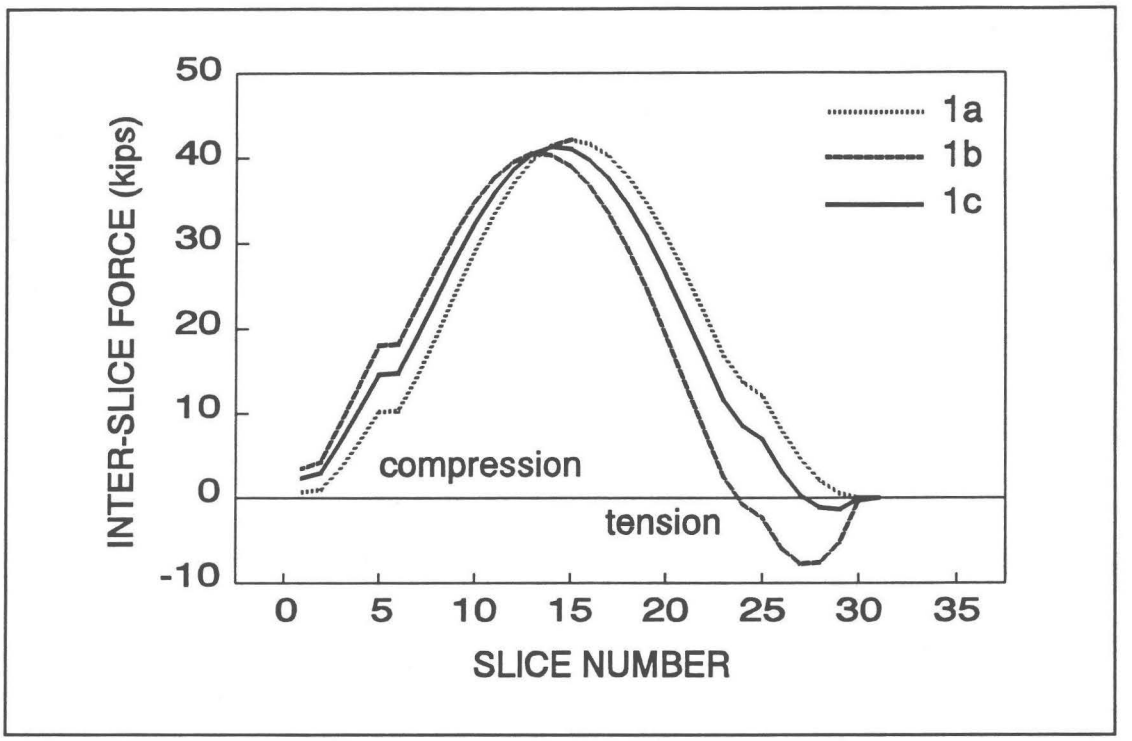

Figure 6.6. Magnitude of interslice forces for example problems: 1(a) – 1(c)

Fig. 6.5 shows the location of the thrust lines for the ϕ-only (1a), c-only (1b) and ϕ - c (1c) soil parameters. From this figure one can readily see that the thrust lines for cases 1b and 1c do not lie within the bounds of the slide mass, suggesting the possibility of *tension* at some of the upper interslice boundaries. This assumption is based on a presumed nonlinear distribution of stress within the slide mass. However if one assumes a linear distribution, the resultant must lie within the "middle-third" to ensure the existence of compressive interslice forces only. The existence of tensile stresses is confirmed by the plot of the interslice forces shown in Fig. 6.6.

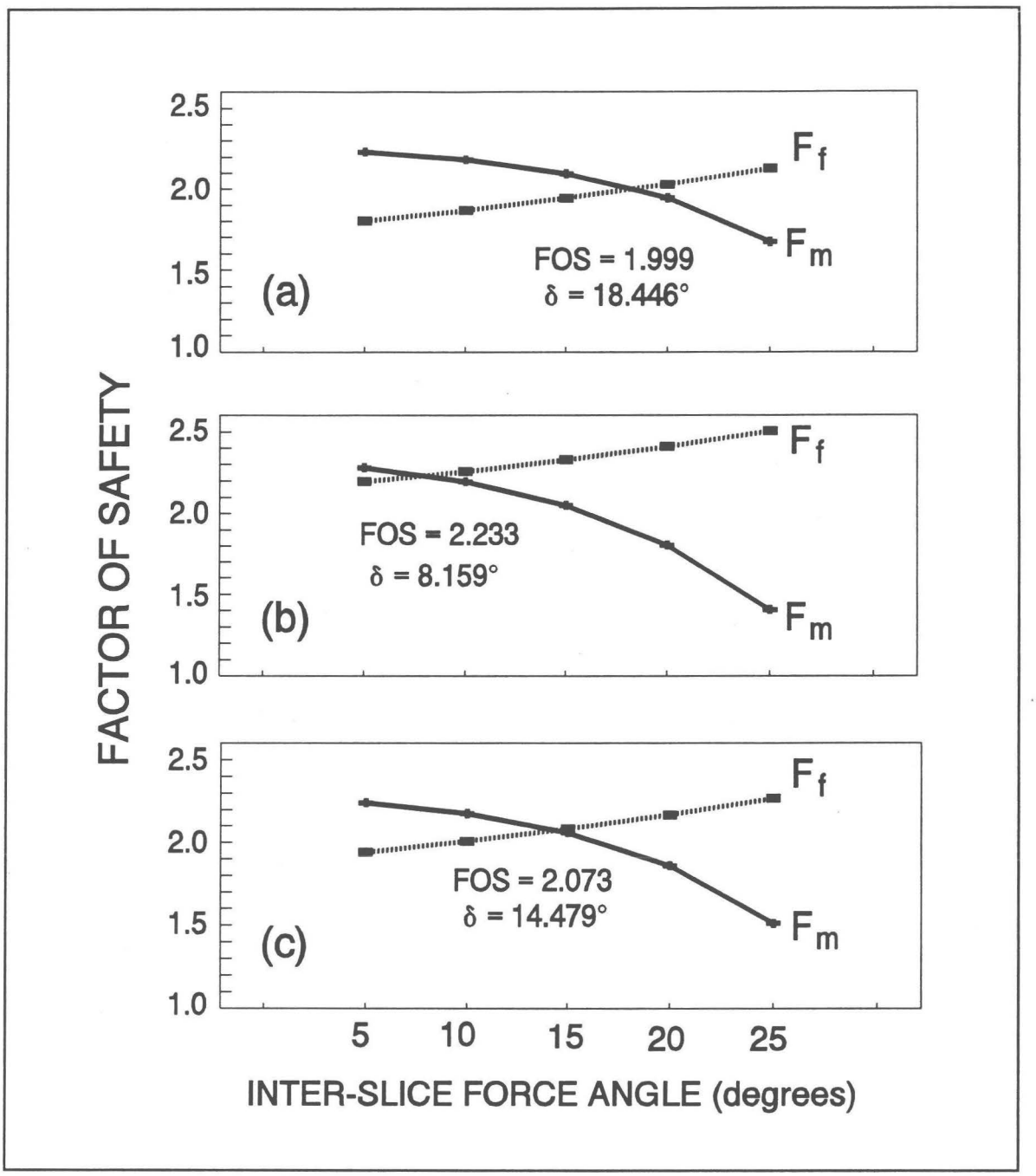

Figure 6.7. Variation of FOS for force and moment equilibrium

For the cases analyzed here, the variation of the factors of safety necessary to satisfy force and moment equilibrium for a range of interslice angles is shown in Fig. 6.7. These three figures, Figs. 6.7(a) - (c), present the calculated FOS and θ corresponding to the point of intersection between the lines representing FOS for force and moment equilibrium. These θ values (at convergence) range between 8.159° and 18.446°. On the basis of these results, it appears that the θ values for the ϕ-only soil are likely to be larger than the ones calculated for the c-only case. Also the tension cracks are more likely to occur in c-only soils. Fig. 6.7(c) shows the two curves for the c-ϕ soil and the results are in good agreement with the values published by Fredlund and Krahn (1977).

Problem 2

The second problem concerns the undrained analysis of a small embankment, as discussed and reported by Edris and Wright (1987) and Leshchinsky (1990). This slope was selected for this study to illustrate the influence of a crack near the crest of the slope. The slope geometry for the two conditions is presented in Figs. 6.8 and 6.9. The circular failure surface is centered at x_c = 30.0 feet and y_c = 80.0 feet and has a radius of 60.83 feet. The crack in Fig. 6.9 is located at a point on the slope where the vertical distance from the ground to failure surface is approximately 6.5 feet. The parameters for the soil have been taken as: γ = 110 pcf, c = 1000 psf and ϕ = 15°.

The iteration revealed a FOS of 3.062 and 2.901 for the intact and cracked slope, respectively. Along with the slope geometry, Fig. 6.8 also shows the location of the thrust line for the intact slope. From this figure one can see that the thrust line is rarely within the required bounds of the slide mass. Such a location of a thrust line indicates the existence of tensile stresses at the interslice boundaries of most slices.

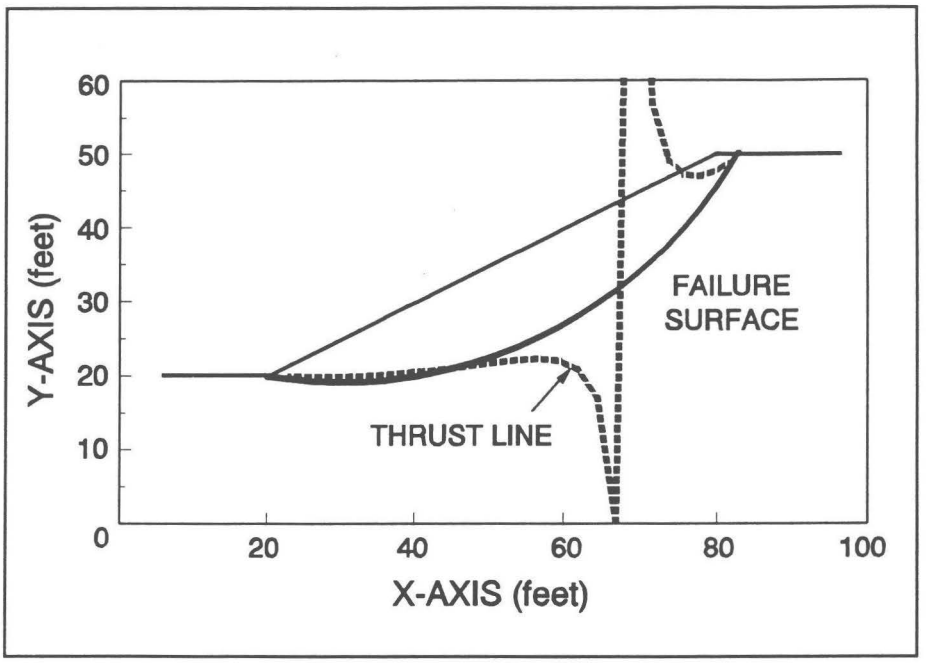

Figure 6.8. Thrust line location for intact slope of problem 2

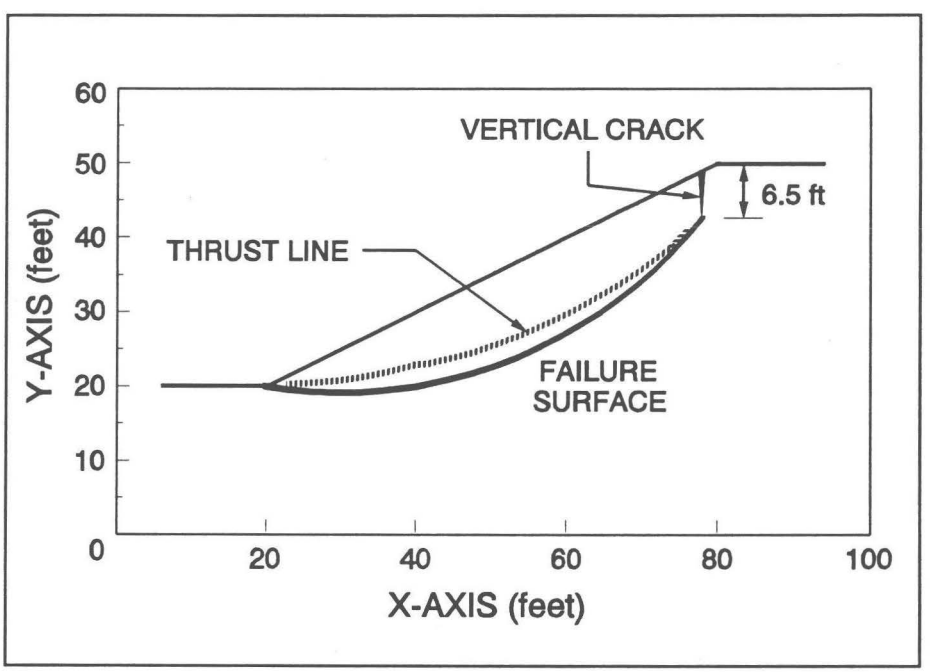

Figure 6.9. Thrust line location for "cracked" slope

The insertion of a crack ***releases*** the tension in the system, allowing the calculation of a more reasonable line of thrust shown in Fig. 6.9. As the strength in the portion of the slip surface beyond the crack is now unavailable for stability, the FOS value is reduced from the higher 3.062 (intact slope) to the more critical 2.901. The effects of a crack are simulated in the spreadsheet program by erasing the slice data for the slices located to the right of the crack. In this example, this procedure eliminated the effects of the last four slices. Please note that after erasing the slice data, one must press **ALT M** to initialize the tabulations. For more information, please consult the help file provided with the program.

The magnitude of the interslice forces is plotted in Fig. 6.10 for both cases. From this figure, one can see that the interslice forces are of a tensile nature for slices 18 to 26 for the intact slope. The prediction of such tensile forces is a direct result of the analysis procedure and may not realistically reflect the expected physical conditions within the slope. However, the insertion of a crack does relieve this tension and results in a more realistic distribution of interslice forces (i.e. all forces are compressive).

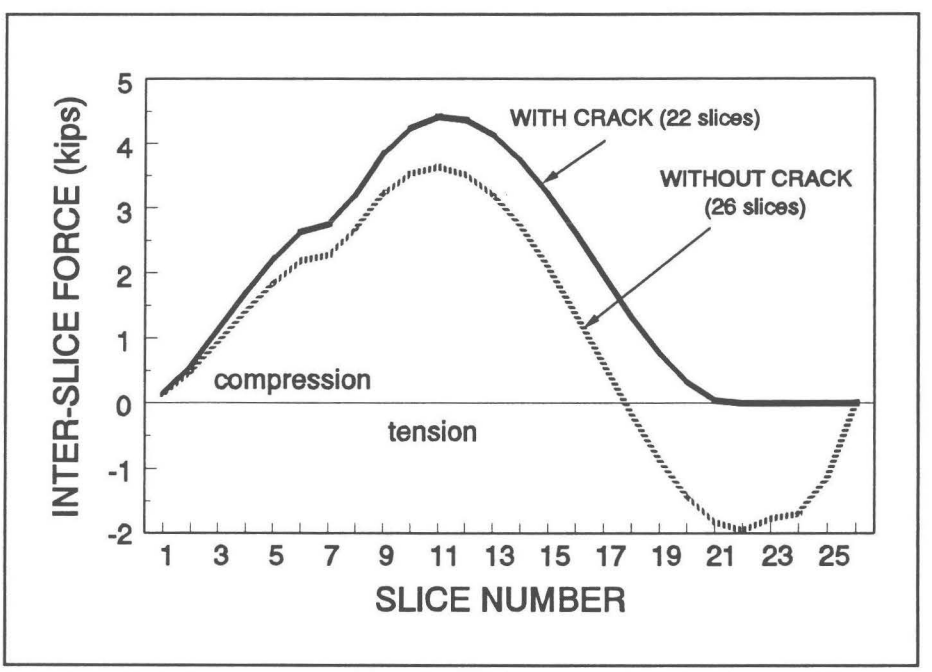

Figure 6.10. Thrust line location for "cracked" slope

The reader should also note that the removal of the tensile forces changes the interslice force inclination angle from $\theta = 7.106°$ to $\theta = 20.561°$. The results of the cracked slope suggest a reasonable factor of safety, as a major portion of the thrust line is now located within the failure mass, which is indicative of a more realistic failure surface.

However, if such a crack is used to determine the minimum factor of safety, the potential for water infiltration must also be recognized and included in the analysis. If water can enter the crack, the analysis must consider a hydrostatic force on the right-hand boundary of the last slice. This boundary condition is implemented by setting Z_R (Equation 1) for the last slice equal to the potential water-force. This force is a destabilizing force and will lead to the calculation of a lower, more critical, factor of safety. In this example, if the crack was completely filled with water to a depth of 6.5 feet, the factor of safety is reduced to 2.769, which is a reduction of about 10 percent in comparison to the intact slope.

If a reasonable factor of safety still cannot be calculated for a slope, the user may wish to employ a variable interslice force angle (θ) (i.e. different for each interslice boundary) as suggested by Spencer (1973).

6.4 Summary

Five different examples for two slopes have been presented to illustrate the calculation procedures proposed by Spencer (1967; 1973). The first example showed the differences that can be expected for ϕ-only or c-only type of soil strength parameters. The second example showed the significant influence that an insertion of a crack may have on the analytical procedure. In this case, the FOS value was reduced by about 4 percent, but this resulted in a much better thrust line and also eliminated the calculated tensile interslice forces.

Bromhead (1986) has noted that the high strengths at the head of the failure surface are an inherent problem due to the basic assumptions of the limit equilibrium theory that all slices have the same factor of safety. Thus if the strengths are high at the upper end of the failure mass, the averaging effect of a global FOS will require tension between slices. For ϕ-only soils, the upper portion will have a relatively small amount of strength due to the steepness of the slice bases, which result in the (unrealistic) calculation of low normal effective stresses.

Thus if a material exhibits high strength in the upper part of the slope (i.e. c-only or a c, ϕ-soil), a crack should be inserted to develop a *more* realistic failure surface. The analysis of such a failure surface will also overcome the potential difficulties associated with the line of thrust, interslice forces and the normal effective stresses at the base of the slices.

If a cracked zone is anticipated, the analyst must also consider the possibility that the water may fill all, or part, of the crack. This infiltration is generally presumed to be a temporary condition (e.g. infiltrating rainwater) and thus will not affect the pore water pressures at the base of the adjacent slices. The force imposed by the water in the crack is a destabilizing force and will thus reduce the FOS value, accordingly.

The proposed interactive method allows the user to examine the graphic location of the thrust line and possible interslice tensile forces. A crack may then be inserted into the potential tensile zone to develop a more reasonable solution. Since the analysis is performed interactively, the effects of different crack locations, and water forces, may be studied readily within the interactive environment.

6.5 Conclusions and Recommendations

Realistically, the shape and location of the slip surface within a slope is fundamentally controlled by the effective stresses within the soil mass (Simons and Menzies, 1974). So if effective stresses are calculated along a selected surface, and at the interslice boundaries, using the limit equilibrium method, these are unlikely to be compatible with the physical model. This failure surface-effective stress incompatibility is one of the major concerns in evaluating the reasonableness of the factor of safety computed using Spencer's Method. Or in other words, the limit equilibrium method is only a "tool" for the assessment of the stability of slopes and cannot be used to effectively model the physical features.

Thus, the engineer has to pay special attention to the results with a view to ensuring that some of the physical assumptions are not grossly violated by the analysis. If an unrealistic factor of safety value is computed, it is usually because an ***unrealistic surface was used to model the potential failure surface.*** Often, the insertion of a crack will lead to a more realistic result as indicated by subsequent analyses using Spencer (1967, 1973) and other limit equilibrium methods.

In view of the very sensitive nature of Spencer's Method, the author can offer the following recommendations:

1. *Assume constant interslice force inclinations (θ)*: this avoids difficulties associated with the selection of one function to represent a variable θ out of a possible infinite number available.

2. *Present a plot of the **effective** thrust line and magnitude of the interslice forces along with the quoted value of the Factor of Safety*: this data will allow the reviewer to make the necessary judgement regarding the validity of the solution.

3. *Use a suitably inserted crack within the tensile zone to define a more realistic failure surface:* this feature should be considered if there are high strength soils (i.e. high "c") in the upper part of the slope.

4. *A water-filled crack should be considered if such a condition is likely to develop due to infiltrating rainwater:* this condition will usually generate the lowest factor of safety for the slope.

REFERENCES

Bishop, A.W. (1955). The Use of the Slip Circle in the Stability Analysis of Slopes, Géotechnique, Vol. 5, No. 1, pp. 7-17, March.

Boutrup, E. (1977). Computerized Slope Stability Analysis for Indiana Highways, Report JHRP-77-25 & 26 (2 Volumes), School of Civil Engineering, Purdue University, West Lafayette, IN 47906.

Bromhead, E.N. (1986). The Stability of Slopes, Surrey University Press, London, England, pp. 140-142.

Charles, J.A. and Soares, M.M. (1984). Stability of compacted rockfill slopes, Géotechnique, Vol. 34, No. 1, pp. 61-70.

Ching, R.K.H. and Fredlund, D.G. (1983). Some difficulties associated with the limit equilibrium method of slices, Canadian Geotechnical Journal, Vol. 20, No. 4, pp. 661-672.

Chowdury, R.N. (1978). Slope Analysis, Developments in Geotechnical Engineering, Vol. 22, Elsevier Scientific Pub. Co., Amsterdam, Netherlands.

Chugh, A.K. (1981). Multiplicity of Numerical solutions for Slope Stability Problems, Int. J. for Num. and Anal. Methods in Geomechanics, Vol. 5, pp. 313-322.

Chugh, A.K. (1981). Pore Water Pressure in Natural Slopes, Int. J. of Numerical & Analytical Methods in Geomechanics, Vol. 5, pp. 449-454.

Duncan, M. and Seed, H.B. (1966). Strength variation along failure surfaces in clay, Journal of Soil Mech. Found. Div., ASCE, Vol. 95, SM6, pp. 81-104.

Edris, E.V. and Wright, S.G. (1987). User's Guide: UTEXAS2 slope stability package, Instruction Report GL-87-1, U.S. Army Corps of Engrs., WES, Vicksburg, MS.

Fellenius, W. (1936). Calculation of the Stability of Earth Dams, Proc., 2nd Congress on Large Dams, Vol. 4, pp. 445-463.

Fredlund, D.G. and Krahn, J. (1977). Comparison of Slope Stability Methods of Analysis, Canadian Geotechnical Journal, Vol. 14, No. 3, pp. 429-439.

Franklin, A.G. and Chang, F.K. (1977). Earthquake Resistance of Earth and Rock-fill Dams: Permanent Displacements of Earth Embankment by Newmark Sliding Block Analysis, USAE, Misc. Paper S-71-17, Report 5, Vicksburg, MS.

Hynes-Griffin, M.E. and Franklin, A.G. (1984). Rationalizing the Seismic Coefficient Method, USAE, Misc. Paper GL-84-13, Vicksburg, MS.

I.S. Designs (1992). **XSTABL**, An Integrated Slope Stability Analysis Program for Personal Computers, Moscow, Idaho.

Janbu, N. (1957). Stability Analysis of Slopes with Dimensionless Parameters, Harvard University, Soil Mechanics Series, No. 46.

Janbu, N. (1973). Slope Stability Computations, in Embankment Dam Engineering, Casagrande Memorial Volume, Hirschfield and Poulos (Editors), John Wiley, New York, pp. 47-86.

Koerner, R.M. (1991). Geosynthetics in Geotechnical Engineering, Chapter 22 in Foundation Engineering Handbook (H.Y. Fang, Editor), Second Edition, Van Nostrand Reinhold, New York, page 802.

Lambe, T.W. and Whitman, R.V. (1969). Soil Mechanics, John Wiley and Sons (Pub.), pp. 359-365.

Leonards, G.A. and Humphrey, D. (1984). End of Construction Pore Pressures in Earth Dam Embankments, Report to American Electric Power Services Corp., Ohio.

Leshchinsky, D. (1990). Slope Stability Analysis: Generalized Approach, ASCE, Vol. 116, GT-5, pp. 851-867.

Little, A.L. and Price, V.E. (1958). The use of an electronic computer for slope stability computation, Géotechnique, Vol. 8, pp. 113-120.

Lovell, C.W., Sharma, S. and Carpenter, J.R. (1984). Slope Stability Analysis with STABL4, Report JHRP-84-19, School of Civil Engineering, Purdue University, West Lafayette, IN 47906.

Morgenstern, N.R. and Price, V.E. (1965). The Analysis of the Stability of General Slip Surfaces, Géotechnique, Vol. 15, No. 1, pp. 79-93, March.

NAVFAC DM7 (1982). Foundations and Earth Structures, Design Manual 7.2, Dept. of the Navy, Naval Facilities Eng. Command, Alexandria, VA, pp. 135-136.

Newmark, N.M. (1965). Effects of earthquakes on dams and embankments, Géotechnique, Vol. 25, No. 2, pp. 139-160.

Press, W.H., Flannery, B.P., Teukolsky, S.A. and Vetterling, W.T. (1986). Numerical Recipes, Cambridge University Press, pp. 195-196.

Sarma, S.K. (1979). Stability Analysis of Embankments and Slopes, ASCE, Vol. 105, GT-5, December, pp. 1511-1524.

Sharma, S. (1988). STBLIN - An Interactive Data Preparation Program for Slope Stability Program, STABL, Final Report to Idaho Transportation Department, Contract 128-K028, Dept. of Civil Engineering, University of Idaho, Moscow, ID 83843.

Sharma, S. and Lovell, C.W. (1983). Strengths and Weaknesses of Slope Stability Analyses, Proceedings of the 34th Annual Highway Geology Symposium, Atlanta, pp. 215-232.

Sharma, S. and Moudud, A. (1992). Interactive Slope Analysis Using Spencer's Method, accepted for publication in the ASCE Specialty Conference on Stability and Performance of Slopes and Embankments, Berkeley, June 29-July 1.

Sherman, W.C. and Clough, G.W. (1968). Embankment Pore Pressures during Construction, ASCE, JSMFD, Vol. 94, No. SM2, March, pp. 527-553.

Siegel, R.A. (1975). Computer Analysis of General Slope Stability Problems, Report JHRP-75-8, School of Civil Engineering, Purdue University, West Lafayette, IN 47906.

Siegel, R.A. (1975). STABL User Manual, Report JHRP-75-9, School of Civil Engineering, Purdue University, West Lafayette, IN 47906.

Siegel, R.A., Kovacs, W.D. and Lovell, C.W. (1980). Random Surface Generation in Stability Analysis, ASCE, VOL. 107, GT-7, pp. 996-1002, July.

Simons, N.E. and Menzies, B.K. (1974). A Note on the Principle of Effective Stress, Géotechnique, Vol. 24, No. 2, pp. 259-261.

Spencer, E. (1973). The Thrust Line Criterion in Embankment Stability Analysis, Géotechnique, Vol. 23, No. 1, pp. 85-100, March.

Spencer, E. (1967). A Method of Analysis of the Stability of Embankments Assuming Parallel Inter-Slice Forces, Géotechnique, Vol. 17, No. 1, pp. 11-26, March.

Wright, S.G. (1969). A Study of Stability and Undrained Shear Strength of Clay Shales, PhD dissertation, University of California, Berkeley.

Wright, S.G. (1974). SSTABI -- A General Computer Program for Slope Stability Analyses, Dept. of Civil Eng., University of Texas, Austin.

APPENDIX

LISTING OF EXAMPLE DATA FILES

		Filename
Pore Pressure Examples:		
1.	PWP-1	FLOW_1.IPT
2.	PWP-2	FLOW_2.IPT
3.	PWP-3	FLOW_3.IPT
4.	PWP-4	FLOW_4.IPT
5.	PWP-5	FLOW_5.IPT
USDA Forest Service Examples:		
6.	Example 1	USFS_1.IPT
7.	Example 2(a)	USFS_2A.IPT
8.	Example 2(b)	USFS_2B.IPT
9.	Example 3(a)	USFS_3A.IPT
10.	Example 3(b)	USFS_3B.IPT
11.	Example 3(c)	USFS_3C.IPT
12.	Example 3(d)	USFS_3D.IPT
13.	Example 3(e)	USFS_3E.IPT
14.	Example 3(f)	USFS_3F.IPT
15.	Example 3(g)	USFS_3G.IPT
16.	Example 3(b)	USFS_3H.IPT
Anisotropic Soils:		
17.	Example 4(a)	ANISO_1.IPT
18.	Example 4(b)	ANISO_2.IPT
19.	Example 4(c)	ANISO_3.IPT
20.	Example 4(d)	ANISO_4.IPT

LISTING OF EXAMPLE DATA FILES

Seismic Analysis

21.	Seismic Coeff., $k_h = 0.4$	EQUAKE.IPT

Nonlinear Mohr-Coulomb Soils:

22.	100 meter slope	NLIN_1.IPT
23.	10 meter slope	NLIN_2.IPT
24.	100 meter slope, Equiv. Linear	NLIN_3.IPT
25.	10 meter slope, Equiv. Linear	NLIN_4.IPT

Reinforced Slope Analysis:

26.	Case 1, Maximum Force	REINF_1.IPT
27.	Case 2, Unreinforced	REINF_2.IPT
28.	Case 3, 7.5 meter zone	REINF_3.IPT
29.	Case 4, 6.0 meter zone	REINF_4.IPT

Effective stress control options:

30.	Negative Effective Stress	NEG_STR.IPT
31.	1500 surface comparison	SCHWTZ_1.IPT

Analysis of Specific Surfaces for use in Spencer's Analysis:

32.	ϕ-only soil	SPENC_1.IPT
33.	c-only soil	SPENC_2.IPT
34.	c-ϕ soil	SPENC_3.IPT
35.	Intact slope	SPENC_4.IPT
36.	Cracked slope	SPENC_5.IPT

Table A1. Input data for example PWP-1

```
PROFIL                                          FILE: FLOW_1      6-01-92
Phreatic Surface Search, PWP-1
   4     3
     5.0        10.0        20.0        10.0    1
    20.0        10.0        50.0        30.0    1
    50.0        30.0        75.0        30.0    1
    20.0        10.0        75.0        10.0    2
SOIL
  2
  125.0    125.0      90.0    32.00     .000         .0     1
  125.0    125.0        .0    40.00     .000         .0     0
WATER
  1       62.40
  20
         5.0         10.0
        28.2         10.0
        28.4         11.0
        28.7         12.0
        29.3         13.1
        30.5         14.2
        31.5         15.2
        33.1         16.3
        35.0         17.2
        37.0         18.3
        39.0         19.2
        41.3         20.2
        44.0         21.3
        47.0         22.5
        50.7         23.5
        54.8         24.4
        59.0         25.5
        63.5         26.4
        68.0         27.5
        75.0         28.0
CIRCL2
   5    20
     20.0        24.0        50.0        70.0
     10.0         5.0         5.0       -20.0
```

Table A2. Input data for example PWP-2

```
PROFIL                                          FILE: FLOW_2      6-01-92
PWP Grid Search, PWP-2
   4     3
      5.0        10.0        20.0        10.0   1
     20.0        10.0        50.0        30.0   1
     50.0        30.0        75.0        30.0   1
     20.0        10.0        75.0        10.0   2
SOIL
  2
  125.0    125.0      90.0    32.00      .000         .0    1
  125.0    125.0        .0    40.00      .000         .0    0
PWGRID
 90
        28.2        10.0          .0
        28.4        11.0          .0
        28.7        12.0          .0
        29.3        13.1          .0
        30.5        14.2          .0
        31.5        15.2          .0
        33.1        16.3          .0
        35.0        17.2          .0
        37.0        18.3          .0
        39.0        19.2          .0
        41.3        20.2          .0
        44.0        21.3          .0
        47.0        22.5          .0
        50.7        23.5          .0
        54.8        24.4          .0
        59.0        25.5          .0
        63.5        26.4          .0
        68.0        27.5          .0
        29.1        10.0          .0
        29.2        10.9         6.2
        29.8        11.5        31.2
        30.4        12.5        43.7
        31.2        13.1        68.6
        32.6        13.9        81.1
        34.0        14.8        93.6
        36.0        15.5       106.1
        37.9        16.1       137.3
        40.0        17.0       137.3
        42.4        17.7       156.0
        45.2        18.4       181.0
        48.5        19.1       212.2
        52.4        19.9       224.6
        56.0        20.5       243.4
        60.4        21.3       262.1
        65.1        22.6       237.1
        69.9        23.4       255.8
```

Table A2. Input data for example PWP-2, continued ...

```
        29.9          10.0            .0
        30.0          10.8          12.5
        34.7          13.0         205.9
        36.6          13.5         230.9
        38.6          14.0         268.3
        40.9          14.5         293.3
        43.2          14.9         330.7
        46.2          15.3         374.4
        49.5          15.9         411.8
        53.0          16.2         455.5
        57.3          16.8         474.2
        61.7          17.1         524.2
        66.6          17.9         530.4
        71.1          18.4         567.8
        30.2          10.0            .0
        30.3          10.2          49.9
        30.6          10.5          93.6
        31.2          10.8         149.8
        32.4          11.0         199.7
        33.8          11.2         249.6
        35.2          11.5         299.5
        37.0          11.8         337.0
        39.0          12.0         393.1
        41.2          12.1         443.0
        43.8          12.3         493.0
        46.6          12.5         549.1
        49.8          12.7         611.5
        53.0          13.0         655.2
        58.0          13.2         698.9
        61.6          13.7         736.3
        67.0          14.1         767.5
        71.7          14.6         805.0
        30.4          10.0            .0
        30.6          10.0          62.4
        30.8          10.0         124.8
        31.5          10.0         199.7
        32.5          10.0         262.1
        33.8          10.0         324.5
        35.4          10.0         393.1
        37.2          10.0         449.3
        39.1          10.0         517.9
        41.4          10.0         574.1
        43.9          10.0         636.5
        46.8          10.0         705.1
        50.0          10.0         780.0
        54.0          10.0         842.4
        58.2          10.0         898.6
        63.0          10.0         967.2
        67.0          10.0        1023.4
        71.5          10.0        1092.0
CIRCL2
   5    20
     20.0         24.0         50.0         70.0
     10.0          5.0          5.0        -20.0
```

Table A3. Input data for example PWP-3

```
PROFIL                                          FILE: FLOW_3      6-01-92
Correct Piezometric Surface, PWP-3
   4     3
      5.0        10.0        20.0        10.0   1
     20.0        10.0        50.0        30.0   1
     50.0        30.0        75.0        30.0   1
     20.0        10.0        75.0        10.0   2
SOIL
  2
  125.0    125.0       90.0    32.00     .000        .0    1
  125.0    125.0         .0    40.00     .000        .0    0
WATER
  1        62.40
 -11
         20.0         10.0
         25.0         10.1
         27.5         10.5
         32.3         14.2
         37.0         17.3
         41.5         19.6
         45.6         22.0
         48.8         22.8
         50.7         23.7
         53.4         27.9
         54.4         29.9
SURB2
    22.49       45.46       20.00       5.00
```

Table A4. Input data for example PWP-4

```
PROFIL                                          FILE: FLOW_4      6-01-92
Solution using Ru Factor, PWP-4
   4     3
      5.0        10.0        20.0        10.0   1
     20.0        10.0        50.0        30.0   1
     50.0        30.0        75.0        30.0   1
     20.0        10.0        75.0        10.0   2
SOIL
  2
  125.0    125.0       90.0    32.00     .157        .0    0
  125.0    125.0         .0    40.00     .000        .0    0
SURB2
    21.67       49.14       20.00       5.00
```

Table A5. Input data for example PWP-5

```
PROFIL                                          FILE: FLOW_5      6-01-92
Incorrect Phreatic Surface, PWP-5
   4     3
      5.0        10.0        20.0        10.0   1
     20.0        10.0        50.0        30.0   1
     50.0        30.0        75.0        30.0   1
     20.0        10.0        75.0        10.0   2
SOIL
  2
  125.0    125.0      90.0    32.00     .000        .0    1
  125.0    125.0        .0    40.00     .000        .0    0
WATER
  1       62.40
 -20
          5.0         10.0
         28.2         10.0
         28.4         11.0
         28.7         12.0
         29.3         13.1
         30.5         14.2
         31.5         15.2
         33.1         16.3
         35.0         17.2
         37.0         18.3
         39.0         19.2
         41.3         20.2
         44.0         21.3
         47.0         22.5
         50.7         23.5
         54.8         24.4
         59.0         25.5
         63.5         26.4
         68.0         27.5
         75.0         28.0
SURB2
    22.49       45.46       20.00       5.00
```

Table A6. Input data for USFS Example 1

```
PROFIL                                          FILE: USFS_1      6-01-92
USFS Example 1
  11      7
     20.0          .0        47.5        33.0    1
     47.5        33.0        63.0        45.8    1
     63.0        45.8        63.1        56.0    2
     63.1        56.0        86.0        56.0    2
     86.0        56.0        90.0        56.0    1
     90.0        56.0        92.0        65.0    1
     92.0        65.0        96.0        70.0    1
     63.0        39.9        63.1        45.8    2
     63.0        38.0        63.1        39.9    2
     63.0        38.0        77.0        38.0    1
     77.0        38.0        86.0        56.0    1
SOIL
  2
  110.0    120.0     350.0    32.00     .000         .0    1
  125.0    135.0      80.0    37.00     .000         .0    1
WATER
  1       62.40
   3
        20.0           .0
        27.0          8.0
       100.0         51.0
BLOCK2
  300   4     10.0
        25.9          4.3         50.0         18.1          .0
        70.0         29.7         76.0         33.2          .0
        77.0         38.0         78.0         38.0          .0
        86.0         56.0         90.0         56.0          .0
```

Table A7. Input data for USFS Example 2(a)

```
PROFIL                                          FILE: USFS_2A     6-01-92
11:06    ft
USFS Example 2(a)
  19    10
       .0        18.0        15.0        23.0   1
     15.0        23.0        46.0        31.0   1
     46.0        31.0        59.0        35.0   1
     59.0        35.0        81.0        43.0   1
     81.0        43.0       141.0        83.0   4
    141.0        83.0       168.0        83.0   4
    168.0        83.0       176.0        82.0   4
    176.0        82.0       184.0        82.0   1
    184.0        82.0       193.0        84.0   2
    193.0        84.0       200.0        90.0   2
     81.0        43.0       130.0        66.0   1
    130.0        66.0       168.0        83.0   1
       .0        16.0        40.0        28.0   2
     40.0        28.0        80.0        42.0   2
     80.0        42.0       132.0        64.0   2
    132.0        64.0       176.0        82.0   2
       .0         8.0        60.0        26.0   3
     60.0        26.0       134.0        51.0   3
    134.0        51.0       200.0        78.0   3
SOIL
  4
   85.0    100.0      50.0    26.00     .000        .0    1
  110.0    120.0     120.0    28.00     .000        .0    2
  120.0    130.0       .0     32.00     .000        .0    2
  125.0    135.0       .0     34.00     .000        .0    1
WATER
  2       62.40
  10
          .0        18.0
         46.0        31.0
         59.0        35.0
         81.0        43.0
        118.0        64.0
        134.0        71.0
        176.0        82.0
        184.0        82.0
        193.0        84.0
        200.0        90.0
  -3
          .0        14.0
        140.0        64.0
        200.0        84.0
LIMITS
   2     2
          .0         6.0       140.0        52.0
        140.0        52.0       200.0        76.0
CIRCL2
   7    50
     40.0        70.0       145.0       170.0
       .0          .0         .0          .0
```

Table A8. Input data for USFS Example 2(b)

```
PROFIL                                          FILE: USFS_2B    6-01-92
USFS Example 2(b)
  19    10
       .0       18.0       15.0       23.0   1
     15.0       23.0       46.0       31.0   1
     46.0       31.0       59.0       35.0   1
     59.0       35.0       81.0       43.0   1
     81.0       43.0      141.0       83.0   4
    141.0       83.0      168.0       83.0   4
    168.0       83.0      176.0       82.0   4
    176.0       82.0      184.0       82.0   1
    184.0       82.0      193.0       84.0   2
    193.0       84.0      200.0       90.0   2
     81.0       43.0      130.0       66.0   1
    130.0       66.0      168.0       83.0   1
       .0       16.0       40.0       28.0   2
     40.0       28.0       80.0       42.0   2
     80.0       42.0      132.0       64.0   2
    132.0       64.0      176.0       82.0   2
       .0        8.0       60.0       26.0   3
     60.0       26.0      134.0       51.0   3
    134.0       51.0      200.0       78.0   3
SOIL
  4
   85.0    100.0      50.0    26.00     .000        .0    1
  110.0    120.0     120.0    28.00     .000        .0    2
  120.0    130.0       .0     32.00     .000        .0    2
  125.0    135.0       .0     34.00     .000        .0    1
WATER
  2       62.40
  10
          .0        18.0
         46.0       31.0
         59.0       35.0
         81.0       43.0
        118.0       64.0
        134.0       71.0
        176.0       82.0
        184.0       82.0
        193.0       84.0
        200.0       90.0
  -3
          .0        14.0
        140.0       64.0
        200.0       84.0
BLOCK2
  300   4     10.0
         81.0       43.0        90.0        47.0        .0
         92.0       47.2       106.0        53.1        .0
        120.0       59.0       140.0        67.5        .0
        141.0       82.9       168.0        82.9        .0
```

Table A9. Input data for USFS Example 3(a)

```
PROFIL                                          FILE: USFS_3A     6-01-92
USFS Ex. 3a, Uniform Load, Rankine
   5     5
     10.0         5.0        54.0        34.0    1
     54.0        34.0        75.2        48.2    1
     75.2        48.2       100.9        65.3    1
    100.9        65.3       101.0        62.3    1
    101.0        62.3       108.0        62.3    1
SOIL
  1
  130.0    135.0         .0    36.00     .000         .0    0
LOADS
  1
       101.0        107.6       2335.0        -15.0
LIMITS
   1     1
        10.0           .0        108.0         51.6
SURFAC
  17
    75.20       48.20
    78.00       48.49
    81.00       48.84
    84.00       49.20
    87.00       49.55
    90.00       49.90
    93.00       50.26
    95.16       50.51
    95.49       50.55
    96.46       50.71
    98.13       51.15
    99.61       51.73
   100.90       52.44
   102.01       53.23
   102.88       54.02
   104.32       55.75
   107.60       62.30
```

Table A10. Input data for USFS Example 3(b)

```
PROFIL                                          FILE: USFS_3B     6-01-92
USFS Ex. 3(b), Uniform load, DM-7
   5     5
     10.0         5.0        54.0        34.0    1
     54.0        34.0        75.2        48.2    1
     75.2        48.2       100.9        65.3    1
    100.9        65.3       101.0        62.3    1
    101.0        62.3       108.0        62.3    1
SOIL
  1
  130.0    135.0         .0    36.00     .000         .0    0
LOADS
  1
       101.0        107.6       2335.0        -15.0
LIMITS
   1     1
        10.0           .0        108.0         51.6
SURFAC
  14
    83.20       53.50
    83.42       53.36
    87.87       51.33
    91.72       50.52
    94.62       50.47
    95.96       50.62
    97.20       50.88
    99.41       51.64
   100.37       52.12
   101.24       52.66
   102.01       53.23
   102.69       53.84
   104.30       55.00
   107.60       62.30
```

Table A11. Input data for USFS Example 3(c)

```
PROFIL                                          FILE: USFS_3C     6-01-92
0:47    ft
USFS Ex. 3(c), nonuniform, Rankine
   4     4
     10.0         5.0        54.0        34.0    1
     54.0        34.0       100.9        65.3    1
    100.9        65.3       101.0        62.3    1
    101.0        62.3       110.0        62.3    1
SOIL
  1
  130.0    135.0         .0    36.00     .000         .0    0
LOADS
  9
        101.0        102.0       2927.0         -8.9
        102.0        103.0       2626.0         -9.9
        103.0        104.0       2324.0        -11.2
        104.0        105.0       2024.0        -12.8
        105.0        106.0       1723.0        -14.9
        106.0        107.0       1421.0        -17.9
        107.0        108.0       1120.0        -22.3
        108.0        109.0        819.0        -29.3
        109.0        110.0        518.0        -41.6
LIMITS
   1     1
        10.0           .0        110.0         52.9
SURFAC
  19
    68.10       43.40
    71.00       43.73
    74.00       44.09
    77.00       44.44
    80.00       44.79
    83.00       45.15
    86.00       45.50
    88.90       45.85
    92.97       46.32
    93.73       46.41
    94.20       46.48
    95.88       46.83
    98.88       47.86
   100.18       48.52
   101.36       49.24
   102.40       50.02
   103.33       50.84
   105.50       53.44
   110.00       62.30
```

Table A12. Input data for USFS Example 3(d)

```
PROFIL                                          FILE: USFS_3D    6-01-92
USFS Ex. 3(d), nonuniform, DM-7
   4     4
     10.0         5.0        54.0        34.0    1
     54.0        34.0       100.9        65.3    1
    100.9        65.3       101.0        62.3    1
    101.0        62.3       110.0        62.3    1
SOIL
  1
  130.0    135.0         .0    36.00     .000         .0    0
LOADS
  9
        101.0        102.0       2927.0         -8.9
        102.0        103.0       2626.0         -9.9
        103.0        104.0       2324.0        -11.2
        104.0        105.0       2024.0        -12.8
        105.0        106.0       1723.0        -14.9
        106.0        107.0       1421.0        -17.9
        107.0        108.0       1120.0        -22.3
        108.0        109.0        819.0        -29.3
        109.0        110.0        518.0        -41.6
LIMITS
   1     1
        10.0           .0        110.0         52.9
SURFAC
  13
    77.78       49.86
    83.23       47.45
    88.45       46.34
    92.39       46.27
    94.20       46.48
    95.88       46.83
    98.88       47.86
   100.18       48.52
   101.36       49.24
   102.40       50.02
   103.33       50.84
   105.50       53.44
   110.00       62.27
```

Table A13. Input data for USFS Example 3(e)

```
PROFIL                                          FILE: USFS_3E     6-01-92
USFS Ex. 3(e), Uniform, Circ. Search
   5     5
     10.0         5.0         54.0        34.0    1
     54.0        34.0         75.2        48.2    1
     75.2        48.2        100.9        65.3    1
    100.9        65.3        101.0        62.3    1
    101.0        62.3        108.0        62.3    1
SOIL
  1
  130.0    135.0         .0    36.00     .000         .0    0
LOADS
  1
       101.0        107.6       2335.0        -15.0
LIMITS
   1     1
        10.0           .0        107.6         51.6
CIRCL2
   5    50
     10.0        20.0        107.6       108.0
       .0        10.0           .0          .0
```

Table A14. Input data for USFS Example 3(f)

```
PROFIL                                          FILE: USFS_3F     6-01-92
USFS Ex. 3(f), Nonuniform, Circ. Search
   5     5
     10.0         5.0        54.0        34.0    1
     54.0        34.0        75.2        48.2    1
     75.2        48.2       100.9        65.3    1
    100.9        65.3       101.0        62.3    1
    101.0        62.3       110.0        62.3    1
SOIL
  1
  130.0    135.0         .0    36.00      .000         .0    0
LOADS
  9
        101.0        102.0       2927.0         -8.9
        102.0        103.0       2626.0         -9.9
        103.0        104.0       2324.0        -11.2
        104.0        105.0       2024.0        -12.8
        105.0        106.0       1723.0        -14.9
        106.0        107.0       1421.0        -17.9
        107.0        108.0       1120.0        -22.3
        108.0        109.0        819.0        -29.3
        109.0        110.0        518.0        -41.6
LIMITS
   1     1
        10.0           .0        110.0         52.9
CIRCL2
   5    50
      10.0        20.0       109.9       110.0
        .0        10.0        30.0        10.0
```

Table A15. Input data for USFS Example 3(g)

```
PROFIL                                          FILE: USFS_3G     6-01-92
USFS Ex. 3(g), External Stab., Block
  12     6
     10.0         5.0         54.0        34.0    1
     54.0        34.0        100.9        65.3    1
    100.9        65.3        102.0        74.3    2
    102.0        74.3        108.0        77.3    2
    108.0        77.3        123.0        77.3    1
    123.0        77.3        126.0        76.3    1
    102.0        74.3        105.0        74.3    2
    105.0        74.3        108.5        65.3    2
    108.5        65.3        110.1        65.3    2
    100.9        65.3        101.0        62.3    1
    101.0        62.3        110.0        62.3    1
    110.0        62.3        110.1        65.3    1
SOIL
  2
  130.0    135.0         .0    36.00     .000          .0    0
  130.0    135.0         .0    45.00     .000          .0    0
LIMITS
   1     1
        10.0           .0        126.0         61.3
BLOCK2
  250   4     10.0
        10.0          5.0         10.0          5.0          .0
        35.0         17.2         75.0         38.4         8.0
       110.0         62.3        110.0         62.3          .0
       112.0         77.3        123.0         77.3          .0
```

Table A16. Input data for USFS Example 3(h)

```
PROFIL                                          FILE: USFS_3H     6-01-92
USFS Ex. 3(h), Ext. Stab., Block + LL
  12     6
     10.0         5.0         54.0        34.0    1
     54.0        34.0        100.9        65.3    1
    100.9        65.3        102.0        74.3    2
    102.0        74.3        108.0        77.3    2
    108.0        77.3        123.0        77.3    1
    123.0        77.3        126.0        76.3    1
    102.0        74.3        105.0        74.3    2
    105.0        74.3        108.5        65.3    2
    108.5        65.3        110.1        65.3    2
    100.9        65.3        101.0        62.3    1
    101.0        62.3        110.0        62.3    1
    110.0        62.3        110.1        65.3    1
SOIL
  2
  130.0    135.0         .0    36.00     .000         .0    0
  130.0    135.0         .0    45.00     .000         .0    0
LOADS
  2
       111.0        112.0       2000.0          .0
       117.0        118.0       2000.0          .0
LIMITS
   1     1
        10.0           .0        126.0        61.3
BLOCK2
  250   4     10.0
        10.0          5.0         10.0         5.0          .0
        35.0         17.2         75.0        38.4         8.0
       110.0         62.3        110.0        62.3          .0
       112.0         77.3        123.0        77.3          .0
```

Table A17. Input data for Anisotropic Strength Example 4(a)

```
PROFIL                                          FILE: ANISO_1     6-01-92
USFS Example 4(a) - Anisotropic Soil
   3     3
       .0        20.0        10.0        20.0   1
     10.0        20.0        50.0        40.0   1
     50.0        40.0        80.0        40.0   1
SOIL
  1
  125.0    125.0         .0       .00      .000         .0     0
ANISO
  1
   1     6
   -45.00          .0       35.00
   -22.50          .0       35.00
      .00          .0       36.00
    22.50          .0       37.00
    45.00          .0       38.00
    90.00          .0       35.00
SURB2
    21.84       66.39       10.00        5.00
```

Table A18. Input data for Anisotropic Strength Example 4(b)

```
PROFIL                                          FILE: ANISO_2     6-01-92
USFS Example 4(b) - Isotropic Soil
   3     3
       .0        20.0        10.0        20.0   1
     10.0        20.0        50.0        40.0   1
     50.0        40.0        80.0        40.0   1
SOIL
  1
  125.0    125.0         .0     34.50      .000         .0     0
SURB2
    21.84       66.39       10.00        5.00
```

Table A19. Input data for Anisotropic Strength Example 4(c)

```
PROFIL                                        FILE: ANISO_3     6-01-92
USFS Example 4(c) - Isotropic Soil
   3     3
       .0        20.0        10.0        20.0   1
     10.0        20.0        50.0        40.0   1
     50.0        40.0        80.0        40.0   1
SOIL
  1
  125.0    125.0         .0    35.00      .000         .0    0
SURB2
    21.84       66.39       10.00       5.00
```

Table A20. Input data for Anisotropic Strength Example 4(d)

```
PROFIL                                        FILE: ANISO_4     6-01-92
USFS Example 4(d) - Isotropic Soil
   3     3
       .0        20.0        10.0        20.0   1
     10.0        20.0        50.0        40.0   1
     50.0        40.0        80.0        40.0   1
SOIL
  1
  125.0    125.0         .0    38.00      .000         .0    0
SURB2
    21.84       66.39       10.00       5.00
```

Table A21. Input data for Anisotropic Strength Example with *Seismic Coefficient*

```
PROFIL                                          FILE: EQUAKE      6-01-92
Anisotropic Soil, Seismic kh = 0.4
   3     3
       .0        20.0        10.0        20.0    1
     10.0        20.0        50.0        40.0    1
     50.0        40.0        80.0        40.0    1
SOIL
  1
  125.0    125.0         .0       .00      .000         .0     0
ANISO
  1
   1     6
   -45.00          .0       35.00
   -22.50          .0       35.00
      .00          .0       36.00
    22.50          .0       37.00
    45.00          .0       38.00
    90.00          .0       35.00
EQUAKE
   .400      .000
SURB2
    21.84       66.39       10.00        5.00
```

Table A22. Input data for Nonlinear Strength Example, 100-meter slope

```
PROFIL                                          FILE: NLIN_1      6-01-92
NL Mohr-Coulomb Env. -- 100 m slope
   3     3
     10.0        10.0        30.0        10.0   1
     30.0        10.0       162.0       110.0   1
    162.0       110.0       235.0       110.0   1
SOIL
  1
   22.0      22.0         .0    30.00      .000         .0    0
NLSOIL
  1
   1    10
          .0           .0
         10.0         28.1
         25.0         55.9
         50.0         94.0
        100.0        158.1
        200.0        265.9
        300.0        360.4
        400.0        447.2
        600.0        606.2
       1200.0       1019.4
CIRCL2
   1   300
     30.0        30.0       162.0       225.0
       .0        20.0          .0          .1
```

Table A23. Input data for Nonlinear Strength Example, 10-meter slope

```
PROFIL                                          FILE: NLIN_2      6-01-92
NL Mohr-Coulomb Env. -- 10 m slope
   3     3
     10.0         5.0        20.0         5.0   1
     20.0         5.0        25.0        15.0   1
     25.0        15.0        35.0        15.0   1
SOIL
  1
   22.0      22.0         .0    30.00      .000         .0    0
NLSOIL
  1
   1    10
          .0           .0
         2.5          9.9
         5.0         16.7
        10.0         28.1
        15.0         38.1
        20.0         47.3
        30.0         64.1
        50.0         94.0
       100.0        158.1
       200.0        265.9
CIRCL2
   1   300
     20.0        20.0        25.0        32.0
       .0         1.0          .0          .1
```

Table A24. Input data for Equivalent Linear Strength Example, 100-meter slope

```
PROFIL                                          FILE: NLIN_3      6-01-92
Linearized Envelope - 100 m slope
   3     3
     10.0        10.0        30.0        10.0   1
     30.0        10.0       162.0       110.0   1
    162.0       110.0       235.0       110.0   1
SOIL
  1
   22.0      22.0         .0     45.30      .000         .0     0
CIRCL2
   1   500
     30.0        30.0       162.0       225.0
       .0        20.0          .0          .1
```

Table A25. Input data for Equivalent Linear Strength Example, 10-meter slope

```
PROFIL                                          FILE: NLIN_4      6-01-92
Linearized Envelope - 100 m slope
   3     3
     10.0         5.0        20.0         5.0   1
     20.0         5.0        25.0        15.0   1
     25.0        15.0        35.0        15.0   1
SOIL
  1
   22.0      22.0         .0     60.90      .000         .0     0
CIRCL2
   1   500
     20.0        20.0        25.0        32.0
       .0         1.0          .0          .1
```

Table A26. Input data for Determining Maximum Reinforcing Force

```
PROFIL                                          FILE: REINF_1     6-01-92
Reinforced Slope Analysis, Case 1
   3     3
      5.0        10.0        13.0        10.0   1
     13.0        10.0        25.0        22.0   1
     25.0        22.0        38.0        22.0   1
SOIL
  1
   20.0      20.0         .0     36.00      .000          .0     0
REINF
  1.500       14.00
LOADS
  1
        25.0         38.0         40.0           .0
CIRCL2
   1   500
     13.0        13.0        25.0        37.0
       .0         3.0          .0          .0
```

Table A27. Input data to determine FOS for unreinforced slope

```
PROFIL                                          FILE: REINF_2     6-01-92
Reinforced Slope Analysis, Case 2
   3     3
      5.0        10.0        13.0        10.0   1
     13.0        10.0        25.0        22.0   1
     25.0        22.0        38.0        22.0   1
SOIL
  1
   20.0      20.0         .0     36.00      .000          .0     0
LOADS
  1
        25.0         38.0         40.0           .0
CIRCL2
   1   500
     13.0        13.0        25.0        37.0
       .0         3.0          .0          .0
```

Table A28. Input data for assumed 7.5 meter reinforced zone

```
PROFIL                                          FILE: REINF_3     6-01-92
Reinforced Slope Analysis, Case 3
   6     4
      5.0        10.0        13.0        10.0   1
     13.0        10.0        25.0        22.0   2
     25.0        22.0        32.5        22.0   2
     32.5        22.0        38.0        22.0   1
     13.0        10.0        20.5        10.0   1
     20.5        10.0        32.5        22.0   1
SOIL
  2
   20.0      20.0         .0     36.00      .000          .0     0
   20.0      20.0         .0     56.04      .000          .0     0
LOADS
  1
        25.0         38.0         40.0           .0
CIRCL2
   1   500
     13.0        13.0        28.0        37.0
       .0         3.0          .0          .0
```

Table A29. Input data for 6.0-meter-wide reinforced zone

```
PROFIL                                          FILE: REINF_4     6-01-92
Reinforced Slope Analysis, Case 4
   6     4
      5.0        10.0        13.0        10.0   1
     13.0        10.0        25.0        22.0   2
     25.0        22.0        31.0        22.0   2
     31.0        22.0        38.0        22.0   1
     13.0        10.0        19.0        10.0   1
     19.0        10.0        31.0        22.0   1
SOIL
  2
   20.0      20.0         .0     36.00      .000          .0     0
   20.0      20.0         .0     56.04      .000          .0     0
LOADS
  1
        25.0         38.0         40.0           .0
CIRCL2
   1   500
     13.0        13.0        28.0        37.0
       .0         3.0          .0          .0
```

Table A30. Input data for control of negative effective stresses, Example 1

```
PROFIL                                          FILE: NEG_STR     6-01-92
Negative Stresses, Example 1
   7     5
      5.0        30.0        20.0        30.0    3
     20.0        30.0        30.0        40.0    3
     30.0        40.0        40.0        50.0    2
     40.0        50.0        50.0        60.0    1
     50.0        60.0        80.0        60.0    1
     40.0        50.0        80.0        50.0    2
     30.0        40.0        80.0        40.0    3
SOIL
  3
  110.0    110.0    1000.0     5.00     .000        .0    0
  110.0    110.0     700.0     7.00     .000        .0    0
  110.0    110.0     400.0    10.00     .000        .0    0
CIRCL2
   6    25
     20.0        30.0        55.0        80.0
       .0         3.0          .0          .0
```

Table A31. Input data for control of negative effective stresses, Example 2

```
PROFIL                                          FILE: SCHWTZ_1   6-01-92
Schwartz +1845 Reinf. Fill, Case 1
  35    13
      .0        14.0        15.0        21.0   1
    15.0        21.0        41.5        40.0   1
    41.5        40.0        43.9        40.0   1
    43.9        40.0        44.1        40.1   4
    44.1        40.1        46.0        43.0   2
    46.0        43.0        46.1        43.1   4
    46.1        43.1        49.0        47.0   2
    49.0        47.0        49.1        47.1   4
    49.1        47.1        52.0        51.0   2
    52.0        51.0        52.1        51.1   4
    52.1        51.1        55.0        55.0   2
    55.0        55.0        57.0        56.0   3
    57.0        56.0        80.0        56.0   3
    55.0        55.0        65.0        55.0   2
    65.0        55.0        72.0        55.0   1
    52.1        51.1        62.1        51.1   4
    52.0        51.0        62.0        51.0   2
    49.1        47.1        59.1        47.1   4
    49.0        47.0        59.0        47.0   2
    46.1        43.1        56.1        43.1   4
    46.0        43.0        56.0        43.0   2
    44.1        40.1        54.1        40.1   4
    43.9        40.0        52.1        40.0   1
    52.1        40.0        53.9        40.0   5
    53.9        40.0        54.1        40.1   5
    54.1        40.1        56.0        43.0   5
    56.0        43.0        56.1        43.1   5
    56.1        43.1        59.0        47.0   1
    59.0        47.0        59.1        47.1   1
    59.1        47.1        62.0        51.0   1
    62.0        51.0        62.1        51.1   1
    62.1        51.1        65.0        55.0   1
      .0         7.0        20.0        17.0   5
    20.0        17.0        52.1        40.0   5
    56.1        43.1        73.5        55.0   5
SOIL
  5
  130.0    135.0     160.0     31.00     .000        .0    1
  130.0    130.0        .0     40.00     .000        .0    1
  130.0    135.0        .0     39.00     .000        .0    1
   60.0     60.0    9999.0       .00     .000        .0    1
  150.0    150.0    2000.0     35.00     .000        .0    1
```

. . . continued on next page

Table A31. Input data for control of negative effective stresses, Example 2 (continued)

```
WATER
  1        62.40
   8
           .0          14.0
         15.0          21.0
         22.0          26.0
         40.0          35.0
         52.1          40.0
         55.9          42.7
         65.0          51.0
         73.5          55.0
LOADS
  1
         57.0          65.0         350.0            .0
LIMITS
   2      2
           .0           3.5          20.0          13.5
         20.0          13.5          74.0          52.0
CIRCL2
  60     25
        .0         30.0         57.0         70.0
        .0          3.0           .0           .0
```

Table A32. Input data for Spencer's Method: Example 1(a), ϕ-only soil

```
PROFIL                                          FILE: SPENC_1     6-01-92
Example for Spencer's FOS, Problem 1
   5      5
     10.0         20.0         25.0         20.0    1
     25.0         20.0         40.0         20.0    1
     40.0         20.0        120.0         60.0    1
    120.0         60.0        140.0         60.0    1
    140.0         60.0        160.0         60.0    1
SOIL
  1
  120.0     120.0         0.0     33.00      .000          .0     0
SURB2
    60.00        90.00        21.30        5.00
```

Table A33. Input data for Spencer's Method: Example 1(b), c-only soil

```
PROFIL                                          FILE: SPENC_2     6-01-92
Example for Spencer's FOS, Problem 2
   5     5
     10.0        20.0        25.0        20.0   1
     25.0        20.0        40.0        20.0   1
     40.0        20.0       120.0        60.0   1
    120.0        60.0       140.0        60.0   1
    140.0        60.0       160.0        60.0   1
SOIL
  1
  120.0    120.0    1400.0      0.00      .000          .0    0
SURB2
    60.00       90.00       21.30       5.00
```

Table A34. Input data for Spencer's Method: Example 1(c), c and ϕ soil

```
PROFIL                                          FILE: SPENC_3     6-01-92
Example for Spencer's FOS, Problem 3
   5     5
     10.0        20.0        25.0        20.0   1
     25.0        20.0        40.0        20.0   1
     40.0        20.0       120.0        60.0   1
    120.0        60.0       140.0        60.0   1
    140.0        60.0       160.0        60.0   1
SOIL
  1
  120.0    120.0     600.0     20.00      .000          .0    0
SURB2
    60.00       90.00       21.30       5.00
```

Table A35. Input data for Spencer's Method: Example 2(a), Intact Section

```
PROFIL                                          FILE: SPENC_4     6-01-92
Example for Spencer's FOS, Problem 4
   5     4
       .0        20.0        20.0        20.0   2
     20.0        20.0        80.0        50.0   1
     80.0        50.0       100.0        50.0   1
    100.0        50.0       120.0        40.0   1
     20.0        20.0       120.0        20.0   2
SOIL
  2
  110.0    110.0    1000.0    15.00     .000         .0    0
  125.0    125.0         .0    35.00     .000         .0    0
SURB2
    30.00       80.00       20.00       3.10
```

Table A36. Input data for Spencer's Method: Example 2(b), Cracked Section

```
PROFIL                                          FILE: SPENC_5     6-01-92
Example for Spencer's FOS, Problem 5
   6     5
       .0        20.0        20.0        20.0   2
     20.0        20.0        77.8        48.9   1
     77.8        48.9        77.9        42.4   1
     77.9        42.4       115.2        42.4   1
    115.2        42.4       120.0        40.0   1
     20.0        20.0       120.0        20.0   2
SOIL
  2
  110.0    110.0    1000.0    15.00     .000         .0    0
  125.0    125.0         .0    35.00     .000         .0    0
SURB2
    30.00       80.00       20.00       3.10
```